

**A COMPARATIVE STUDY OF ANALYTICAL
HIERARCHY PROCESS AND PROBABILITY
ANALYSIS FOR LANDSLIDE SUSCEPTIBILITY
ZONATION IN LOWER MAE CHAEM WATERSHED,
NORTHERN THAILAND**

Narumon Intarawichian

**A Thesis Submitted in Partial Fulfillment of the Requirements for the
Degree of Doctor of Philosophy in Geoinformatics**

Suranaree University of Technology

Academic Year 2008

การศึกษาเปรียบเทียบกระบวนการวิเคราะห์ตามลำดับชั้นและ
การวิเคราะห์ความน่าจะเป็นสำหรับการกำหนดเขตเสี่ยงภัยดินถล่ม
ในเขตลุ่มน้ำแม่แจ่มตอนล่าง ภาคเหนือ ประเทศไทย

นางสาวนฤมล อินทวิเชียร

วิทยานิพนธ์นี้เป็นส่วนหนึ่งของการศึกษาตามหลักสูตรปริญญาวิทยาศาสตรดุษฎีบัณฑิต
สาขาวิชาภูมิสารสนเทศ
มหาวิทยาลัยเทคโนโลยีสุรนารี
ปีการศึกษา 2551

**A COMPARATIVE STUDY OF ANALYTICAL HIERARCHY
PROCESS AND PROBABILITY ANALYSIS FOR LANDSLIDE
SUSCEPTIBILITY ZONATION IN LOWER MAE CHAEM
WATERSHED, NORTHERN THAILAND**

Suranaree University of Technology has approved this thesis submitted in fulfillment of the requirements for the Degree of Doctor of Philosophy.

Thesis Examining Committee

S. Sarapirom

(Asst. Prof. Dr. Sunya Sarapirome)

Chairperson

S. Dasananda

(Asst. Prof. Dr. Songkot Dasananda)

Member (Thesis Advisor)

S. Thammathaworn

(Assoc. Prof. Dr. Sompong Thammathaworn)

Member

Kaew Nualchawee

(Assoc. Prof. Dr. Kaew Nualchawee)

Member

Autcha.K.

(Assoc. Prof. Autcha K.buakasorn)

Member

P. Sattaya Khum

(Prof. Dr. Pairote Sattayatham)

Vice Rector for Academic Affairs

P. Manym

(Assoc. Prof. Dr. Prapan Manyum)

Dean of Institute of Science

นฤมล อินทรวชิเชียร : การศึกษาเปรียบเทียบกระบวนการวิเคราะห์ตามลำดับชั้นและการวิเคราะห์ความน่าจะเป็นสำหรับการกำหนดเขตเสี่ยงภัยดินถล่ม ในเขตลุ่มน้ำแม่แจ่มตอนล่าง ภาคเหนือ ประเทศไทย (A COMPARATIVE STUDY OF ANALYTICAL HIERARCHY PROCESS AND PROBABILITY ANALYSIS FOR LANDSLIDE SUSCEPTIBILITY ZONATION IN LOWER MAE CHAEM WATERSHED, NORTHERN THAILAND) อาจารย์ที่ปรึกษา : ผู้ช่วยศาสตราจารย์ ดร.ทรงกต ทศานนท์, 172 หน้า.

การศึกษานี้มีวัตถุประสงค์เพื่อประเมินผล เปรียบเทียบ และตรวจสอบ เขตเสี่ยงภัยดินถล่มซึ่งมาจากการวิเคราะห์ 3 วิธีการ ได้แก่ กระบวนการวิเคราะห์ตามลำดับชั้น แบบจำลองอัตราส่วนความถี่ และการประสมประสานค่าน้ำหนักของกระบวนการวิเคราะห์ตามลำดับชั้นและแบบจำลองอัตราส่วนความถี่ ในพื้นที่ลุ่มน้ำแม่แจ่มตอนล่าง บริเวณภาคเหนือของประเทศไทย โดยใช้ข้อมูลการรับรู้จากระยะไกล การสำรวจภาคสนาม และระบบสารสนเทศภูมิศาสตร์ ซึ่งปัจจัยที่ใช้ในการวิเคราะห์ทั้งหมด 10 ปัจจัย ได้แก่ ระดับความสูงของพื้นที่ ทิศด้านลาดของความลาดชัน ค่ามุมของความลาดชัน ระยะห่างจากทางน้ำ ชนิดของหิน ระยะห่างจากรอยแตกแยกและรอยเลื่อนของหิน อนุภาคของดิน ปริมาณน้ำฝน ลักษณะการใช้ที่ดิน และดัชนีความสมบูรณ์ของพืชพรรณ ทั้งนี้แผนที่เขตเสี่ยงภัยดินถล่มสร้างมาจากการคำนวณค่าดัชนีความเสี่ยงต่อการเกิดดินถล่ม โดยการให้ค่าน้ำหนักกับปัจจัยแต่ละประเภท ตามกระบวนการของทั้ง 3 วิธีการ ซึ่งการจำแนกค่าดัชนีด้วยวิธี เนเชอรัลเบรก (Natural Breaks) สามารถแบ่งเขตเสี่ยงภัยต่อการเกิดดินถล่มออกเป็น 5 ระดับ ได้แก่ เขตเสี่ยงภัยสูงมาก เขตเสี่ยงภัยสูง เขตเสี่ยงภัยปานกลาง เขตเสี่ยงภัยต่ำ และเขตเสี่ยงภัยต่ำมาก

แผนที่เขตเสี่ยงภัยดินถล่มที่ได้จากผลการวิเคราะห์ทั้ง 3 วิธีการ จะถูกนำไปตรวจสอบกับแผนที่ตำแหน่งดินถล่มที่เคยเกิดขึ้นแล้วจำนวน 25 จุด ซึ่งบันทึกข้อมูลโดยเจ้าหน้าที่ของหน่วยงานท้องถิ่น ในช่วงเวลา 10 ปีที่ผ่านมา ด้วยวิธีการหาพื้นที่ได้ไค้เพื่อประเมินค่าความถูกต้องของการทำนาย โดยการสร้างเส้นไค้และคำนวณพื้นที่ได้ไค้ ทั้งนี้ค่าที่ได้จากการคำนวณจะอธิบายถึงแบบจำลองและปัจจัยที่ใช้ในการวิเคราะห์ว่าสามารถทำนายการเกิดดินถล่มได้ดีมากน้อยเพียงใด

ผลจากการตรวจสอบความถูกต้องดังกล่าวพบว่า กระบวนการวิเคราะห์ตามลำดับชั้นแบบจำลองอัตราส่วนความถี่ และการประสมประสานค่าน้ำหนักของกระบวนการวิเคราะห์ตามลำดับชั้นและแบบจำลองอัตราส่วนความถี่ มีค่าความถูกต้องของการทำนาย 64.90% 84.82% และ 91.22% ตามลำดับ ผลจากการเปรียบเทียบแสดงให้เห็นว่า วิธีการประสมประสานค่าน้ำหนักของกระบวนการวิเคราะห์ตามลำดับชั้นและแบบจำลองอัตราส่วนความถี่ มีค่าความถูกต้องของการทำนายสูงที่สุด ผลจากการศึกษาในครั้งนี้สามารถสรุปได้ว่า วิธีการประสมประสานค่าน้ำหนักของ

กระบวนการวิเคราะห์ตามลำดับชั้นและแบบจำลองอัตราส่วนความถี่ให้ผลลัพธ์ที่ดีที่สุด ซึ่งผลที่ได้สามารถนำไปใช้เป็นแนวทางในการป้องกันและบรรเทาพิบัติภัยจากดินถล่ม รวมทั้งการวางแผนการใช้ที่ดินและการก่อสร้างในอนาคต

สาขาวิชาการรับรู้จากระยะไกล
ปีการศึกษา 2551

ลายมือชื่อนักศึกษา 
ลายมือชื่ออาจารย์ที่ปรึกษา 

NARUMON INTARAWICHIAN : A COMPARATIVE STUDY OF
ANALYTICAL HIERARCHY PROCESS AND PROBABILITY
ANALYSIS FOR LANDSLIDE SUSCEPTIBILITY ZONATION IN
LOWER MAE CHAEM WATERSHED, NORTHERN THAILAND.
THESIS ADVISOR : ASST. PROF. SONGKOT DASANANDA, Ph.D.
172 PP.

LANDSLIDE SUSCEPTIBILITY/ANALYTICAL HIERARCHY PROCESS/
FREQUENCY RATIO/GIS/REMOTE SENSING

The main objective of this research is to evaluate, compare and verify landslide susceptibility zonation using three different methods namely; analytical hierarchy process (AHP), frequency ratio (FR) model and integrated AHP and FR model in lower Mae Chaem watershed, northern Thailand. The study was carried out using remote sensing data, field surveys and geographic information system (GIS) tools. The ten factors that influence landslide occurrence, such as elevation, slope aspect, slope angle, distance from drainage, lithology, distance from lineament, soil texture, precipitation, land use/land cover (LULC) and NDVI. Using these methods, the landslide susceptibility index (LSI) was calculated using the defined weight and rating, and the three landslide susceptibility maps were produced based on values of the index. These LSI values were divided into five classes according to the natural breaks range which represent five different zones in the landslide susceptibility map. These are very high susceptibility (VHS), high susceptibility (HS), moderate susceptibility (MS), low susceptibility (LS) and very low susceptibility (VLS) zones.

Results of analysis were verified with the known landslide locations map containing 25 points recorded by the local authorities in the last decade. For the verification, the area under curve (AUC) method was used where the rate curves were created and their areas under curve were calculated for being the prediction accuracy. The rate explains how well the model and factor predict the landslide occurrences.

It was found that prediction accuracy of analytical hierarchy process (AHP), the frequency ratio (FR) model, and integrated AHP and FR model are 64.90%, 84.82% and 91.22% respectively. The comparison results showed that the integrated AHP and FR model gave the highest percentage of prediction accuracy in the study area. Therefore, it can be concluded that the integrated AHP and FR model provides the best result in this study. This knowledge can be used for the landslide hazard prevention and mitigation, and proper planning for land use and construction in the future.

School of Remote Sensing

Academic Year 2008

Student's Signature N. Intarawichian

Advisor's Signature S. Dasanamda

ACKNOWLEDGEMENTS

I would like to express my sincere appreciation to Asst. Prof. Dr. Songkot Dasananda, thesis advisor, for his valuable suggestions and critical comments which greatly improved the quality of the work done in this thesis.

I would like to thank Asst. Prof. Dr. Sunya Sarapirome, Assoc. Prof. Dr. Kaew Nualchawee, Assoc. Prof. Autcha K.buakasorn, Assoc. Prof. Dr. Sompong Thammathaworn and Dr. Suwit Ongsomwang for their guidance and valuable contributions through the progress report discussions.

Thanks to the Geo-Informatics and Space Technology Development Agency (Public Organization), or GISTDA, for providing Landsat-5 TM satellite images of the study area, Ministry of Agriculture and Cooperatives for providing aerial photographs, Department of Mineral Resources for providing the geological data, Land Development Department for providing soil data and Thai Meteorological Department and the GAME-T project for providing rainfall data for the research. Special thanks to Mae Chaem District Office and its staffs for providing valuable background information on the landslides in the study area and their help in the field surveys.

I would also like to thank School of Remote Sensing, Institute of Science, Suranaree University of Technology, for giving the opportunity to pursue a Ph.D. program in geoinformatics and to learn more about geoinformatics techniques which are useful for doing my own research in the future.

Thanks are also extended to Mrs. Phenkhae Petchmai, Mrs. Warunee Tanissara, and Mrs. Ratchaneekorn Chatuthai, the secretary of School of Remote Sensing, Institute of Science, Suranaree University of Technology, for their help and assistance in doing several paper works during the study.

Thanks and appreciation to Mrs. Suree Teerarungsigul, geologist of Department of Mineral Resources, for her invaluable guidance on knowledge as well as her encouragement and suggestions on this thesis. Thanks are due to Mr. Rattana Boonprasert, Mr. Rawee Rattanakom and Miss Siriwan Ruamkaew, my friends, for their kind help and warm encouragement during the time of my study.

I would also like to express my deep sense of gratitude to my parents and my two younger brothers for their continuous motivation, ultra-patience, and endless trust. In addition, special thanks to my husband, Mr. Surat Jiaranaiwiwat of Burapha University, for his great technical supports and for giving me his infinite love, patience, sacrifices and understanding during the study at Suranaree University of Technology.

Finally, my appreciation is devoted to my passed-away mother for giving me inspiration and her continuous love and care.

This research was supported by grant from the Commission on Higher Education, the Ministry of Education of Thailand.

Narumon Intarawichian

CONTENTS

	Page
ABSTRACT IN THAI.....	I
ABSTRACT IN ENGLISH.....	III
ACKNOWLEDGEMENTS.....	V
CONTENTS.....	VII
LIST OF TABLES.....	XII
LIST OF FIGURES.....	XVII
LIST OF ABBREVIATIONS.....	XXI
CHAPTER	
I INTRODUCTION.....	1
1.1 Introduction to this Study.....	1
1.2 Research Objectives.....	5
1.3 Scope and Limitations of the Study.....	5
1.4 Study Area.....	6
1.4.1 Location.....	6
1.4.2 Topography.....	6
1.4.3 Climate.....	8
1.4.4 Land Use Patterns.....	8
1.4.5 Population.....	8
1.5 Characteristic of the Problem.....	9
1.6 Expected Results.....	11

CONTENTS (Continued)

	Page
II LITERATURE REVIEW	12
2.1 Definition of Landslide and Terminology.....	12
2.2 Classifications of Landslides.....	12
2.2.1 Types of Materials.....	13
2.2.2 Types of Landslides.....	14
2.2.3 Causes of Landslides.....	22
2.2.4 Multiple Causes of Landslides.....	23
2.2.4.1 Landslides and Water.....	24
2.2.4.2 Landslides and Seismic Activity.....	27
2.2.4.3 Landslides and Volcanic Activity.....	27
2.3 Use of Remote Sensing in Landslide Susceptibility Assessment.....	27
2.4 Remote Sensing in Landslides Spatial Analysis and Hazard Prediction...	28
2.5 Geographical Information Systems (GIS) and Landslide Hazard Assessment.....	29
2.6 GIS and Landslide Analysis.....	33
2.7 GIS Based Landslide Hazard Zoning Techniques.....	34
2.8 Landslide Susceptibility Approaches.....	35
2.9 Landslide Hazard or Susceptibility Mapping.....	43
2.10 Trends in Landslide Hazard Zonation.....	44
2.11 Landslide Hazard in Thailand.....	45
2.12 Comparison and Verification of the Results.....	47

CONTENTS (Continued)

	Page
III MATERIALS AND METHODOLOGY	49
3.1 Instrumentation.....	49
3.1.1 Hardware.....	49
3.1.2 Software.....	50
3.1.3 Data.....	50
3.2 Data Input and Preparation.....	50
3.3 Landslide Location Detection.....	65
3.4 Factors Influencing Landslides.....	68
3.4.1 Elevation.....	72
3.4.2 Slope Aspect.....	72
3.4.3 Slope Angle.....	73
3.4.4 Distance from Drainage.....	74
3.4.5 Lithology.....	74
3.4.6 Distance from Lineament.....	75
3.4.7 Soil Texture.....	76
3.4.8 Precipitation.....	76
3.4.9 Land Use/Land Cover.....	77
3.4.10 NDVI.....	77
3.5 Research Methodology.....	78
3.5.1 Analytical Hierarchy Process (AHP).....	80
3.5.2 Probability Analysis–Frequency Ratio (FR) Model.....	81

CONTENTS (Continued)

	Page
3.5.3 Integrated AHP and FR Model.....	82
3.6 Area Under the Curve (AUC) Method.....	84
IV RESULTS	85
4.1 Landslide Susceptibility Zones Map.....	85
4.2 Application of AHP and Susceptibility Map.....	86
4.3 Application of Probability Analysis–Frequency Ratio (FR) Model and Susceptibility Map.....	92
4.3.1 Relationship between Landslides and Landslide Related Factors.....	92
4.3.2 Landslide Susceptibility Mapping.....	95
4.4 Application of Integrated AHP and FR Model and Susceptibility Map.....	97
4.5 Comparison and Verification of the Results.....	102
V CONCLUSIONS AND DISCUSSION	105
5.1 Conclusions.....	105
5.2 Discussion.....	106
5.2.1 Landslide Occurrence in the Low Risk Zone.....	108
5.2.2 Comparison with the Susceptibility Maps Developed from Some Agencies.....	109
REFERENCES	111

CONTENTS (Continued)

	Page
APPENDICES.....	132
APPENDIX A QUESTIONNAIRE AND LIST OF EXPERTS.....	133
APPENDIX B THE PAIR-WISE COMPARISON METHOD:	
AHP'S FACTOR WEIGHTS.....	140
APPENDIX C THE PAIR-WISE COMPARISON METHOD:	
AHP'S CLASS WEIGHTS.....	145
APPENDIX D AVERAGE ANNUAL RAINFALL DATA AND	
STATION.....	167
CURRICULUM VITAE.....	172

LIST OF TABLES

Table	Page
1.1 Summary of the crucial landslide incidences in the study area (Source: Department of Mineral Resources, Mae Chaem District Office and internet resource).....	10
2.1 Types of landslides. Abbreviated version of Varnes' classification of slope movements (Varnes, 1978).....	14
2.2 Schematic overview of landslide damage types, related to different types of landslides, elements at risk and the location of the elements at risk in relation to the landslide (modified from Van Westen et al., 2006).....	25
2.3 Usefulness of specific combinations of hazard approaches and risk approaches for GIS-based landslide risk zonation at medium scales.....	41
2.4 The trends in landslide hazard zonation (Van Westen, 1993).....	45
3.1 Overview of remotely-sensed data of the study area.....	53
3.2 Spatial data layers used in the study.....	54
3.3 Distribution of landslide occurrence points for various data layers in the study area.....	69
3.4 Lithologic groups and geological ages in the study area.....	75
3.5 Scale of preference between two parameters in AHP (Saaty, 2000).....	81
4.1 The pair-wise comparison matrix, factor weights, class weights (rating) and consistency ratio.....	87

LIST OF TABLES (Continued)

Table	Page	
4.2	Landslide susceptibility classes, susceptibility index values and coverage percentage of the study area based on AHP.....	91
4.3	Frequency ratio of landslide occurrence.....	93
4.4	Landslide susceptibility classes, susceptibility index values and coverage percentage of the study area based on FR model.....	96
4.5	Weights from integrated AHP and FR model.....	98
4.6	Landslide susceptibility classes, susceptibility index values and coverage percentage of the study area based on integrated AHP and FR model.....	100
4.7	Compare percentage of area occupied by each landslide susceptibility class and the susceptibility index values between AHP, FR model and integrated AHP and FR model. The LSI ranges used in the classification were assigned using natural breaks algorithm.....	101
5.1	Allocation of the 25 referred landslide events to each susceptibility class defined by the AHP, FR model, and integrated AHP and FR model.....	108
A1	Scale of preference between two parameters in AHP (Saaty, 2000).....	134
A2	Questionnaire.....	135
A3	List of experts.....	139
B1	Factor weights from questionnaires.....	141
B2	Step I: Generation of the pair-wise comparison matrix for each factor.....	143
B3	Step II: Computation of the criterion weights for each factor.....	143
B4	Step III: Estimation of the consistency ratio for each factor.....	144

LIST OF TABLES (Continued)

Table	Page
C1	Step I: Generation of the pair-wise comparison matrix for each elevation's class..... 146
C2	Step II: Computation of the criterion weights for each elevation's class..... 147
C3	Step III: Estimation of the consistency ratio for each elevation's class..... 147
C4	Step I: Generation of the pair-wise comparison matrix for each slope aspect's class..... 148
C5	Step II: Computation of the criterion weights for each slope aspect's class..... 148
C6	Step III: Estimation of the consistency ratio for each slope aspect's class..... 149
C7	Step I: Generation of the pair-wise comparison matrix for each slope angle's class..... 150
C8	Step II: Computation of the criterion weights for each slope angle's class..... 150
C9	Step III: Estimation of the consistency ratio for each slope angle's class..... 151
C10	Step I: Generation of the pair-wise comparison matrix for each distance from drainage's class..... 152
C11	Step II: Computation of the criterion weights for each distance from drainage's class..... 152

LIST OF TABLES (Continued)

Table	Page
C12 Step III: Estimation of the consistency ratio for each distance from drainage's class.....	153
C13 Step I: Generation of the pair-wise comparison matrix for each lithology's class.....	154
C14 Step II: Computation of the criterion weights for each lithology's class.....	154
C15 Step III: Estimation of the consistency ratio for each lithology's class.....	155
C16 Step I: Generation of the pair-wise comparison matrix for each distance from lineament's class.....	156
C17 Step II: Computation of the criterion weights for each distance from lineament's class.....	156
C18 Step III: Estimation of the consistency ratio for each distance from lineament's class.....	157
C19 Step I: Generation of the pair-wise comparison matrix for each soil texture's class.....	158
C20 Step II: Computation of the criterion weights for each soil texture's class.....	158
C21 Step III: Estimation of the consistency ratio for each soil texture's class.....	159
C22 Step I: Generation of the pair-wise comparison matrix for each precipitation's class.....	160

LIST OF TABLES (Continued)

Table	Page
C23	Step II: Computation of the criterion weights for each precipitation's class..... 160
C24	Step III: Estimation of the consistency ratio for each precipitation's class..... 161
C25	Step I: Generation of the pair-wise comparison matrix for each land use/land cover's class..... 162
C26	Step II: Computation of the criterion weights for each land use/land cover's class..... 163
C27	Step III: Estimation of the consistency ratio for each land use/land cover's class..... 164
C28	Step I: Generation of the pair-wise comparison matrix for each NDVI's class..... 165
C29	Step II: Computation of the criterion weights for each NDVI's class..... 165
C30	Step III: Estimation of the consistency ratio for each NDVI's class..... 165
D1	Average annual rainfall data are available from 1996 to 2005..... 168

LIST OF FIGURES

Figure	Page
1.1 Location map of the study area, the lower Mae Chaem watershed.....	7
1.2 Photographs of landslide occurrences in the study area.....	11
2.1 An idealized slump-earth flow showing commonly used nomenclature for labeling the parts of a landslide (modified from USGS Fact Sheet 2004-3072 in USGS, 2004).....	15
2.2 Major types of landslide movement (modified from Varnes, 1978 and DOE., 1990).....	16
2.3 GIS and its related software systems as components of GIS (modified from Sgzen, 2002).....	30
2.4 The phases of a GIS (modified from Sgzen, 2002).....	30
2.5 The questions of a well-built GIS should answer (modified from Sgzen, 2002).....	31
2.6 A schematic illustration of landslide susceptibility mapping methods used commonly at present (modified from Ayalew et al., 2005).....	40
3.1 Elevation map of the study area based on DEM from topographic map of 1:50,000 scale (Source: Royal Thai Survey Department).....	55
3.2 Slope aspect map of the study area based on DEM from topographic map of 1:50,000 scale (Source: Royal Thai Survey Department).....	56
3.3 Slope angle map of the study area based on DEM from topographic map of 1:50,000 scale (Source: Royal Thai Survey Department).....	57

LIST OF FIGURES (Continued)

Figure	Page
3.4 Distance from drainage map of the study area from topographic map of 1:50,000 scale (Source: Royal Thai Survey Department).....	58
3.5 Lithology map of the study area (Source: Department of Mineral Resources).....	59
3.6 Distance from lineament map of the study area (Source: Department of Mineral Resources).....	60
3.7 Soil texture map of the study area (Source: Land Development Department).....	61
3.8 Precipitation map of the study area (1996-2005) based on kriging interpolation method (Source: Thai Meteorological Department and the GAME-T project, 2006).....	62
3.9 Land use/land cover map of the study area modified from Land Development Department, 2001, and based on unsupervised classification method (ISODATA) from Landsat-5 TM image, path 131/row 47, acquired on 12 February 2001, and field surveys (Source: Geo-Informatics and Space Technology Development Agency (Public Organization)).....	63
3.10 Normalized difference vegetation index (NDVI) map of the study area derived from Landsat-5 TM image, path 131/row 47, acquired on 12 February 2001 (Source: Geo-Informatics and Space Technology Development Agency (Public Organization)).....	64

LIST OF FIGURES (Continued)

Figure	Page
3.11 High resolution satellite images (IKONOS) and aerial photographs show landslide locations in the study area.....	66
3.12 101 landslide locations map with hill-shaded map in the study area.....	67
3.13 Histograms showing frequency ratio of landslide occurrence with (a) elevation; (b) slope aspect; (c) slope angle; (d) distance from drainage; (e) lithology; (f) distance from lineament; (g) soil texture; (h) precipitation; (i) land use/land cover; (j) NDVI.....	72
3.14 Flow diagram showing research procedure.....	79
3.15 Flow chart of integrated AHP and FR model.....	83
4.1 The landslide susceptibility map based on AHP with 25 known landslide locations on the basis of natural breaks classification.....	91
4.2 The landslide susceptibility map based on FR model with 25 known landslide locations on the basis of natural breaks classification.....	96
4.3 The landslide susceptibility map based on integrated AHP and FR model with 25 known landslide locations on the basis of natural breaks classification.....	100
4.4 Histograms showing relative distribution of landslide susceptibility classes generated by AHP, FR model and integrated AHP and FR model...	101
4.5 Illustration of cumulative frequency diagram showing landslide susceptibility index rank (x-axis) occurring in cumulative percent of landslide occurrence (y-axis).....	102

LIST OF FIGURES (Continued)

Figure	Page
4.6 Histograms showing the percentage of prediction accuracy based on AUC method.....	103
5.1 Susceptibility maps of the study area derived in this thesis and by different Thai agencies. (a) AHP; (b) FR model; (c) integrated AHP and FR model; (d) LDD (2001); (e) DMR (2005); (f) Chiang Mai University (2006).....	110
D1 Graph showing the pattern distribution of average annual rainfall data are available from 1996 to 2005 on each station/guage (Source: Thai Meteorological Department and the GAME-T project).....	171

LIST OF ABBREVIATIONS

AHP	=	Analytical Hierarchy Process
FR	=	Frequency Ratio
WLC	=	Weighted Linear Combination
CR	=	Consistency Ratio
AUC	=	Area Under the Curve
GIS	=	Geographic Information System
TM	=	Thematic Mapper
DEM	=	Digital Elevation Model
GCP	=	Ground Control Point
LSI	=	Landslide Susceptibility Index
LSZ	=	Landslide Susceptibility Zonation
VHS	=	Very High Susceptibility
HS	=	High Susceptibility
MS	=	Moderate Susceptibility
LS	=	Low Susceptibility
VLS	=	Very Low Susceptibility
LULC	=	Land Use/Land Cover
NDVI	=	Normalized Difference Vegetation Index
GISTDA	=	Geo-Informatics and Space Technology Development Agency (Public Organization)

CHAPTER I

INTRODUCTION

1.1 Introduction to this Study

Landslide is typically defined by a wide range of ground movement, such as rock falls, deep failure of slopes, and shallow debris flows. Landslide hazard results in great loss of life and property. These damages can be avoided if the cause and effect relationships of the events are known. Landslide is one of the complex natural hazards, involving multitude of factors and need to be studied systematically in order to evaluate effectively. A landslide susceptibility map depicts areas likely to have landslides in the future by correlating some of the principal factors that contribute to landslides with the past distribution of slope failures (Brabb, 1984).

Over the past decade, the provinces in the north of Thailand most at risk are Chiang Mai and Mae Hong Son where flash floods and landslides have resulted in serious agricultural and property damage, and sometimes substantial loss of lives. Several areas in the lower Mae Chaem watershed are also prone to landslide disaster, especially ones that locate close to steeply sloping small mountain. Consequently, the effective landslide hazard assessment of the area is seriously needed and this is fulfilled in this study.

Landslide susceptibility mapping relies on a rather complex knowledge of slope movements and their controlling factors. The reliability of landslide susceptibility maps depends mostly on the amount and quality of available data, the

working scale and the selection of the appropriate methodology of analysis and modeling. The process of creating these maps involves several qualitative or quantitative approaches (e.g., Soeters and Van Westen, 1996; Aleotti and Chowdhury, 1999; Guzzetti et al., 1999). Early attempts defined susceptibility classes by qualitative overlaying of geological and morphological slope-attributes to landslide inventories (Nielsen et al., 1979). More sophisticated assessments involved AHP, bivariate, multivariate, logistics regression, fuzzy logic, artificial neural network, etc. analysis.

Qualitative methods depend on expert opinions. The most common types of qualitative methods simply use landside inventories to identify sites of similar geological and geomorphological properties that are susceptible to failure. Some qualitative approaches, however, incorporate the idea of ranking and weighting, and may evolve to be semi-quantitative in nature. The application of the analytical hierarchy process (AHP) method, developed by Saaty (1980), for landslide susceptibility has been shown before (e.g., Barredo et al., 2000; Mwasi, 2001; Nie et al., 2001; Yagi, 2003), and weighted linear combination (WLC) by Ayalew et al. (2004). AHP involves building a hierarchy of decision elements (factors) and then making comparisons between possible pairs in a matrix to give a weight for each element and also a consistency ratio. It is based on three principles: decomposition, comparative judgment and synthesis of priorities (Malczewski, 1999). WLC is a concept to combine maps of landslide-controlling parameters by applying a standardized score (primary-level weight) to each class of a certain parameter and a factor weight (secondary-level weight) to the parameters themselves. Being partly subjective, results of these approaches vary depending on the knowledge of experts.

Hence, qualitative or semi-quantitative methods are often useful for regional studies (Soeters and Van Westen, 1996; Guzzetti et al., 1999).

Quantitative methods are based on numerical expressions of the relationship between controlling factors and landslides. There are two types of quantitative methods: deterministic and statistical (Aleotti and Chowdhury, 1999). Deterministic quantitative methods depend on engineering principles of slope instability expressed in terms of the factor of safety. Due to the need for exhaustive data from individual slopes, these methods are often effective for mapping only small areas. Landslide susceptibility mapping using either multivariate or bivariate statistical approaches analyzes the historical link between landslide-controlling factors and the distribution of landslides (Guzzetti et al., 1999).

The increasing computer-based tools are found to be useful in the hazard mapping of landslides. One of such significant tools for hazard mapping of landslides is geographic information systems (GIS). A GIS is defined as a powerful set of tools for collecting, storing, retrieving at will, displaying, and transforming spatial data (Burrough and McDonnel, 1998). One of the main advantages of the use of this technology is the possibility of improving hazard occurrence models, by evaluating their results and adjusting the input variables. An important aspect of landslide investigations is the possibilities to store, treat, and analyze spatiotemporal data that are available. The feature extraction of some factors can be interpreted satellite images. With the increase in efficient digital computing facilities, the digital remote sensing data and their analysis have gained enormous importance. Then the spatial and temporal thematic information derived from remote sensing and ground based information need to be integrated for data analysis. This can be very well achieved

using GIS which has the capabilities to handle voluminous spatial data. With the help of GIS, it is possible to integrate the spatial data of different layers to determine the influence of the parameters on landslide occurrence. The process of GIS aided landslide susceptibility mapping at present involves several methods that can be considered as either qualitative or quantitative. Qualitative methods depend on expert opinions, and are often useful for regional assessments (Soeters and van Westen, 1996; Aleotti and Chowdhury, 1999). Quantitative methods rely on observed relationships between controlling factors and landslides (Guzzetti et al., 1999).

In this study, the three different methods namely, AHP, FR model and integrated AHP and FR model, to produce and later compare three landslide susceptibility maps of the selected area. The first method, AHP is a semi-qualitative method, which involves a matrix-based pair-wise comparison of the contribution of different factors for landslide. The AHP is a Multi-Criteria Decision Making (MCDM) tool at the core of which lies a method for converting subjective assessments of relative importance to a set of overall scores or weights. The second method, FR model is a quantitative method. The spatial relationships between the landslide location and each landslide-related factor were analyzed by using the probability analysis–FR model. The frequency ratio, a ratio between the occurrence and absence of landslides in each cell, was calculated for each factor's type (or range) that had been identified as significant with respect to causing landslides. An area ratio for each factor's type (or range) to the total area was calculated. Finally, frequency ratios for each factor's type (or range) were calculated by dividing the landslide occurrence ratio by the area ratio. The last method, integrated AHP and FR model is a hybrid method between qualitative and quantitative methods (Ayalew et al., 2004). Finally, all the

weighted factor maps are overlaid and a landslide susceptibility maps are produced and represented in term of landslide susceptibility zone (LSZ).

There are five categories of LSZ assigned which are very high susceptibility (VHS), high susceptibility (HS), moderate susceptibility (MS), low susceptibility (LS) and very low susceptibility (VLS) zones. The validity of three landslide susceptibility maps obtained from each model were carried out using the map overlay technique provided in ArcGIS software (v 9.0). Finally, the validity of the output map was verified and compared using the known landslide locations.

1.2 Research Objectives

This research will focus on the three following main objectives:

1.2.1 To find relative importance of the chosen landslide influencing factors.

1.2.2 To evaluate landslide susceptibility zonation in the chosen area by using analytical hierarchy process (AHP), frequency ratio (FR) model and integrated AHP and FR model.

1.2.3 To compare and verify the results of three landslide susceptibility maps by using known landslide locations.

1.3 Scope and Limitations of the Study

In this study, the three different methods namely, AHP, FR model and integrated AHP and FR model have been used to produce and later compare and verify, three landslide susceptibility maps of lower Mae Chaem watershed. Relevant thematic layers pertaining the causative factors are generated using remote sensing data, field surveys and geographic information system (GIS) tools. There are ten landslide inducing parameters considered which are elevation, slope aspect, slope

angle, distance from drainage, lithology, distance from lineament, soil texture, precipitation, land use/land cover and NDVI. In order to store the information of these parameter maps in a concise thematic database a 25×25 meter grid is overlaid to the area.

1.4 Study Area

1.4.1 Location

The lower Mae Chaem watershed is a significant watershed of Mae Ping River, which is the main river in the upper north of Thailand and the largest tributary of central Thailand's Chao Phraya River. It is located approximately between latitudes 18°06'00"N to 18°38'24"N and longitudes 98°04'12"E to 98°38'24"E, covering area of about 1,932 km² in Chiang Mai and Mae Hong Son Provinces. There are three districts (Amphoe) located within Chiang Mai border and two districts (Amphoe) located within Mae Hong Son border.

1.4.2 Topography

Topography of lower Mae Chaem watershed is relatively steep with elevation ranging from 260 m to 2,540 m and small narrow floodplains appear close to the river (Figure 1.1). About 90% of its areas are high mountains covered with diversified plant communities that form various types of forest, where rice and other agricultural productions, especially vegetables and orchards, are normally cultivated in the low area.

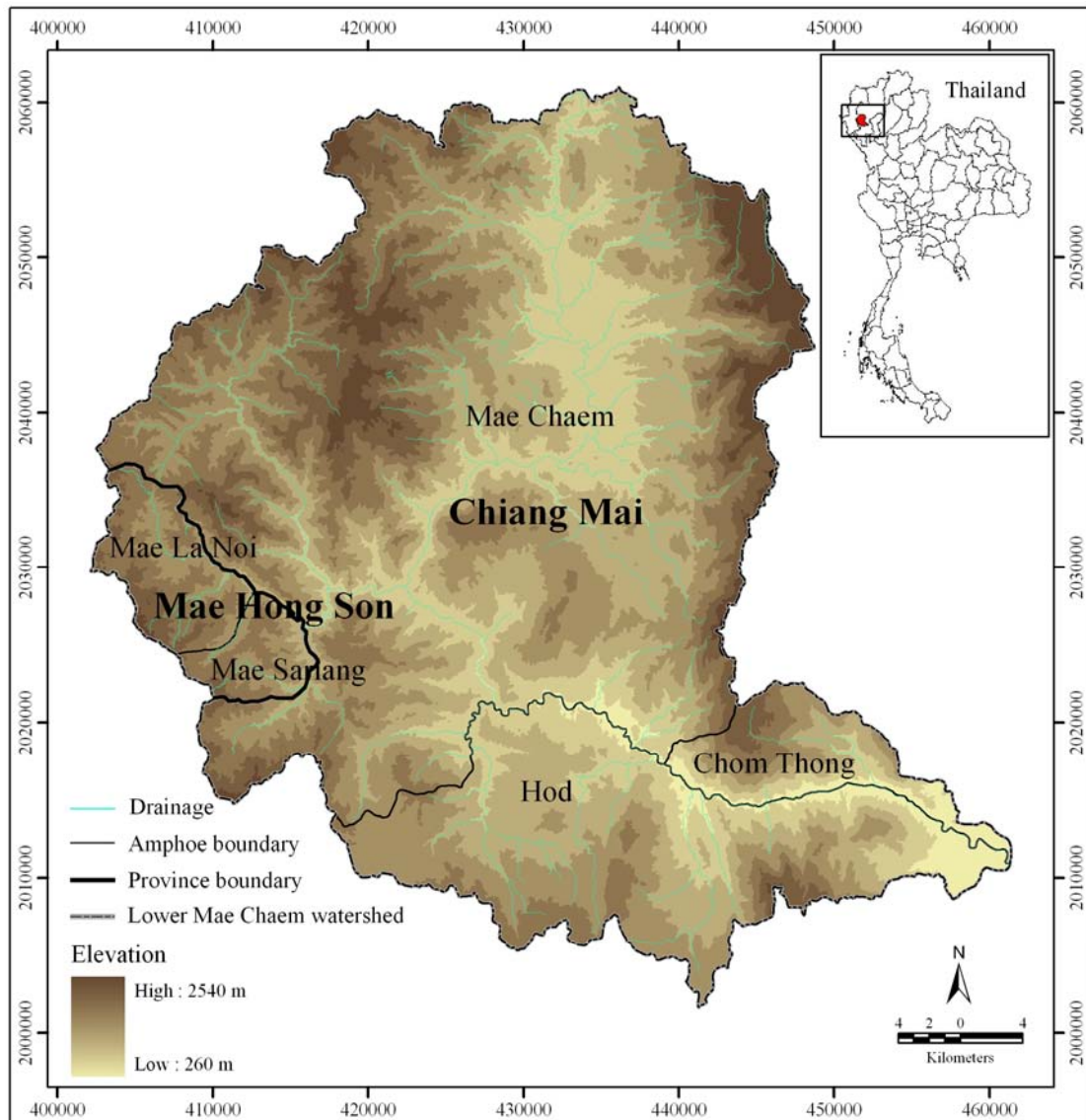


Figure 1.1 Location map of the study area, the lower Mae Chaem watershed.

Altitude variation induces different climatic zones with distinctive types of natural land cover. Dominant vegetation includes dry dipterocarp and mixed deciduous forests below 1,000 m, tropical mixed pine forest from 900 to 1,500 m alternating with hill evergreen forest that extends up to 2,000 m, and tropical montane cloud forest above 2,000 m (Dairaku et al., 2000; Kuraji et al., 2001). Steep hillsides with slopes exceeding 25% are a common landscape element, resulting in rates of soil erosion that prevent advanced soil development. Thus, soils are relatively shallow and

have limited water-holding capacity (Hansen, 2001). Dominant soil textures are sandy clay loam and clay loam.

1.4.3 Climate

The climate of this mountainous basin is defined by large variations in seasonal and annual rainfall that are influenced by Pacific-born typhoons, superimposed on the south-west monsoon (Walker, 2002). The orographic effect induces an altitudinal increase of spatial rainfall distribution (Dairaku et al., 2000; Kuraji et al., 2001). In this area, annual rainfall is highly variable from year to year with 95% of rain occurring in the wet season from May to October and the average annual temperature ranges from 20 °C to 34 °C.

1.4.4 Land Use Patterns

Land use patterns in lower Mae Chaem watershed have undergone substantial change during the past several decades. As recently as the 1960s, the agriculture mosaic was comprised of highland (above 1,000 m) pioneer shifting cultivation that often included opium, mid-elevation (600–1,000 m) rotational forest fallow shifting cultivation with a decade long fallow period, and paddy and home garden-centered cultivation in the lowlands (Thomas et al., 2002; Walker, 2003).

1.4.5 Population

The population of lower Mae Chaem watershed is ethnically diverse and distributed among numerous small villages. Ethnic Karen make up more than 60 percent of the total population, northern Thai (khon muang) nearly 30 percent, and Hmong less than 10 percent; a few ethnic Lua and Lisu communities are also located in the study area.

Ethnic Hmong and Lisu communities are located mainly in the highland zone, while most Karen and Lua are in the middle zone and northern Thai (khon muang) occupy most of the lowlands. The majority Karen and Lua ethnic groups live primarily in mid-elevation zones between 600 and 1,000 m, with some communities extending into higher elevations. Ethnic northern Thai (khon muang) villages are mostly clustered in lowland areas below 600 m, whereas Hmong and Lisu ethnic groups live mostly in highland villages located above 1,000 m.

1.5 Characteristic of the Problem

Due to its hilly and mountainous landscape, landslide is a recurrent problem which happens throughout most of northern Thailand. Most severe landslides were triggered by a period of continuous heavy rainfall and could result in significant damage to property and agriculture, and to the tragic loss of human life also. Typically, the predominant type of landslide found in northern Thailand is the rainfall-triggered shallow landslide which caused by the intense and continuous rainfall (Yumuang, 2006). Shallow failures occur due to saturation of top soil layer along the terrain slope which shifts slope from marginally stable to unstable state. This could result in the rapid movement of soil cover down hill to the surrounded low area (Liu and Wu, 2008). During this period, the landslide might transform into a debris avalanche, with increasing velocity and volume. If the landslide material flows into a gully at the base of the slope, then the run-out of the material can reach long distance (Revellino et al., 2004).

In recent years, the lower Mae Chaem watershed has experiences several massive landslide incidences which brought vast damage to the properties and natural

environment, and some loss of human life (Table 1.1). Though, the area is long known to be in the landslide risk zone but it still lacks of studies that assess risk of landslide occurrence in this area thoughtfully and this is the main objective of this research. Photographs of some landslide occurrences found in the study area are shown in Figure 1.2.

Table 1.1 Summary of the crucial landslide incidences in the study area (Source: Department of Mineral Resources, Mae Chaem District Office and internet resource).

Date/Place	The effect of the disaster
September 15, 2002 Mae Chaem, Chiang Mai	The infrastructures were affected such as bridge, road, drainage systems and agricultural areas.
October 2, 2002 Mae Sariang, Mae Hong Son	The infrastructures were affected such as bridge, road, drainage systems and agricultural areas with several casualties.
May 6, 2004 Mae Chaem, Chiang Mai	1 people died, 3 houses were destroyed, agricultural areas and property were affected.
September 14, 2005 Mae Sariang and Mae La Noi, Mae Hong Son	The infrastructures were affected such as bridge, road.
September 19, 2005 Mae Chaem, Chiang Mai	Some houses were destroyed, and infrastructures were affected such as bridge, road, drainage systems and agricultural areas.



Figure 1.2 Photographs of landslide occurrences in the study area.

1.6 Expected Results

1.6.1 Determination of triggering factors and a suitable methodology for predicting on landslides occurrences and landslide susceptibility zonation maps in the study area.

1.6.2 The landslide susceptibility maps produced in the chosen area by using analytical hierarchy process (AHP), frequency ratio (FR) model and integrated AHP and FR model.

1.6.3 Knowledge of the potential landslide prone areas that could be used for explaining existing landslide locations, making emergency decisions, avoiding and mitigating of future landslide hazard.

CHAPTER II

LITERATURE REVIEW

Landslide is simply the down slope movement (sliding or falling) of soil, rock, or some mixture of the two, under the influence of gravity. Landslides are natural processes, but can be triggered or accelerated by one or more of the factors, especially when the factors occur in combination.

2.1 Definition of Landslide and Terminology

According to Cruden (1991), landslide is defined as “the movement of a mass of rock, debris or earth down a slope”. Mass movement is defined as “the outward and downward gravitational movement of earth material without the aid of running water as a transporting agent” (Crozier, 1986). These are internationally accepted and most widely used definitions of the phenomenon. Although, several more definitions may be found, but in essence, they all lead to the same conclusion that landslide is involved mass transportation down the slope in which a hazardous activity for humans can occur.

2.2 Classifications of Landslides

The various types of landslides can be differentiated by the kinds of material involved and the mode of movement. A typical classification system based on these parameters is shown in Table 2.1. Classification of landslides is based on a two-term descriptor; the first term describing material type prior to failure and the second term

describing the type of movement (Varnes, 1978). As can be seen in Table 2.1, there are five basic types of landslides that occur in three types of material. Falls, topples, slides, lateral spreads, and flows can occur in bedrock, debris, or earth. While individual landslide types can occur in nature, most landslides are complex, or composed of combinations of basic types of landslides. Other classification systems incorporate additional variables, such as the rate of movement and the water, air, or ice content of the landslide material.

2.2.1 Types of Materials

The material types involved in landslide can be classified into two groups; bedrock and soil (Table 2.1). Soil is generally unconsolidated surficial material. It is further subdivided into debris and earth depending upon its textures.

Bedrock: Bedrock refers to earth materials that have been created by rock forming processes. Its strength depends on the rock type, degree of weathering, density and orientation of discontinuities, which are generally the planes of weakness in the rock mass. For instance, if a dense and hard granite rock contains many fractures, the rock mass may be less strong than a coarse-grained soil.

Debris: Debris is composed of predominantly coarse-grained soil including boulder to gravel and sandy materials. It can also include pieces of highly fractured bedrock. The strength of coarse-grained soil generally depends on the friction between the grains. Woody debris such as tree or logs, or other organic material, is sometime mixed with the inorganic debris.

Earth: Earth refers to predominantly fine-grained soil (silt and clay size materials). The strength of fine-grained soil generally depends on cohesion, chemical and electrical bonding between small particles.

Table 2.1 Types of landslides. Abbreviated version of Varnes' classification of slope movements (Varnes, 1978).

Type of Movement	Type of Material		
	Bedrock	Engineering Soils	
		Predominantly coarse	Predominantly fine
FALLS	Rock fall	Debris fall	Earth fall
TOPPLES	Rock topple	Debris topple	Earth topple
SLIDES			
ROTATIONAL	Rock slide	Debris slide	Earth slide
TRANSLATIONAL			
LATERAL SPREADS	Rock spread	Debris spread	Earth spread
FLOWS	Rock flow	Debris flow	Earth flow
	(deep creep)		(soil creep)
COMPLEX	Combination of two or more principal types of movement		

2.2.2 Types of Landslides

The term "landslide" describes a wide variety of processes that result in the downward and outward movement of slope-forming materials including rock, soil, artificial fill, or a combination of these. Landslides are portrayed according to the types of movements namely, fall, topple, slide, spread and flow. Figure 2.1 shows a graphic illustration of a landslide, with the commonly accepted terminology describing its features.

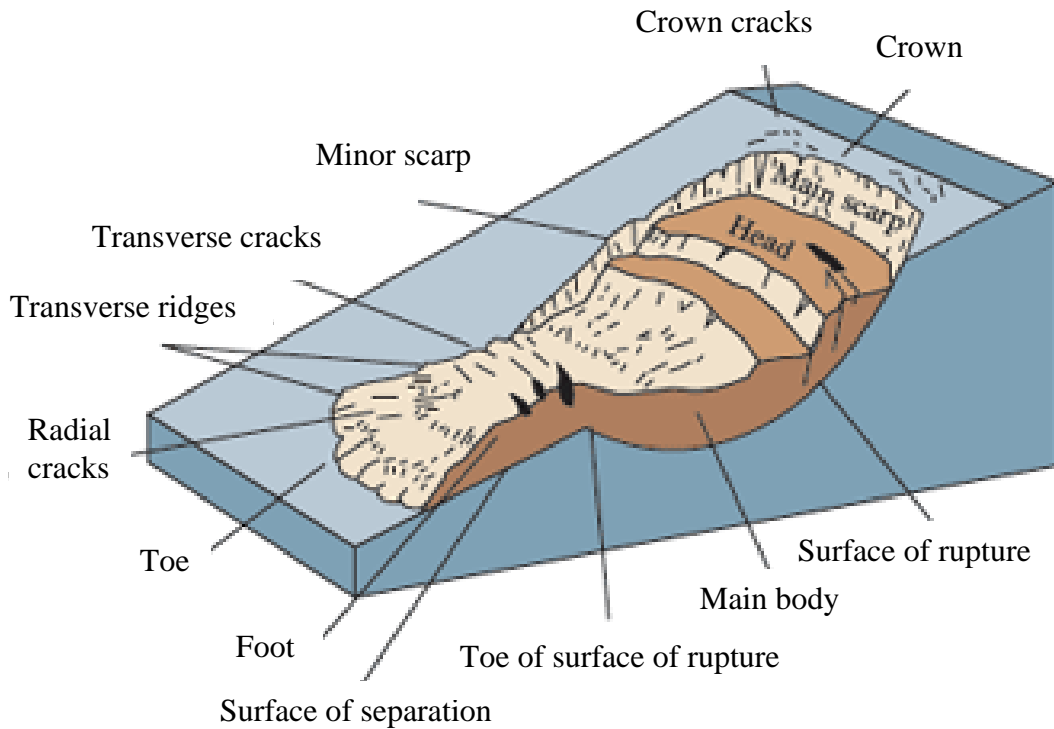


Figure 2.1 An idealized slump-earth flow showing commonly used nomenclature for labeling the parts of a landslide (modified from USGS Fact Sheet 2004-3072 in USGS, 2004).

Although landslides are primarily associated with mountainous regions, they can also occur in areas of generally low relief. In low-relief areas, landslides occur as cut-and-fill failures (roadway and building excavations), river bluff failures, lateral spreading landslides, collapse of mine-waste piles (especially coal), and a wide variety of slope failures associated with quarries and open-pit mines. The most common types of landslides are described as follows and are illustrated in Figure 2.2.

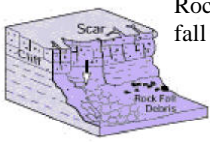
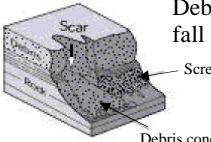
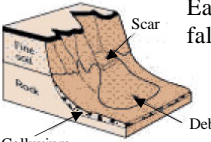
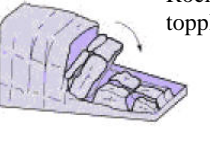
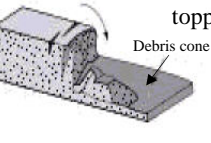
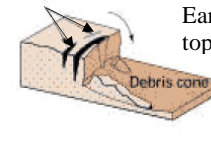
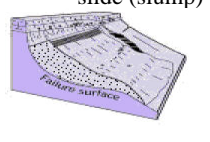
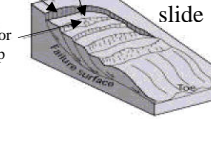
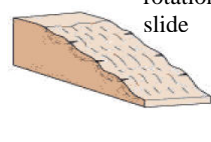
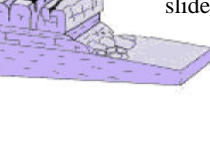
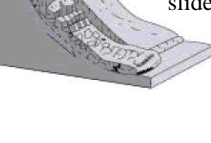
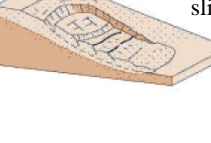
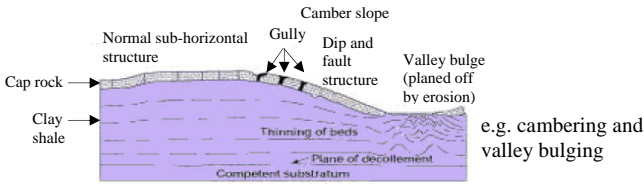
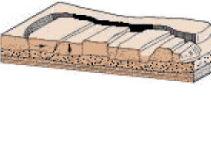
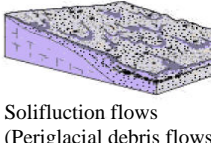
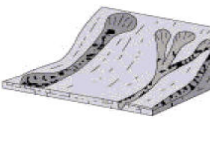
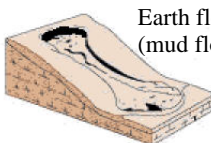
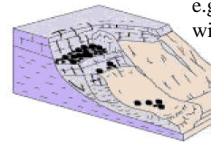
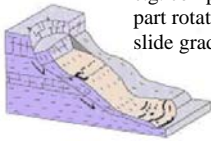
Type of movement	Type of material		
	ROCK	DEBRIS	EARTH
FALLS	 <p>Rock fall</p>	 <p>Debris fall</p>	 <p>Earth fall</p>
TOPPLES	 <p>Rock topple</p>	 <p>Debris topple</p>	 <p>Earth topple</p>
SLIDES	<p>Rotational</p>  <p>Single rotational slide (slump)</p>	 <p>Multiple rotational slide</p>	 <p>Successive rotational slide</p>
	<p>Translational (Planar)</p>  <p>Rock slide</p>	 <p>Debris slide</p>	 <p>Earth slide</p>
LATERAL SPREADS			 <p>Earth spread</p>
FLOWS	 <p>Solifluction flows (Periglacial debris flows)</p>	 <p>Debris flow</p>	 <p>Earth flow (mud flow)</p>
COMPLEX	 <p>e.g. slump-earthflow with rockfall debris</p>		 <p>e.g. composite, non-circular part rotational/part translational slide grading to earthflow at toe</p>

Figure 2.2 Major types of landslide movement (modified from Varnes, 1978 and DOE., 1990).

The landslide glossary for the UNESCO working party on world landslide inventory in 1993 has given these following definitions related to landslide phenomenon (Cruden, 1993).

Accumulation: The volume of the displaced material, which lies above the original ground surface.

Crown: The practically undisplaced material still in place and adjacent to the highest parts of the main scarp.

Depleted mass: The volume of the displaced material, which overlies the rupture surface but underlies the original ground surface.

Depletion: The volume bounded by the main scarp, the depleted mass and the original ground surface.

Displaced material: Material displaced from its original position on the slope by movement in the landslide. It forms both the depleted mass and the accumulation.

Flank: The undisplaced material adjacent to the sides of the rupture surface. Compass directions are preferable in describing the flanks but if left and right are used, they refer to the flanks as viewed from the crown.

Foot: The portion of the landslide that has moved beyond the toe of the surface of rupture and overlies the original ground surface.

Head: The upper parts of the landslide along the contact between the displaced material and the main scarp.

Main body: The part of the displaced material of the landslide that overlies the surface of rupture between the main scarp and the toe of the surface of rupture.

Main scarp: A steep surface on the undisturbed ground at the upper edge of the landslide, caused by movement of the displaced material away from the

undisturbed ground. It is the visible part of the surface of rupture.

Minor scarp: A steep surface on the displaced material of the landslide produced by differential movements within the displaced material.

Original ground surface: The surface of the slope that existed before the landslide took place.

Surface of rupture: The surface which forms (or which has formed) the lower boundary of the displaced material below the original ground surface.

Surface of separation: The part of the original ground surface overlain by the foot of the landslide.

Tip: The point of the toe farthest from the top of the landslide.

Toe: The lower, usually curved margin of the displaced material of a landslide, it is the most distant from the main scarp.

Toe of surface of rupture: The intersection (usually buried) between the lower part of the surface of rupture of a landslide and the original ground surface.

Top: The highest point of contact between the displaced material and the main scarp.

Zone of depletion: The area of the landslide within which the displaced material lies below the original ground surface.

Zone of accumulation: The area of the landslide within which the displaced material lies above the original ground surface.

The most common types of landslide are fall, topple, rotational slide, translational slide, lateral spread, flow and complex landslide as seen in Figure 2.2. Their brief information is as follows.

Falls: Falls are abrupt movements of masses of geologic materials, such as rocks and boulders, that become detached from steep slopes or cliffs. Separation occurs along discontinuities such as fractures, joints, and bedding planes, and movement occurs by free-fall, bouncing, and rolling. Falls are strongly influenced by gravity, mechanical weathering, and the presence of interstitial water.

Topples: Toppling failures are distinguished by the forward rotation of a unit or units about some pivotal point, below or low in the unit, under the actions of gravity and forces exerted by adjacent units or by fluids in cracks.

Slides: Although many types of mass movements are included in the general term "landslide," the more restrictive use of the term refers only to mass movements, where there is a distinct zone of weakness that separates the slide material from more stable underlying material. The two major types of slides are rotational slides and translational slides.

1) Rotational slide: This is a slide in which the surface of rupture is curved concavely upward and the slide movement is roughly rotational about an axis that is parallel to the ground surface and transverse across the slide.

2) Translational slide: In this type of slide, the landslide mass moves along a roughly planar surface with little rotation or backward tilting. A block slide is a translational slide in which the moving mass consists of a single unit or a few closely related units that move downslope as a relatively coherent mass.

Lateral Spreads: Lateral spreads are distinctive because they usually occur on very gentle slopes or flat terrain. The dominant mode of movement is lateral extension accompanied by shear or tensile fractures. The failure is caused by liquefaction, the

process whereby saturated, loose, cohesionless sediments (usually sands and silts) are transformed from a solid into a liquefied state. Failure is usually triggered by rapid ground motion, such as that experienced during an earthquake, but can also be artificially induced. When coherent material, either bedrock or soil, rests on materials that liquefy, the upper units may undergo fracturing and extension and may then subside, translate, rotate, disintegrate, or liquefy and flow. Lateral spreading in fine-grained materials on shallow slopes is usually progressive. The failure starts suddenly in a small area and spreads rapidly. Often the initial failure is a slump, but in some materials movement occurs for no apparent reason. Combination of two or more of the above types is known as a complex landslide.

Flows: There are five basic categories of flows that differ from one another in fundamental ways.

1) Debris flow: A debris flow is a form of rapid mass movement in which a combination of loose soil, rock, organic matter, air, and water mobilize as a slurry that flows downslope. Debris flows include <50% fines. Debris flows are commonly caused by intense surface-water flow, due to heavy precipitation or rapid snowmelt, that erodes and mobilizes loose soil or rock on steep slopes. Debris flows also commonly mobilize from other types of landslides that occur on steep slopes, are nearly saturated, and consist of a large proportion of silt- and sand-sized material. Debris-flow source areas are often associated with steep gullies, and debris-flow deposits are usually indicated by the presence of debris fans at the mouths of gullies. Fires that denude slopes of vegetation intensify the susceptibility of slopes to debris flows.

2) Debris avalanche: This is a variety of very rapid to extremely rapid debris flow.

3) Earth flow: Earth flows have a characteristic "hourglass" shape. The slope material liquefies and runs out, forming a bowl or depression at the head. The flow itself is elongate and usually occurs in fine-grained materials or clay-bearing rocks on moderate slopes and under saturated conditions. However, dry flows of granular material are also possible.

4) Mudflow: A mudflow is an earth flow consisting of material that is wet enough to flow rapidly and that contains at least 50 percent sand, silt, and clay-sized particles. In some instances, for example in many newspaper reports, mudflows and debris flows are commonly referred to as "mudslides."

5) Creep: Creep is the imperceptibly slow, steady, downward movement of slope-forming soil or rock. Movement is caused by shear stress sufficient to produce permanent deformation, but too small to produce shear failure. There are generally three types of creep: (1) seasonal, where movement is within the depth of soil affected by seasonal changes in soil moisture and soil temperature; (2) continuous, where shear stress continuously exceeds the strength of the material; and (3) progressive, where slopes are reaching the point of failure as other types of mass movements. Creep is indicated by curved tree trunks, bent fences or retaining walls, tilted poles or fences, and small soil ripples or ridges.

Complex Landslides: In general, complex landslides are involving the combination of two or more types of movement. Commonly one type of movement starts the materials moving, such as debris slide, and once underway the materials take on the character of another type of movement such as a debris flow. For example, the

combination of the type of movement between debris slide and debris flow called as a debris slide-debris flow. The rate of movement depends on the types of movements in addition, material.

2.2.3 Causes of Landslides

The causes of landslides are usually related to instabilities in slopes. It is usually possible to identify one or more landslide causes and one landslide trigger. The difference between these two concepts is subtle but important. The landslide causes are the reasons that a landslide occurred in that location and at that time. Landslide causes are listed in the following Table 2.1, and include geological factors, morphological factors, physical factors and factors associated with human activity. Landslide causes are as following: (USGS, 2004)

•Geological Causes

- 1) Weak or sensitive materials
- 2) Weathered materials
- 3) Sheared, jointed, or fissured materials
- 4) Adversely oriented discontinuity (bedding, schistosity, fault, unconformity, contact, and so forth)
- 5) Contrast in permeability and/or stiffness of materials

•Morphological Causes

- 1) Tectonic or volcanic uplift
- 2) Glacial rebound
- 3) Fluvial, wave, or glacial erosion of slope toe or lateral margins
- 4) Subterranean erosion (solution, piping)

- 5) Deposition loading slope or its crest
- 6) Vegetation removal (by fire, drought)
- 7) Thawing
- 8) Freeze-and-thaw weathering
- 9) Shrink-and-swell weathering

•Human Causes

- 1) Excavation of slope or its toe
- 2) Loading of slope or its crest
- 3) Drawdown (of reservoirs)
- 4) Deforestation
- 5) Irrigation
- 6) Mining
- 7) Artificial vibration
- 8) Water leakage from utilities

2.2.4 Multiple Causes of Landslides

Causes may be considered to be factors that made the slope vulnerable to failure, that predispose the slope to becoming unstable. The trigger is the single event that finally initiated the landslide. Thus, causes combine to make a slope vulnerable to failure, and the trigger finally initiates the movement. Landslides can have many causes but can only have one trigger. Usually, it is relatively easy to determine the trigger after the landslide has occurred (although it is generally very difficult to determine the exact nature of landslide triggers ahead of a movement event).

The three multiple types of landslides that the most important causes of the damaging landslides around the world. Landslide multiple causes are following: (USGS, 2004)

2.2.4.1 Landslides and Water

Slope saturation by water is a primary cause of landslides. This effect can occur in the form of intense rainfall, snowmelt, changes in ground-water levels, and water-level changes along coastlines, earth dams, and the banks of lakes, reservoirs, canals, and rivers.

Landslide and flood are closely allied because both are related to precipitation, runoff, and the saturation of ground by water. In addition, debris flows and mudflows usually occur in small, steep stream channels and often are mistaken for floods; in fact, these two events often occur simultaneously in the same area.

Landslides can cause flooding by forming landslide dams that block valleys and stream channels, allowing large amounts of water to back up. This causes backwater flooding and, if the dam fails, subsequent downstream flooding. Also, solid landslide debris can "bulk" or add volume and density to otherwise normal streamflow or cause channel blockages and diversions creating flood conditions or localized erosion. Landslides can also cause overtopping of reservoirs and/or reduced capacity of reservoirs to store water.

Table 2.2 Schematic overview of landslide damage types, related to different types of landslides, elements at risk and the location of the elements at risk in relation to the landslide (modified from Van Westen et al., 2006).

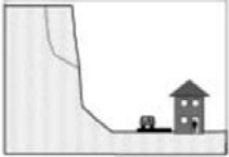
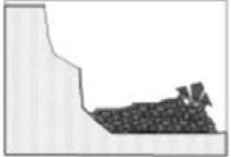
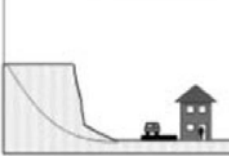
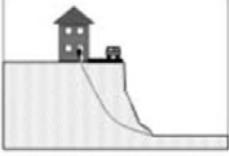
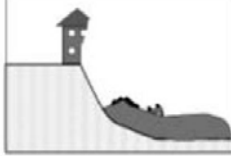
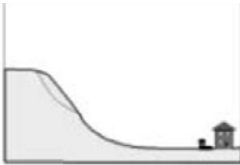
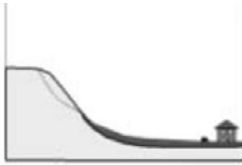
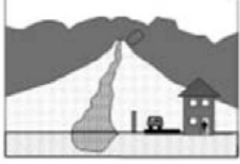
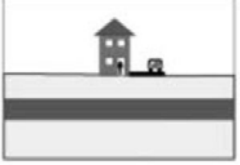
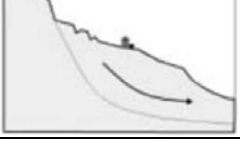
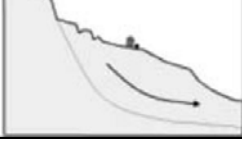
Type	Before	After	Likely damage to elements at risk	Factors determining risk
Impact by large rockmass			<p>Buildings: Total collapse likely Persons in buildings: Loss of life/major injury likely Infrastructure: Coverage and obstruction/destruction of surface Persons in traffic: Loss of life major injury possible</p>	<ul style="list-style-type: none"> • Volume of rockfall mass • Location of source zone • Distance to elements at risk • Triggering factors • Local topography along track • Intermediate obstacles • Precursory events
Impact by single blocks			<p>Buildings: Total collapse not likely. Localized damage Persons in buildings: Minor to major injury likely Infrastructure: Coverage and obstruction of traffic Persons in traffic: Loss of life major injury possible</p>	<ul style="list-style-type: none"> • Volume of rockfall blocks • Number of rockfall blocks • Location of source zone • Distance to elements at risk • Triggering factors • Local topography along track • Intermediate obstacles
Impact by landslides mass			<p>Buildings: Collapse/major damage depending on volume Persons in buildings: None persons are normally able to escape Infrastructure: Coverage and obstruction of traffic Persons in traffic: None persons are normally able to escape</p>	<ul style="list-style-type: none"> • Volume of landslide mass • Water content • Landslide material type • Triggering factors • Distance to elements at risk • Local topography along track • Speed of landslide movement
Loss of support due to undercutting			<p>Buildings: Collapse/major damage likely Persons in buildings: None persons are normally able to escape Infrastructure: Complete destruction of road surface Persons in traffic: None persons are normally able to escape</p>	<ul style="list-style-type: none"> • Volume of landslide mass • Water content • Landslide material type • Triggering factors • Retrogressive landslide • Cliff erosion • Speed of landslide movement
Differential settlement/tilting due to slow movement			<p>Buildings: Tilted buildings with cracks. Normally no collapse Persons in buildings: None, slow movement. People not in danger Infrastructure: Tilting and cracks, traffic slowed down Persons in traffic: None, slow movement</p>	<ul style="list-style-type: none"> • Volume of landslide mass • Water content • Landslide material type • Triggering factors • Speed of landslide movement • Amount of displacement

Table 2.2 Schematic overview of landslide damage types, related to different types of landslides, elements at risk and the location of the elements at risk in relation to the landslide (modified from Van Westen et al., 2006) (Continued).

Type	Before	After	Likely damage to elements at risk	Factors determining risk
Impact by debris flow on slope			<p>Buildings: Filled by mud, damage to contents Persons in buildings: Minor - major injuries. Depends on speed Infrastructure: Coverage of road surface. Obstruction of traffic Persons in traffic: Minor - major injuries. Depends on speed</p>	<ul style="list-style-type: none"> • Volume of landslide mass • Water content • Slope steepness • Local topography • Landslide material type • Triggering factors • Speed of movement • Size of blocks transported
Flooding by debris flow on alluvial fan			<p>Buildings: Filled by mud, damage to contents Persons in buildings: None persons are normally able to escape Infrastructure: Coverage Persons in traffic: None persons are normally able to escape</p>	<ul style="list-style-type: none"> • Volume of debris flow • Water & sediment content • Local topography of fan • Triggering factors • Distance from source • Distance from lahar channel • Speed
Impact by Sturzstrom			<p>Buildings: Total collapse Persons in buildings: Loss of life Infrastructure: Total destruction Persons in traffic: Loss of life</p>	<ul style="list-style-type: none"> • Volume of rockfall mass • Location of source zone • Distance to elements at risk • Triggering factors • Local topography along track • Distance from source zone • Precursory events
Liquefaction			<p>Buildings: Differential settlement, cracks Persons in buildings: Minor injuries or no-injuries Infrastructure: Differential settlement, cracks Persons in traffic: No-injuries</p>	<ul style="list-style-type: none"> • Soil types • Soil strength • Grainsize distribution • Foundation types • Earthquake intensity • Water table
Deep seated creep movement			<p>Buildings: Differential settlement, tilting, cracks Persons in buildings: Minor injuries or no-injuries Infrastructure: Differential settlement, cracks, broken pipes Persons in traffic: No-injuries</p>	<ul style="list-style-type: none"> • Speed of movement • Local geological situation • Age of landslide • Seasonality of movement

2.2.4.2 Landslides and Seismic Activity

Many mountainous areas that are vulnerable to landslides have also experienced at least moderate rates of earthquake occurrence in recorded times. The occurrence of earthquakes in steep landslide-prone areas greatly increases the likelihood that landslides will occur, due to ground shaking alone or shaking-caused dilation of soil materials, which allows rapid infiltration of water. Widespread rockfalls also are caused by loosening of rocks as a result of ground shaking.

2.2.4.3 Landslides and Volcanic Activity

Landslides due to volcanic activity are some of the most devastating types. Volcanic lava may melt snow at a rapid rate, causing a deluge of rock, soil, ash, and water that accelerates rapidly on the steep slopes of volcanoes, devastating anything in its path. These volcanic debris flows (also known as lahars) reach great distances, once they leave the flanks of the volcano, and can damage structures in flat areas surrounding the volcanoes.

2.3 Use of Remote Sensing in Landslide Hazard Assessment

The phenomenon, landslide is affecting the earth's surface, hence it also falls in to the research and application areas of both aerial and space born remote sensing. The nature of this phenomenon as it is occurring at the surface of earth lets earth scientists to exploit this fact using remotely sensed data. On the other hand, again the nature of this phenomenon limits the applications, as being dynamic and sometimes being quite small in terms of conservative remote sensing language. Furthermore they reveal very small information when they are observed in planar 2-D, however, they contain large amounts of data when explored in 3-D. Basing on this fact the use of

stereo-remote sensing products seems to be indispensable, which reveals the true morphodynamical features of the landslides. These information are providing the diagnostic information regarding the type of the movement (Crozier, 1973). The general application fields of remote sensing in landslide business are monitoring the change of landslide activities through time (change detection) and mapping out where the hazard occurs.

The landslide information extracted from the remotely sensed products is mainly related with the morphology, vegetation and the hydrological conditions of the slope. The slope morphology is best examined with stereographical coverages.

2.4 Remote Sensing in Landslides Spatial Analysis and Hazard

Prediction

Previous works (Soeters and Van Westen, 1996; Van Westen et al., 1997) have grouped methods for landslide hazard assessment into inventory, heuristic, statistical and deterministic approaches. A landslide inventory map based on aerial photo-interpretation, satellite images, ground survey and database of historical occurrence of landslide in an area as done by He et al. (2003) is the most straightforward approach (Mantovani et al., 1996). The output provides the spatial distribution of mass movements, represented as polygons or points (Wieczorek, 1984). Such maps can be used as an elementary form of hazard map because they show the spatial location of recorded landslides, though they fail to identify areas that may be susceptible to landsliding unless landslides have already occurred (Dai et al., 2002). Furthermore, Mantovani et al. (1996) mention this approach provide information for the period shortly preceding the date of remote data collection or field

checking, without an insight into the temporal changes in mass movement distribution. Therefore, a refinement is the construction of landslide activity maps, based on multi-temporal aerial photo or satellite interpretation as done by Nagarajan et al. (1998), Zhou et al. (2002), Van Westen and Getahun (2003), Cheng et al. (2004).

2.5 Geographical Information Systems (GIS) and Landslide Hazard Assessment

GIS is defined as a “powerful set of tools for collecting, storing, retrieving at will, transforming, and displaying spatial data from the real world for particular set of purposes” (Burrough, 1986). A more specific definition is given by Bonham-Carter (1996) as follows: “a geographic information system, or simply GIS, is a computer system for managing spatial data. The word geographic implies that the locations of the data items are known, or can be calculated, in terms of geographical coordinates. The word information implies that the data in GIS are organized to yield useful knowledge, often as colored maps and images, but as also statistical graphics, tables and various on-screen responses to interactive queries. The word system implies that a GIS is made up from several interrelated and linked components with different functions. Thus, GIS has functional capabilities for data capture, input, manipulation, transformation, visualization, combination, query, analysis, modeling and output.”

These international valid definitions of GIS directly oppose to the belief that GIS is only a CAD software or only a drawing tool. CAD can only constitute a small portion of the whole integrated system, in which an ideal GIS and its possible components are shown in Figure 2.3.

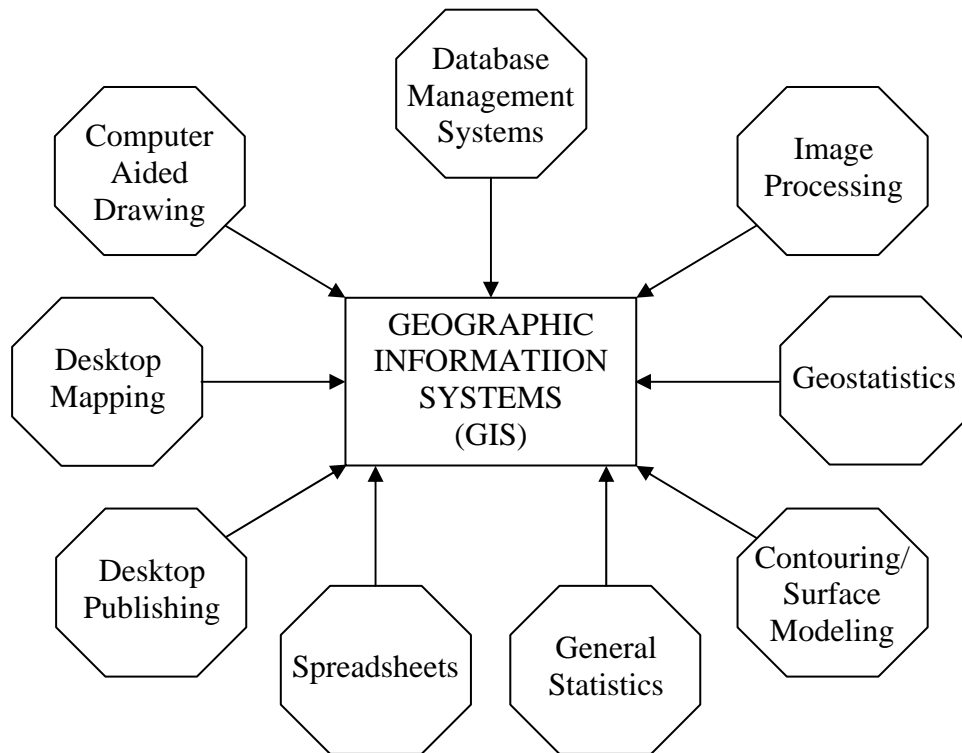


Figure 2.3 GIS and its related software systems as components of GIS (modified from Sgzen, 2002).

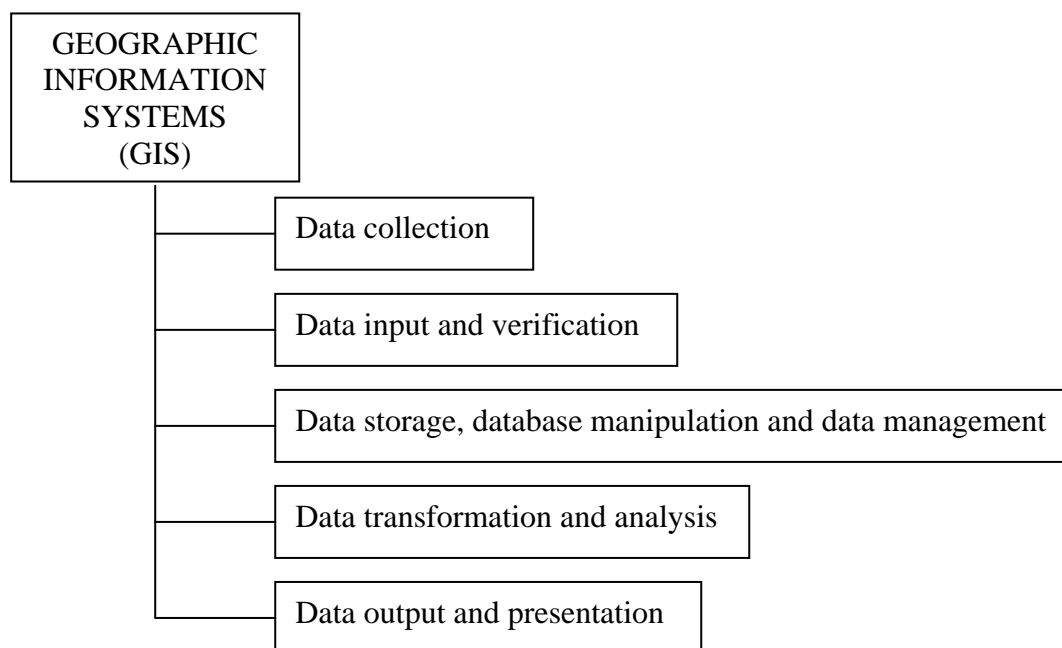


Figure 2.4 The phases of a GIS (modified from Sgzen, 2002).

Generally a GIS consists of the five phases namely; data collection; data input and verification; data storage, database manipulation and data management; data transformation and analysis; and data output and presentation (Figure 2.4). A GIS if based over the former components should answer the following questions; location, condition, trends, patterns, and modeling (Figure 2.5).

More and more the products of mapping and inventory are being stored in data banks for their ultimate retrieval or combination with data from other sources. Often they are incorporated in GIS or LIS (Land Information Systems) which serve as a base for programmable data manipulation and selective information extraction for planning and project assessment.

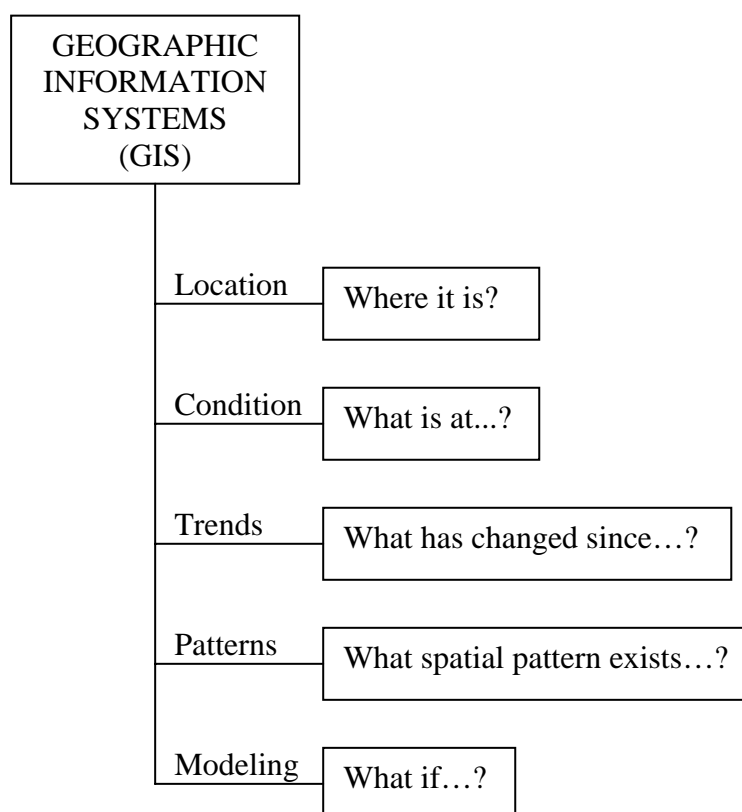


Figure 2.5 The questions of a well-built GIS should answer (modified from Sgzen, 2002).

The development of GIS and LIS systems is of considerable interest in the context of satellite surveying, change detection and monitoring. The flexibility of digital data processing, combined with quick input of new data (possible from updating on the basis of satellite remote sensing records) offers new possibilities to the surveyor, cartographer and planner.

It is clear that in a rapidly developing society, change detection is of great importance. In modern society, mapping suffers from high rate of change: change in land use in rural and urban areas; change in requirements for maps and inventories; change in concepts in the various disciplines of earth and social sciences, leading to different interpretations of the same data and change in the economical and technical factors on which mapping methods were based.

In order to refine the discussion around landslide hazard one can say that, the occurrence of slope failure depends generally on complex interactions among a large number of partially interrelated factors. Analysis of landslide hazard requires evaluation of the relationships between various terrain conditions and landslide occurrences. An experienced earth scientist has the capability to mentally assess the overall slope conditions and to extract the critical parameters. However, an objective procedure is often desired to quantitatively support the slope instability assessment. This procedure requires the evaluation of the spatially varying terrain conditions as well as the spatial representation of landslides. A GIS allows for the storage and manipulation of information concerning the different terrain factors as distinct data layers and thus provides an excellent tool for slope stability hazard zonation.

The advantages of GIS for assessing landslide hazard include the followings:

1) A much larger variety of hazard analysis techniques become attainable. Because of the speed of calculation, complex techniques requiring a large number of map overlays and table calculations become feasible.

2) It is possible to improve models by evaluating their results and adjusting the input variables. Users can achieve maximum results by a process of trial and error, running the models several times, whereas it is difficult to use these models even once in the conventional manner. Therefore, more accurate results can be expected.

The disadvantages of GIS for assessing landslide hazard include the followings:

1) A large amount of time is needed for data entry. Digitizing is especially time consuming

2) There is a danger in placing too much emphasis on data analysis as much as the expense of data collection and manipulation based on professional experience. A number of different techniques of analysis are theoretically possible, but often the necessary data are missing. In other words, the tools are available but cannot be used because of the lack or uncertainty of the data.

2.6 GIS and Landslide Analysis

Geographic information system (GIS), as a computer-based system for data capture, input, manipulation, transformation, visualization, combination, query, analysis, modeling and output, with its excellent spatial data processing capacity, has attracted great attention in natural disaster assessment (Carrara et al., 1999).

Landslides are one of the complex analyses, involving multitude of factors and need to be studied systematically in order to evaluate the hazard. The increasing

computer-based tools are found to be useful in the hazard mapping of landslides. One of such significant tools for hazard mapping of landslides is geographic information systems (GIS). A GIS is defined as a powerful set of tools for collecting, storing, retrieving at will, displaying, and transforming spatial data (Burrough and McDonnel, 1998). One of the main advantages of the use of this technology is the possibility of improving hazard occurrence models, by evaluating their results and adjusting the input variables. An important aspect of landslide investigations is the possibilities to store, treat, and analyze spatio-temporal data that are available.

As the typical landslide analysis demands, collection of numerous data, storage of them and using them in the analysis could be handled well in the GIS environment. Any spatially-distributed data with a geo-reference to real world could be stored as points, lines and polygons (vector model) or as continuous fields (raster data model). Beyond GIS being used as a spatial database, it assists in modeling applications through handling a special form of data that would otherwise be compromised in conventional analysis (Miles and Ho, 1999). Also, GIS does not only serve as a database for parameter data, rather qualitative and quantitative data can be integrated through spatial relationships rather than through relationships between attributes that may not exist (Frost et al., 1997).

2.7 GIS Based Landslide Hazard Zoning Techniques

Recently, the geographical information system (GIS) has become an important tool for landslide susceptibility mapping because it provides the various functions of handling, processing, analyzing, and reporting geospatial data. An ideal map of slope instability hazard should provide information on the spatial probability, temporal

probability, type, magnitude, velocity, run out distance and retrogression limit of the mass movements predicted in a certain area (Hartlen and Viberg, 1988). A reliable landslide inventory defining the type and activity of all landslides, as well as their spatial distribution, is essential before any analysis of the occurrence of landslides and their relationship to environmental conditions are undertaken. Even the inventory of historical periods are of great use in the final analyses. The differentiation of slope instability according to type of movement is important, not only because different types of mass movement will occur under different terrain conditions, but also because the impact of slope failures on the environment has to be evaluated according to type of failure.

2.8 Landslide Susceptibility Approaches

Overviews and classification of GIS-based landslide hazard assessment methods can be found in Soeters and Van Westen (1996), Carrara et al. (1995, 1999), Guzzetti et al. (1999), Aleotti and Chowdury (1999) and Van Westen (2000). There is a general consensus that a classification may involve four different approaches:

- Landslide inventory-based probabilistic approach
- Heuristic approach (qualitative maps of direct-geomorphological mapping or indirect-combination)
- Statistical approach (bivariate or multivariate statistics)
- Deterministic approach (Soeters and Van Westen, 1996)

The number of publications on landslide susceptibility assessment is still rather modest, but recently some good overview publications on landslide susceptibility methods have been published (e.g., Cruden and Fell, 1997; Guzzetti,

2000; Dai et al., 2002) including a recent textbook by Lee and Jones (2004). The classification of the published landslide susceptibility assessment methods is still not very detailed but that proposed by the Sub-committee on Landslide Risk Management of the Australian Geomechanics Society has been generally adopted. This classification is based on the level of quantification dividing the landslide susceptibility assessment methods into:

- Qualitative methods (probability and losses expressed in qualitative terms)
- Semi-quantitative methods (indicative probability, qualitative terms), and
- Quantitative methods (probability and losses quantified)

The review of literature related to landslide susceptibility assessment methods indicates that a lot of developments have taken place by several authors in the last couple of decades. Some important literatures pertaining to the advancement of the assessment methods in recent years are the focus of this review.

Qualitative or semi-quantitative methods depend on expert opinions. The most common types of qualitative methods simply use landside inventories to identify sites of similar geological and geomorphological properties that are susceptible to failure. Some qualitative approaches, however, incorporate the idea of ranking and weighting, and may evolve to be semi-quantitative in nature. Qualitative or semi-quantitative methods are often useful for regional studies (Soeters and Van Westen, 1996; Guzzetti et al., 1999). The application of the analytical hierarchy process (AHP) method, developed by Saaty (1980), for landslide susceptibility has been used by Barredo et al. (2000), Mwasi (2001), Nie et al. (2001), Yagi (2003), Ayalew et al. (2005), Komac (2006) and Yalcin (2008).

Quantitative methods are based on numerical expressions of the relationship between controlling factors and landslides. There are two types of quantitative methods: deterministic and statistical (Aleotti and Chowdhury, 1999). Deterministic quantitative methods depend on engineering principles of slope instability expressed in terms of the factor of safety. Due to the need for exhaustive data from individual slopes, these methods are often effective for mapping only small areas. Landslide susceptibility mapping using either multivariate or bivariate statistical approaches analyzes the historical link between landslide-controlling factors and the distribution of landslides (Guzzetti et al., 1999). More sophisticated assessments involved bivariate, multivariate, logistics regression, fuzzy logic, artificial neural network, etc. analysis.

A variety of multivariate statistical approaches (MSA) exist, but those commonly used to map landslide susceptibility include discriminant analyses and logistic regression. Stepwise discriminant analyses have been used by Carrara et al. (1991, 1995, 2003, 2008) to classify stable and unstable slope-units in Italy. The method was also reported to be significant to define landslide susceptibility classes in the Spanish Eastern Pyrenees (Baeza and Corominas, 2001).

Recently, there have been studies on landslide hazard evaluation using quantitative methods, and many of these studies have applied logistic regression, for examples, Lee and Min (2001), Dai et al. (2001), Dai and Lee (2002, 2003), Ohlmacher and Davis (2003) and Ayalew and Yamagishi (2004), Ayalew and Yamagishi (2005), Ayalew et al. (2005), Yesilnacar and Topal (2005), Lee (2005), Lee and Sambath (2006), Lee and Pradhan (2006a, 2007), Lee (2007b) Akgun and Bulut (2007) and Oh et al. (2008).

Fuzzy logic has also been applied to landslide susceptibility mapping by Chung and Fabbri (2001), Ercanoglu and Gokceoglu (2002, 2004), Kanungo et al. (2006) and Lee (2007a).

Artificial neural network (ANN) has been applied for susceptibility mapping by various researchers including Lee et al. (2003a, b, 2004b), Ermini et al. (2005), Go´mez and Kavzoglu (2005), Yesilnacar and Topal (2005) and Kanungo et al. (2006).

In the last decade, many studies have used frequency ratio (FR) model with reasonably satisfied results by Jibson et al. (2000), Luzi et al. (2000), Lee and Min (2001), Clerici et al. (2002), Donati and Turrini (2002), Lee et al. (2002, 2004a), Lee and Choi (2003), Zezere et al. (2004), Lee and Talib (2005), Lee and Dan (2005), Lee and Sambath (2006), Lee and Lee (2006), Lee and Pradhan (2006a, b, 2007), Akgun et al. (2007), Vijith and Madhu (2008) and Oh et al. (2008).

Hybrid methods are combined between qualitative and quantitative methods. As mentioned earlier, qualitative methods depend on expert opinions, and are often useful for regional assessments (Soeters and Van Westen, 1996; Aleotti and Chowdhury, 1999). Quantitative methods rely on observed relationships between controlling factors and landslides (Guzzetti et al., 1999). As a new approach to landslide susceptibility evaluation using GIS, there are many studies have used these methods applied for landslide susceptibility mapping can be found in Ayalew et al. (2004), Kanungo et al. (2006), Akgun and Bulut (2007) and Akgun et al. (2007).

The lack of standardization in analytical methods is also another issue that could be linked with the accountability of landslide susceptibility or hazard maps. As known, there are several qualitative and quantitative methods in literature. Some are

simple, especially those which rely on subjective assessments. Others, however, depend on complex mathematical concepts and are difficult to understand easily. Good reviews of those methods developed in the last few decades and evaluations of the subsequent approaches are given in Mantovani et al. (1996), Soeters and Van Westen (1996), Aleotti and Chowdhury (1999) and Guzzetti et al. (1999). But some old approaches have long disappeared, some underwent a sort of refinement, and new methods are always coming. Figure 2.6 shows a schematic illustration of the methods used frequently at present. Many of these methods are not yet available in known commercial GIS packages either as built-in functions or additional modules. So, data is usually transformed to external software products for core analyses. Despite the claims otherwise, many landslide susceptibility mapping efforts share only the data storage and visualization services of GIS and some functional tools including map crossing procedures. The fate of the final susceptibility map is often decided by the theoretical bases and assumptions that build the method in use (Carrara et al., 1999), and the core analyses in the external software.

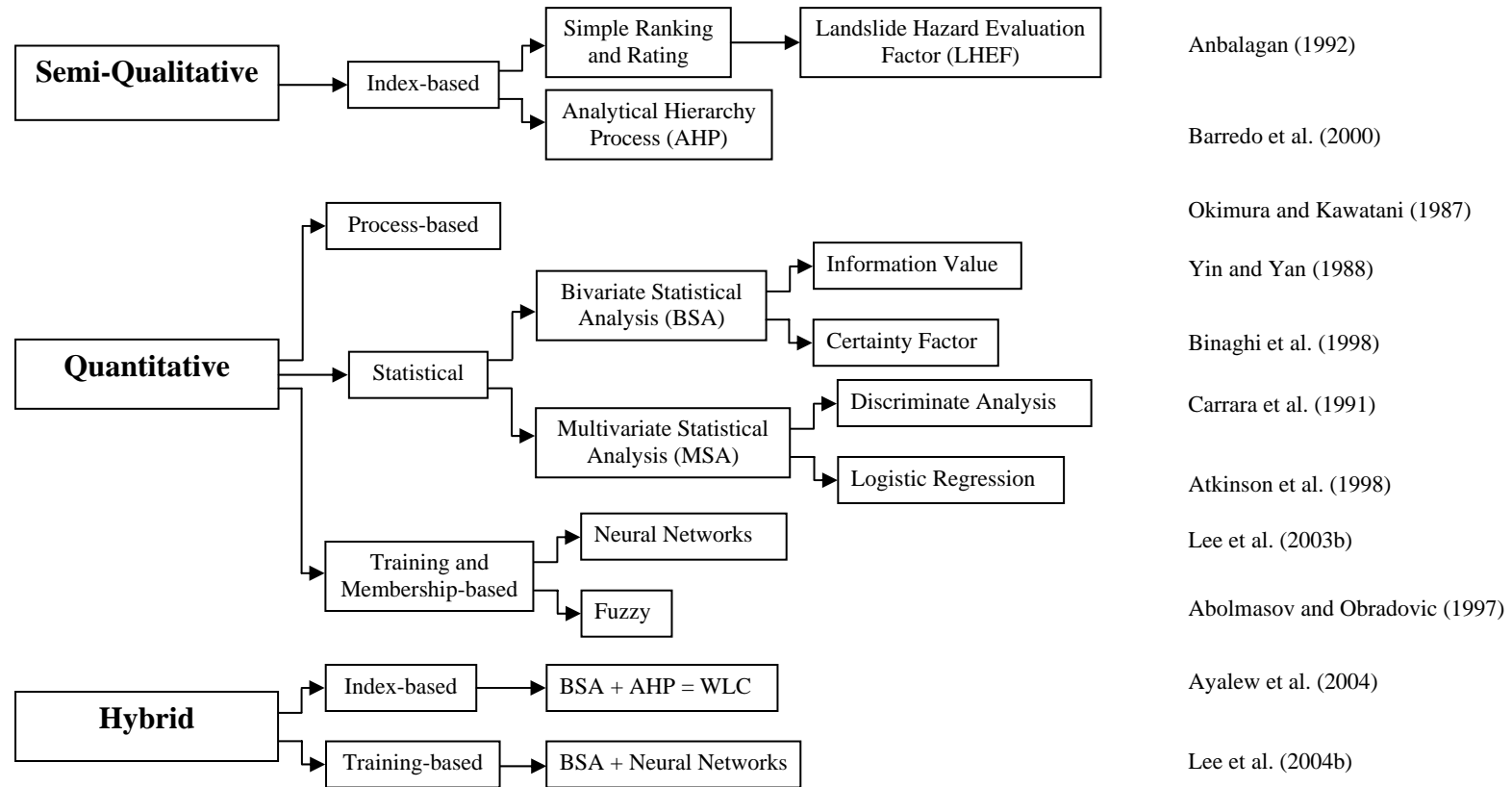


Figure 2.6 A schematic illustration of landslide susceptibility mapping methods used commonly at present (modified from Ayalew et al., 2005).

If the methods described for landslide susceptibility assessment are combined with the methods reported for calculating the hazard component, the value of a number of combinations is more obvious. Table 2.3 gives an indication of the usefulness of particular hazard approaches for the three types of landslide susceptibility assessment methods, given that they are carried out over relatively large areas at medium scales (1:10,000–1:50,000) using GIS-based methods for susceptibility zonation. The following sections give an inventory of recent developments in each of the four above-mentioned hazard approaches (Table 2.3).

Table 2.3 Usefulness of specific combinations of hazard approaches and susceptibility approaches for GIS-based landslide susceptibility zonation at medium scales.

Hazard approaches	Susceptibility approaches		
	Qualitative	Semi-quantitative	Quantitative
Inventory-based probabilistic approach	2	2	2
Heuristic/geomorphological/direct mapping/expert-based approach	3	3	0
Statistical approach (bivariate or multivariate)	3	2	2
Deterministic and dynamic modelling approach	0	1	3

The numbers in Table 2.3 have the following explanation:

- 0: The hazard method is not appropriate for the susceptibility method.
- 1: Moderately useful combination. The hazard method is less appropriate for the susceptibility method.
- 2: Highly useful combination. The hazard method could be the best method for susceptibility assessment, but this depends on the availability of data (e.g., historical landslide records).

•3: Most useful combination, which will result in the best susceptibility assessment given the available input data.

For quantitative susceptibility assessment, landslide inventory based probabilistic methods are generally the best methods, assuming that the occurrence of landslide events in the past is a good indication of the likelihood of the phenomena occurring in the future. However, the method requires fairly complete historical landslide records and may be less useful for the susceptibility assessment in areas that have had large environmental changes in the past or where, as a consequence of climate change, the landslide frequency is expected to change significantly.

Generally speaking, the best option for quantitative landslide susceptibility assessment is the application of deterministic slope stability models, combined with dynamic models for hillslope hydrology. These may provide scenarios of potential instability under varying environmental and climatic conditions (Van Beek, 2002), but are very data demanding over larger areas and require a substantial degree of simplification of the landslide types and depths.

Statistical hazard methods are good for assessing the spatial probability but there are problems in evaluating either temporal probability or the effects of future environmental changes. They are mostly used in qualitative susceptibility assessment but if combined with landslide inventory maps for different triggering events, might be the best method for quantitative susceptibility assessment over larger areas.

Heuristic approaches are suitable for qualitative and semi-quantitative susceptibility assessment and can provide reliable maps over larger areas with limited costs, provided they are carried out by (teams of) experts.

2.9 Landslide Hazard or Susceptibility Mapping

The practicality of landslide hazard or susceptibility maps is profoundly affected by conceptual differences. The term hazard is defined by Varnes (1984) as the probability of occurrence of a potentially damaging phenomenon within a specified period of time and area.

The concept of hazard zonation (e.g., maps that show the spatial distribution of hazard classes) is central to the phase of spatial analysis and hazard prediction of landslide occurrence. According to Varnes (1984), zonation refers to the division of the land in homogeneous areas and their ranking according to degree of actual or potential hazard caused by mass movements. Consequently, it requires knowledge of the factors determining the probability of landslide for a particular slope or area, which according to Dai et al. (2002) can be grouped into two categories: (1) preparatory variables which make the slope susceptible to failure without triggering it, such as geology, slope gradient and aspect, elevation, soil geotechnical properties, vegetation cover and long term drainage patterns and weathering; and (2) the triggering variables such as heavy rainfall, glacier outburst.

As mentioned in section (2), the mapping requirements for input data for landslide hazard is scale dependant, with generally three scales of spatial analysis being defined (Mantovani et al., 1996): a regional scale (<100,000), a medium scale (1:50,000–1:25,000) and a large scale (>1:10,000). Dai et al. (2002) mention that when assessing the probability of landsliding on regional scales, it might be feasible considering landslide susceptibility (e.g., omitting the inclusion of triggering factors in the spatial analysis) as the probability of landsliding. This is based on the assumption that long-term historical landslide records tend to smooth out the spatio-

temporal effect of triggering factors on landslide occurrence. For large scale hazard assessments, in which work is undertaken over relatively small areas or specific slopes, data collection at this scale should relate to the quantitative parameters needed for slope stability modelling (Dai et al., 2002).

In addition, landslide hazard mapping was defined by Guzzetti et al. (1999) as the quantitative prediction of the spatial distribution of both landslide deposits and slopes which are likely to be sites of failures, whose movement or reactivations will take place in a way and within a time period defined from information that is not directly incorporated in the analysis. Generally, the purpose of landslide hazard or susceptibility mapping is to highlight the regional distribution of potentially unstable slopes based on a detailed study of the factors responsible for landsliding. The resulting maps are useful to establish standards and requirements for the use of land on and around slopes that are likely to fail, to assess the susceptibility that a proposed use of land will affect the stability of an area, and to develop and review mitigation options.

These maps are amended upon the receipt of corrected, updated and refined data or during the revision of studies on which they were initially based. Since hazard analysis or susceptibility mapping involves the handling and interpreting of a large amount of data, the use of GIS is proved to be very important.

2.10 Trends in Landslide Hazard Zonation

A large amount of research on hazard zonation has been done in last 30 years, as the consequence of an urgent demand for slope instability hazard mapping. Overviews of the various slope instability hazard zonation techniques can be found in

Hansen (1984), Varnes (1984), Hartlen and Viberg (1988). The general trends in landslide hazard zonation are given in Table 2.4. The distribution analyses and qualitative analyses are generally used for very large areas with very low detail such as national hazard maps. The deterministic and frequency analyses are used generally for very small areas such as specific large engineering projects like dams, nuclear power plants, highway strips, open pit mine slopes and spoils. Monitoring and laboratory analyses are indispensable for these analyses. The statistical analyses have the most flexibility in scale and in data type and will be investigated in detail in the following sections.

Table 2.4 The trends in landslide hazard zonation (Van Westen, 1993).

Type of landslide hazard analysis	Main characteristics
A. Distribution analysis	Direct mapping of mass movement features resulting in a map, which gives information only for those sites where landslides have occurred in the past.
B. Qualitative analysis	Direct, or semi-direct, methods in which the geomorphological map is re-numbered to a hazard map, or in which several maps are combined into one using subjective decision rules, based on the experience of the earth scientist.
C. Statistical analysis	Indirect methods in which statistical analyses are used to obtain predictions of the mass movement hazard from a number of parameter maps.
D. Deterministic analysis	Indirect methods in which parameter maps are combined in slope stability calculations.
E. Landslide frequency analysis	Indirect methods in which earthquake and/or rainfall records or hydrological models are used for correlation with known landslide dates, to obtain threshold values with a certain frequency.

2.11 Landslide Hazard in Thailand

Landslides are recurrent and devastated incidences commonly found in Thailand especially in the mountainous regions and their vicinity. The predominant type of landslides discovered is the rainfall-triggered shallow landslide caused by the

intense and continuous rainfalls where most vulnerable geologic formation is the granite terrain which can be easily weathered into thin layers of the landslide prone residual soils (Soralump, 2007). Shallow failures occur due to saturation of top soil layer along the terrain slope which shifts slope property from marginally stable to unstable state. This could result in the rapid movement of soil cover down hill to the surrounded low area (Liu and Wu, 2008). During this period, the landslide may transform into a debris avalanche, with increasing velocity and volume. If the landslide material flows into a gully at the base of the slope, then the run-out of the material can reach long distance (up to several kilometers) (Revellino et al., 2004).

To reduce risk from the current widespread landslide activity, the landslide susceptibility assessment is crucially needed in all areas that are potentially prone to landsliding. However, reports on this issue for Thailand are still infrequent and they typically focused only on small areas where the catastrophic landslides have occurred before (e.g. Naramngam and Tangtham, 1997; Yumuang, 2006; Akkrawinrawong et al., 2008; Oh et al., 2008) but the investigation on basin or regional scales are still rarely found in literature (e.g. LDD, 2001; DMR, 2005). In most cases, only few causative factors were taken into account and the verification process was largely ignored. To assist the effective susceptibility analysis in broader scale, In this research, the formulation of landslide susceptibility map at basin scale for local Thailand based on three different methods namely; analytical hierarchy process (AHP), frequency ratio (FR) model and integrated AHP and FR model in lower Mae Chaem watershed, northern Thailand.

2.12 Comparison and Verification of the Results.

As Carrara et al. (1999) indicated, the popular misconception is that a GIS-based landslide susceptibility map is more accurate and objective than a product where the qualitative hazard classes are derived mainly through expert knowledge. This has also been the objective of several studies, which compared different types of landslide hazard assessment (Irigaray et al., 1996; Van Westen et al., 1999; Guzzetti et al., 1999; 2000).

Binaghi et al. (1998) made a comparison between two methodologies for landslide susceptibility mapping: a probabilistic approach using certainty factors, and one based on Fuzzy Logic integrated with the Dempster–Shafer theory. These methodologies are applied to an area in Italy.

Suzen and Doyuran (2003) made a comparison of bivariate and multivariate methods in the same area. They used the so-called “seed cell” approach to create a buffer around the crown of the landslide for which the input values were sampled from the various factor maps. They concluded that although 80% of the area was classified similarly in general the bivariate susceptibility map was overestimating the susceptibility classes relative to the multivariate map.

Chung and Fabbri (2003) give an overview of methods that can be used for the classification of hazard scores into meaningful susceptibility classes, the use of success rates and prediction rates and the validation of landslide susceptibility maps made through statistical methods, using time, space and random partition methods. An example of time partition methods is given by Irigaray et al. (1999) who verified a landslide susceptibility map which was made using a statistical method with new landslides that were generated during an extreme rainfall event, and concluded that

about 85 % of the new landslides occurred in areas, that were classified as “high” or “very high” in the susceptibility map.

In literature, there are different validation methods. Lee et al. (2004a) used the area under curve (AUC) method. In this method, they compared the known landslide location data with the produced landslide susceptibility maps and made rate curves so that he can assess the prediction accuracy using the area under curve.

Suzen and Doyuran (2004) developed the “seed cell area index (SCAI)” method to compare the two landslide susceptibility maps which were constructed by bivariate and logistic regression methods. In this method, the area percent values are divided with the landslide seed cell percent values to find density of landslides among the classes.

Ayalew et al. (2005) used simple overlay method. In this method, two susceptibility maps were separately overlaid with the active landslide zones map and the landslide occurrence percentage in all susceptibility classes for both maps were determined.

CHAPTER III

MATERIALS AND METHODOLOGY

The first stage in all the landslide susceptibility assessment studies consists in the collecting of existing information and data for the investigation area (Aleotti and Chowdhury, 1999). In this study, data acquisition and methods used for data processing, procedure for preparation of thematic maps and factors used for identification of landslide susceptibility zonation (LSZ) using GIS and remote sensing. Data preparation is a first fundamental and essential step for landslide susceptibility analysis. The spatial database is mainly composed of two parts such as landslide location map and landslide affecting factors.

3.1 Instrumentation

The equipments (hardware, software) and data used to generate chosen factors are as follows:

3.1.1 Hardware

- 1) Global positioning system (GPS): Garmin GPS III+
- 2) PC computer: Intel core 2 duo processor 2 GHz, 2 GB DDR2, 250 GB HDD
- 3) Digital camera
- 4) Laser printer

3.1.2 Software

1) Geographic information system (GIS) software packages, ArcView 3.3, and ArcGIS 9.0 version were used for spatial management and data manipulation.

2) Remote sensing (RS) software packages, PCI Geomatica 9.0, and ERDAS Imagine 9.0 version were used for image processing.

3) Operation system: Microsoft Windows XP Professional

3.1.3 Data

1) Landsat-5 TM path 131/row 47, IKONOS satellite images and aerial photographs (see Table 3.1).

2) Topographic maps at 1:50,000 scale (series number: L7018; and sheet number: 4645 I, 4645 II, 4645 III, 4645 IV, 4746 II, 4646 III, 4745 III, 4745 IV and 4746 III).

3.2 Data Input and Preparation

In this study, ten factors were considered which are elevation, slope aspect, slope angle, distance from drainage, lithology, distance from lineament, soil texture, precipitation, land use/land cover and NDVI. The first eight factors were extracted and calculated from their associated database while LULC and NDVI map were derived from Landsat-5 TM satellite images (Tables 3.1-3.2 and Figures 3.1-3.10). These factors can be divided into three broad categories which are geological, topographical and environmental conditioning parameters. The working scale of geographic maps was chosen at 1:50,000.

Identification and mapping of a suitable set of instability factors related to the slope failures require a priori knowledge of the main causes of landslides (Guzzetti et

al., 1999). These instability factors include surface and bedrock lithology and structure, seismicity, slope steepness and morphology, stream evolution, groundwater conditions, climate, vegetation cover, land use, and human activity. The availability of thematic data varies widely, depending on the type, scale, and method of data acquisition. To apply the three methods, a spatial database that considers landslide related factors was designed and constructed. These data are available in Thailand either as paper or as digital maps. Details of spatial database constructed are shown in Table 3.2.

There were ten related factors considered in the calculation of the landslide susceptibility (Figures 3.1-3.10). These factors were extracted from the constructed GIS-based spatial database. The digital elevation model (DEM) portrays accurate representation of land surface which was suitable for medium scale mapping (Tomlin, 1990; Nagarajan et al., 1998). For DEM creation, 10 meter interval contours and surveyed base points showing the elevation values were extracted from the 1:50,000 scale topographic maps. Using the DEM, elevation, slope aspect, and slope angle were calculated.

Slope aspect derives from a raster surface, and it identifies the downslope direction of the maximum rate of change in value from each cell to its neighbors. Slope aspect can be thought of as the slope direction. The values of the output raster will be the compass direction of the slope aspect.

Slope angle identifies the steepest downhill slope for a location on a surface. Slope angle is calculated for each triangle in TIN and for each cell in raster. For a TIN, this is the maximum rate of change in elevation across each triangle. For raster, it is the maximum rate of change in elevation over each cell and its eight neighbors. The

slope angle command takes an input surface raster and calculates an output raster containing the slope angle at each cell. The lower the slope angle value, the flatter the terrain; the higher the slope angle value, the steeper the terrain. The output slope angle raster can be calculated as percent slope angle or degree of slope angle.

In addition, the distance from drainage was calculated using the topographic database. The drainage buffer was calculated in 100 meter intervals. The lithology map was prepared from a 1:50,000 scale geological map. The distance from lineament was calculated in 100 meter intervals. The soil texture was prepared from 1:50,000 scale soil map. The precipitation data were provided by Thai Meteorological Department and the GAME-T project for the whole northern Thailand over the last 10 years, and the kriging interpolation method was used to produce rainfall intensity map of the study area.

LULC data were classified from Landsat-5 TM satellite images using an unsupervised classification method (ISODATA) and field surveys where twelve classes, which are paddy field, mixed field crop, longan, truck crop, mixed swidden cultivation, hill evergreen forest, mixed deciduous forest, mixed forest plantation, grass and scrub, mine, urban, and water, were extracted for land use mapping (Figure 3.9).

Finally, the normalized difference vegetation index (NDVI) map was generated from Landsat-5 TM satellite images (resolution of 25 m). The NDVI involves a non-linear transformation of the visible or red and near-infrared bands of satellite images (Rouse et al., 1973; Jackson et al., 1983; Tucker et al., 1991), consequently NDVI results from the difference between the visible or red and near-infrared (NIR) bands, and can be considered a measure of vegetation in terms of

biomass, leaf area index, and percentage of vegetation cover. NDVI values range from -1 to +1 (pixel values 0–255) and is represented by calculated using formula $NDVI = (NIR - R) / (NIR + R)$, where NIR is the energy reflected in the near infrared portion of the electromagnetic spectrum, and R is the energy reflected in the red portion of the spectrum.

The collected data were converted to a raster grid with 25 m × 25 m cells for application of the three different methods namely, analytical hierarchy process (AHP), frequency ratio (FR) model and integrated AHP and FR model. The total cell number is 3,091,791. In this study, the weights and ratings for each factor were determined based on the three different methods mentioned above. These values were then used to calculate the landslide susceptibility index and the index was mapped to represent landslide susceptibility. Finally, accuracy of the output map was verified based on known landslide locations and the success rate was calculated.

Table 3.1 Overview of remotely-sensed data of the study area.

No.	Data	Path/Row	Resolution	Acquisition date	Data source
1	Landsat-5 TM	131/47	25 m × 25 m	12 February 2001	GISTDA
2	Landsat-5 TM	131/47	25 m × 25 m	26 February 2006	GISTDA
3	IKONOS	-	1 m × 1 m	taken during 2003 to 2007	www.PointAsia.com
4	Aerial photographs	-	1:4,000	taken during 2000 to 2002	Ministry of Agriculture and Cooperatives

Table 3.2 Spatial data layers used in the study.

Category	Layer	Data type	Scale	Data Source
Landslide location map	Aerial photographs (taken during 2000 to 2002)	Point	1:4,000	Ministry of Agriculture and Cooperatives
	IKONOS (taken during 2003 to 2007)	Point	1 m × 1 m	
Topographic map	Elevation Slope aspect Slope angle	Point and line	1:50,000	Royal Thai Survey Department
Drainage map	Distance from drainage	Polygon	1:50,000	
Geological map	Lithology	Polygon	1:50,000	Department of Mineral Resources
Lineament map	Distance from lineament	Polygon	1:50,000	
Soil map	Soil texture	Polygon	1:50,000	Land Development Department
Precipitation map	Precipitation	GRID	1:50,000	1.Thai Meteorological Department 2.The GAME-T project
LULC map	Land use/land cover	GRID	25 m × 25 m	Derivation from Landsat-5 TM images provided by GISTDA
NDVI map	NDVI	GRID	25 m × 25 m	

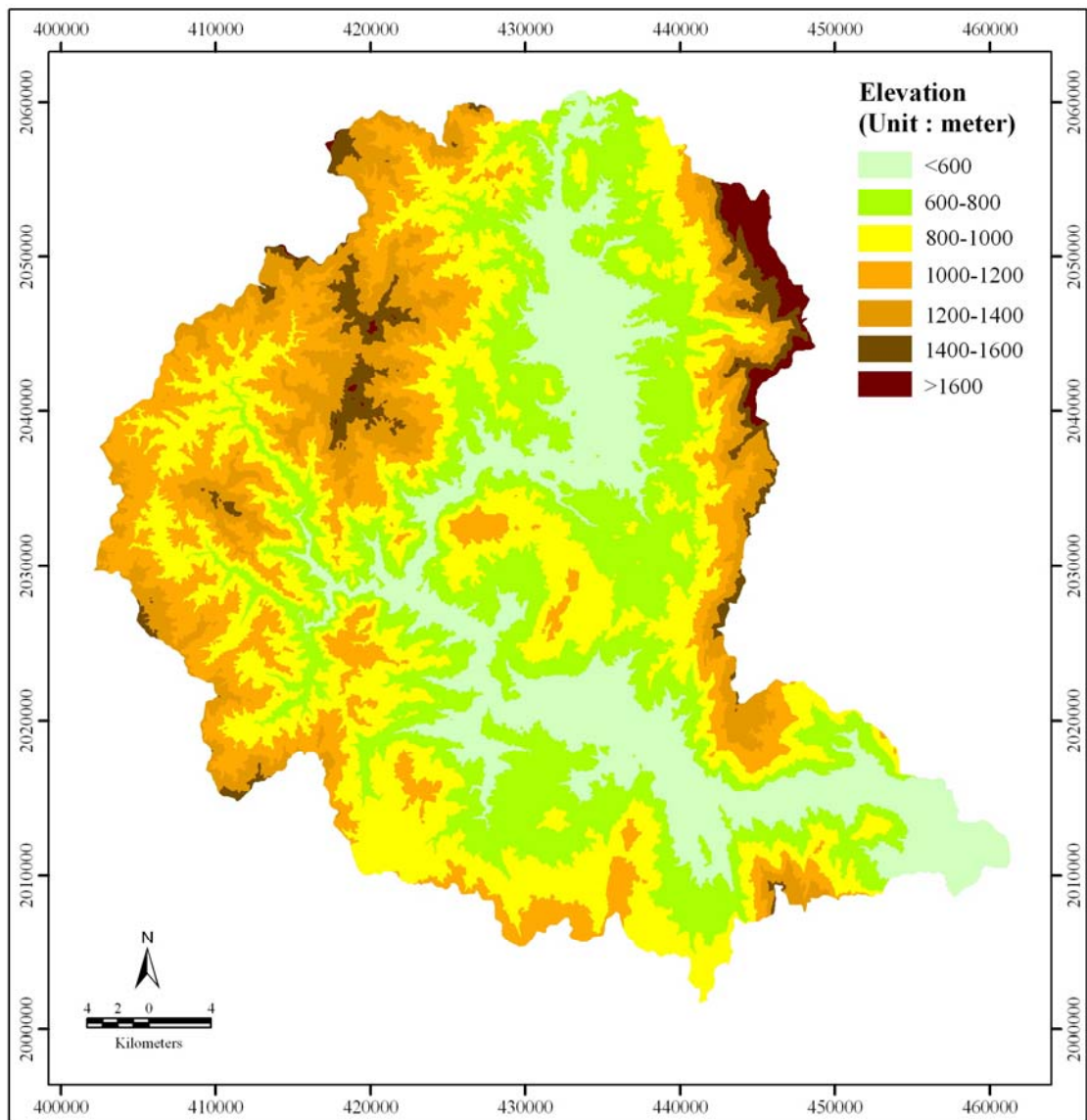


Figure 3.1 Elevation map of the study area based on DEM from topographic map of 1:50,000 scale (Source: Royal Thai Survey Department).

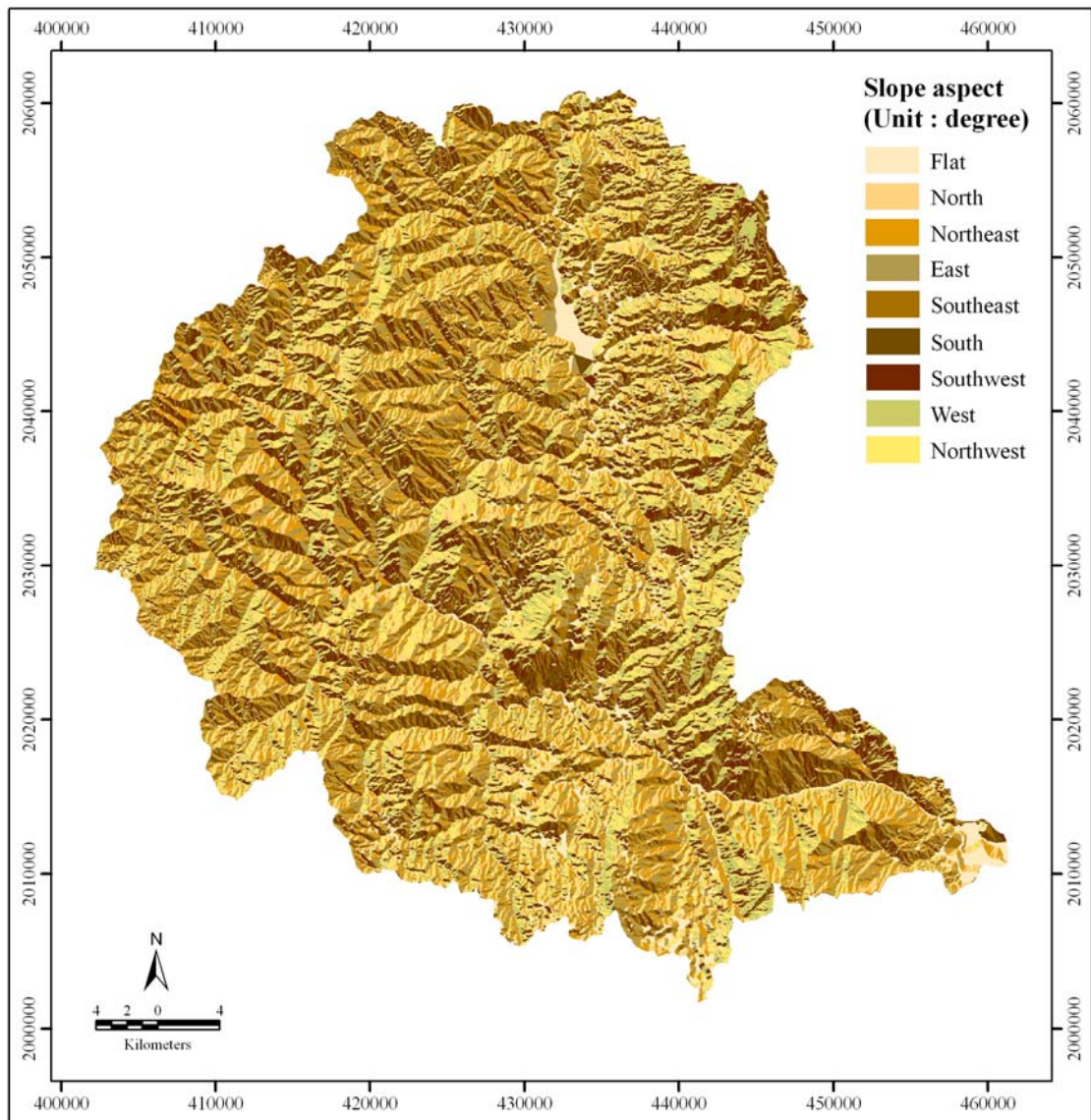


Figure 3.2 Slope aspect map of the study area based on DEM from topographic map of 1:50,000 scale (Source: Royal Thai Survey Department).

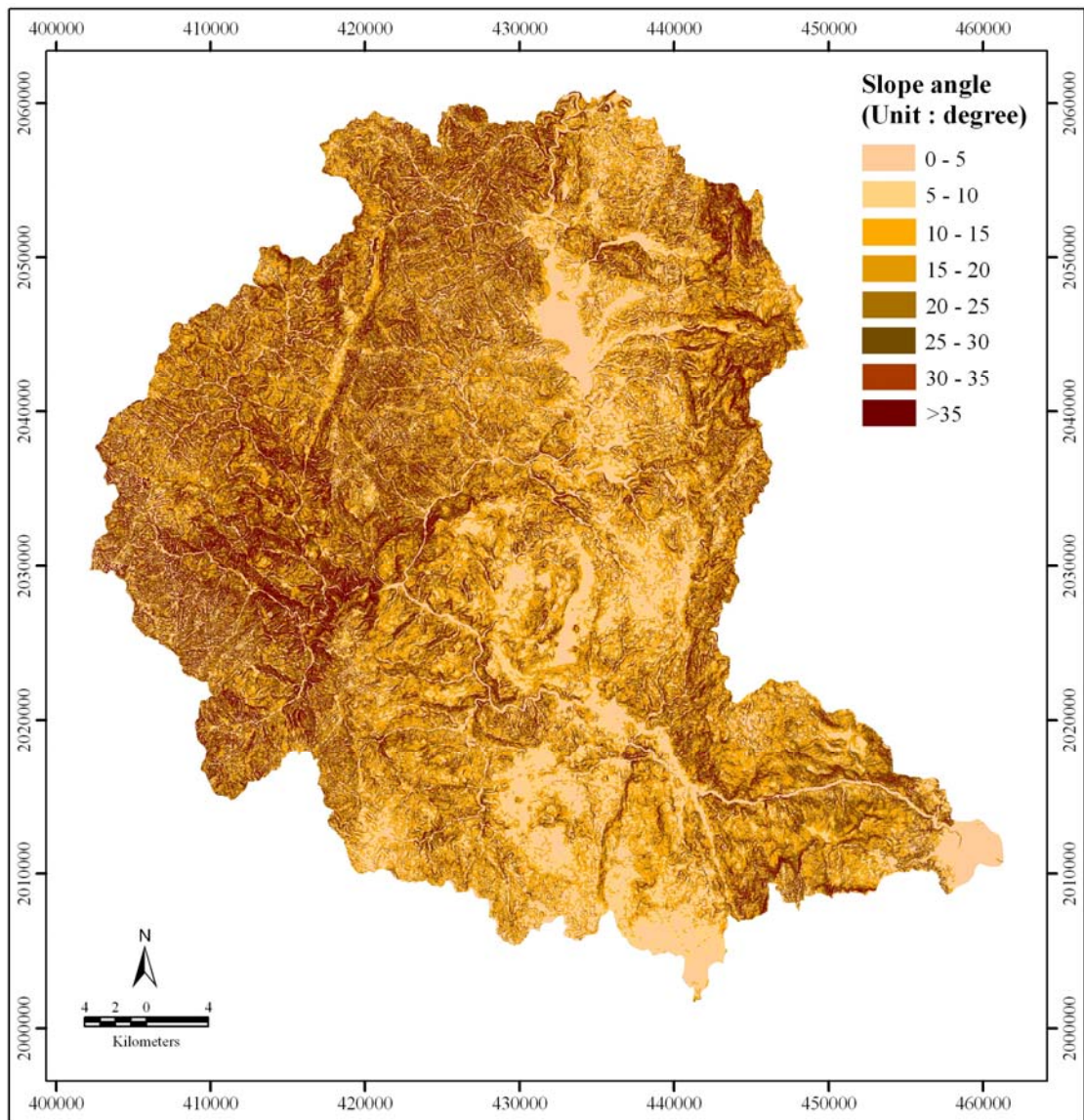


Figure 3.3 Slope angle map of the study area based on DEM from topographic map of 1:50,000 scale (Source: Royal Thai Survey Department).

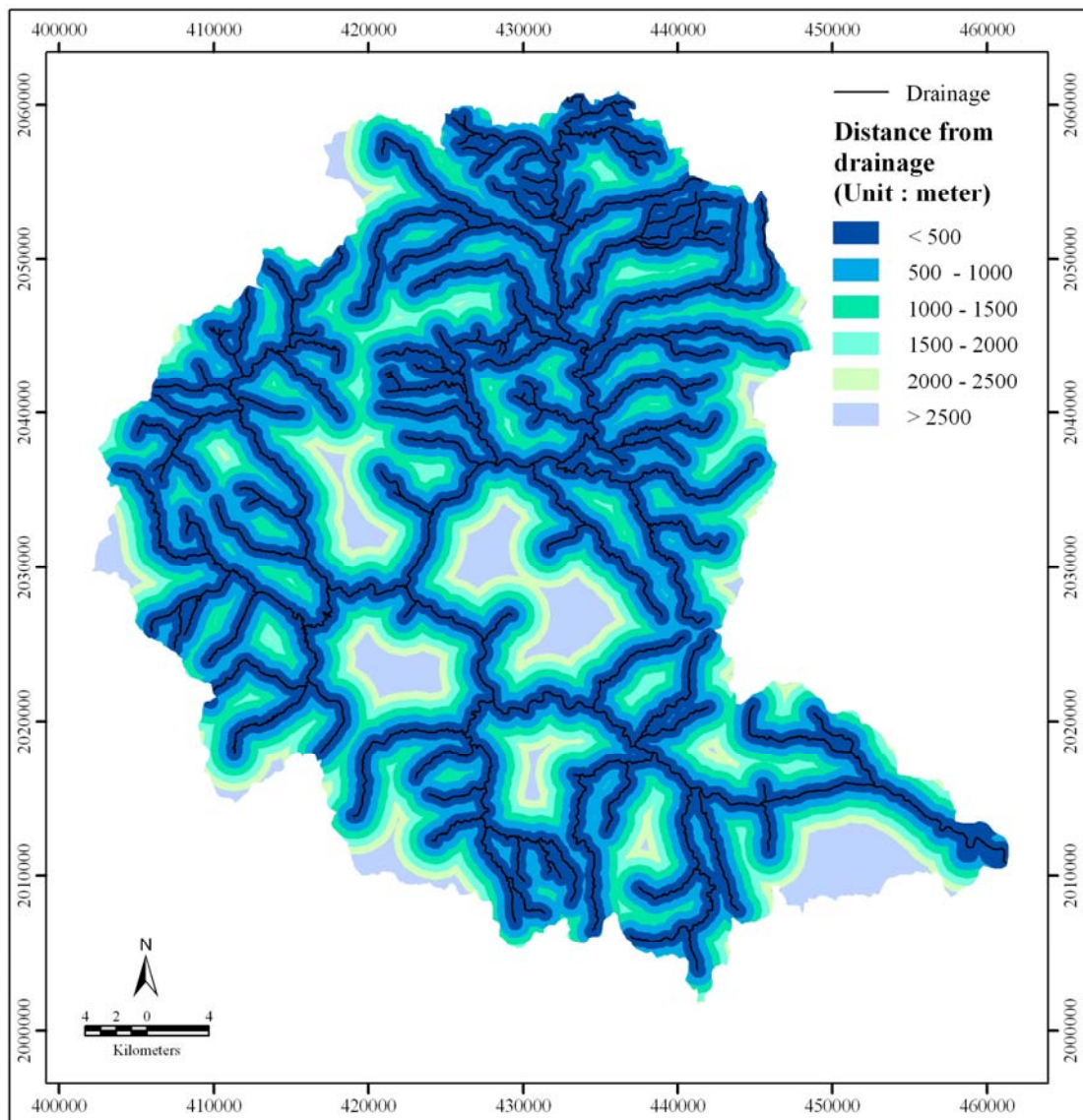


Figure 3.4 Distance from drainage map of the study area from topographic map of 1:50,000 scale (Source: Royal Thai Survey Department).

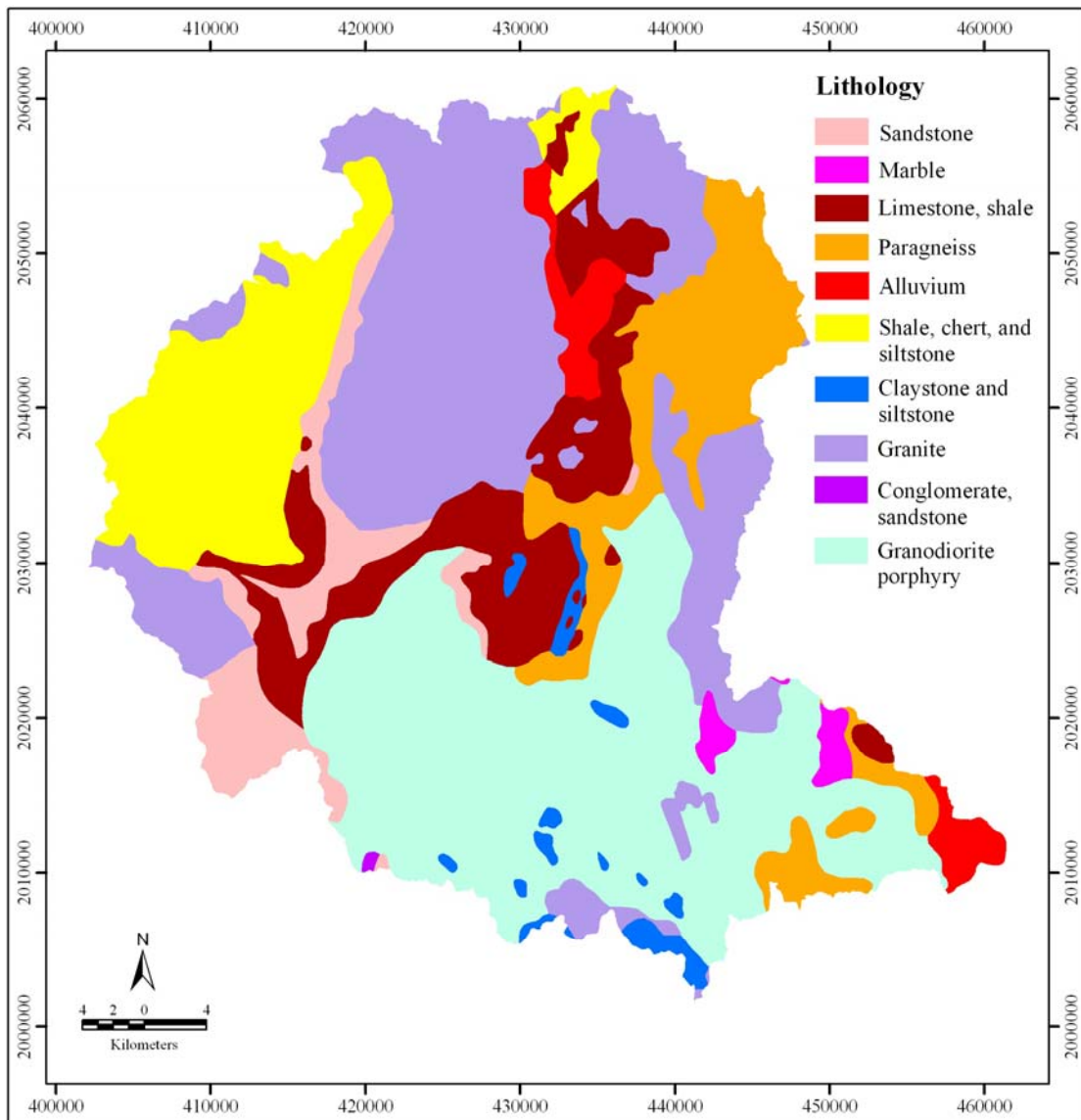


Figure 3.5 Lithology map of the study area (Source: Department of Mineral Resources).

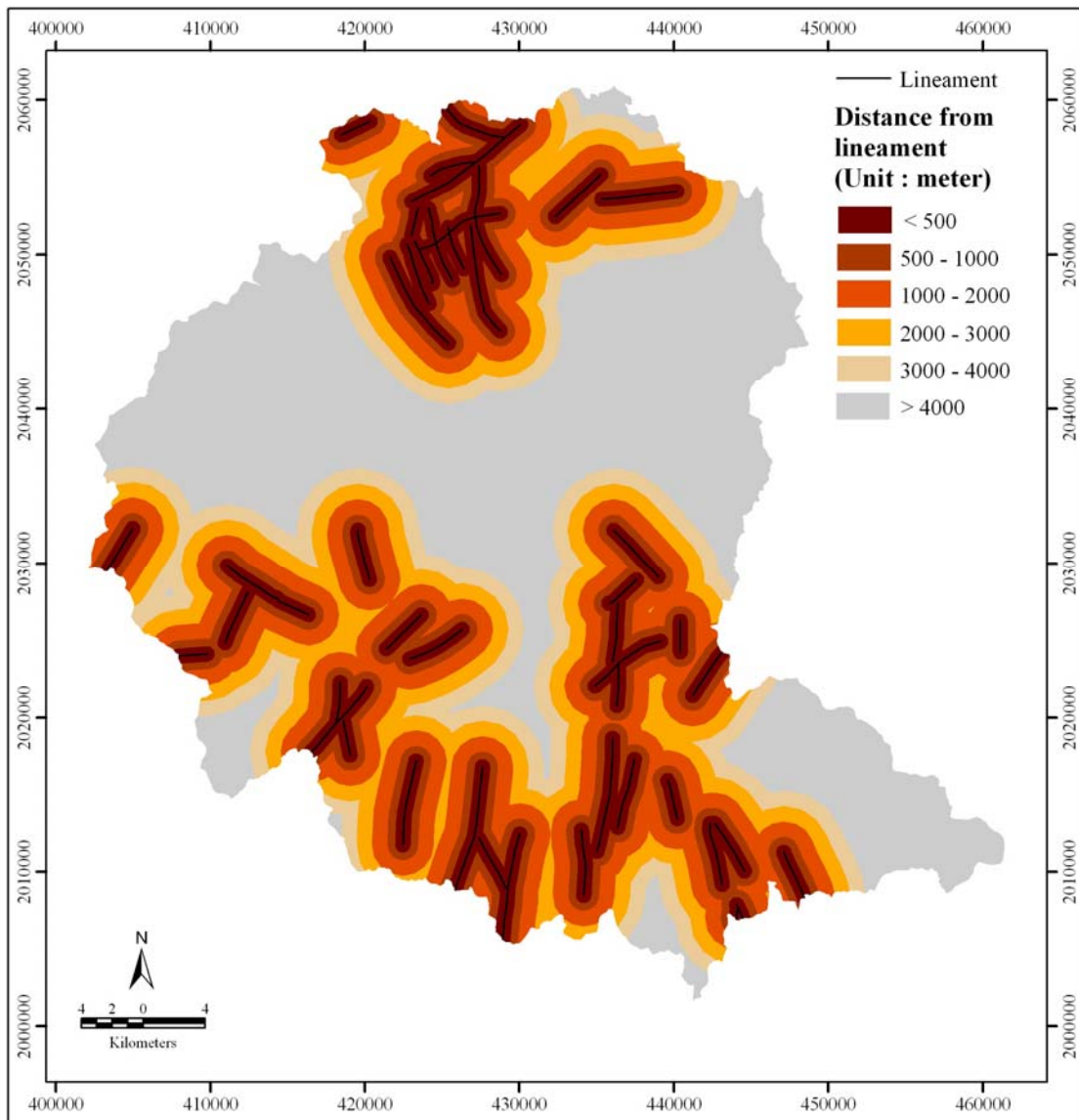


Figure 3.6 Distance from lineament map of the study area (Source: Department of Mineral Resources).

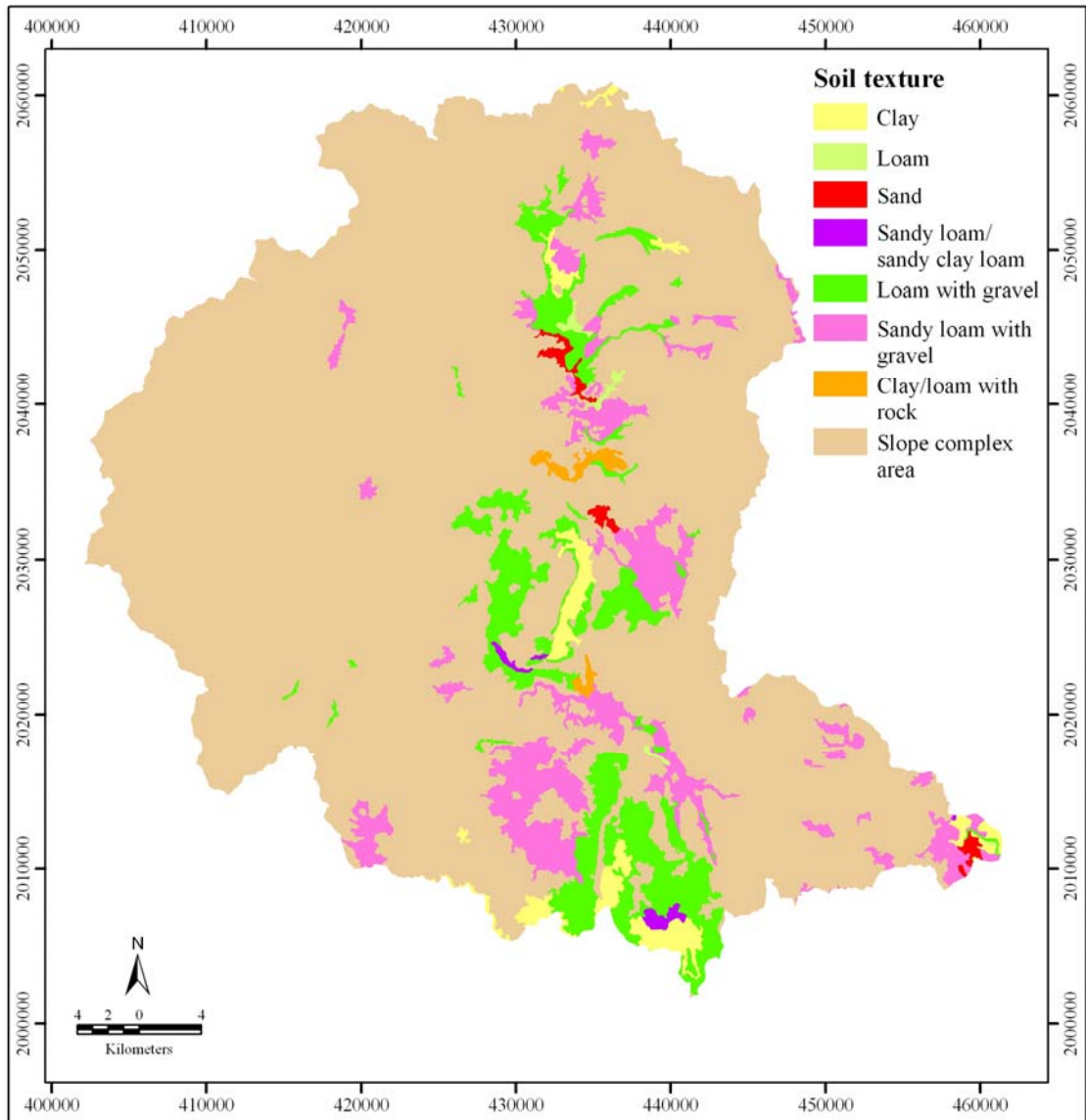


Figure 3.7 Soil texture map of the study area (Source: Land Development Department).

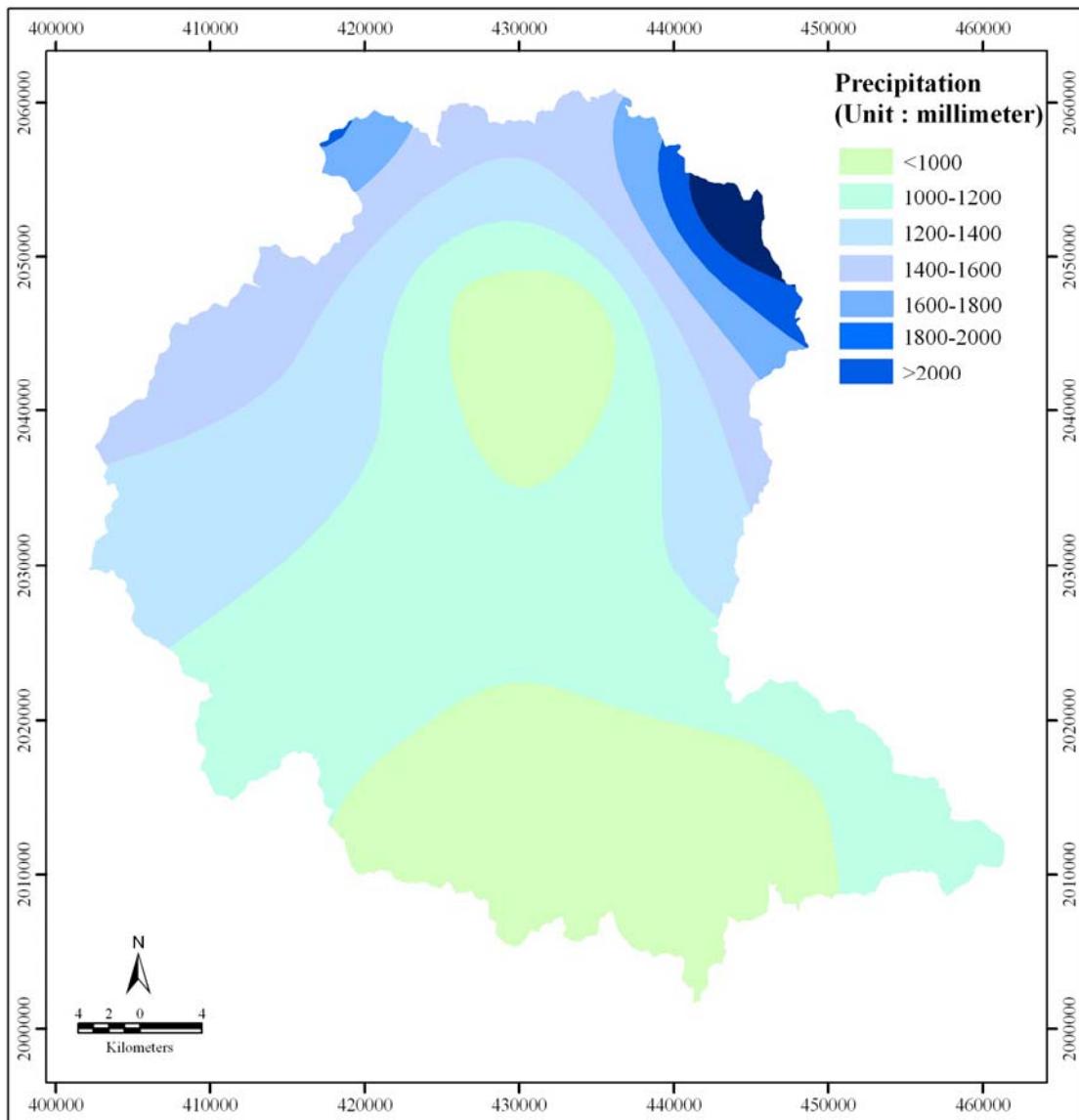


Figure 3.8 Precipitation map of the study area (1996-2005) based on kriging interpolation method (Source: Thai Meteorological Department and the GAME-T project, 2006).

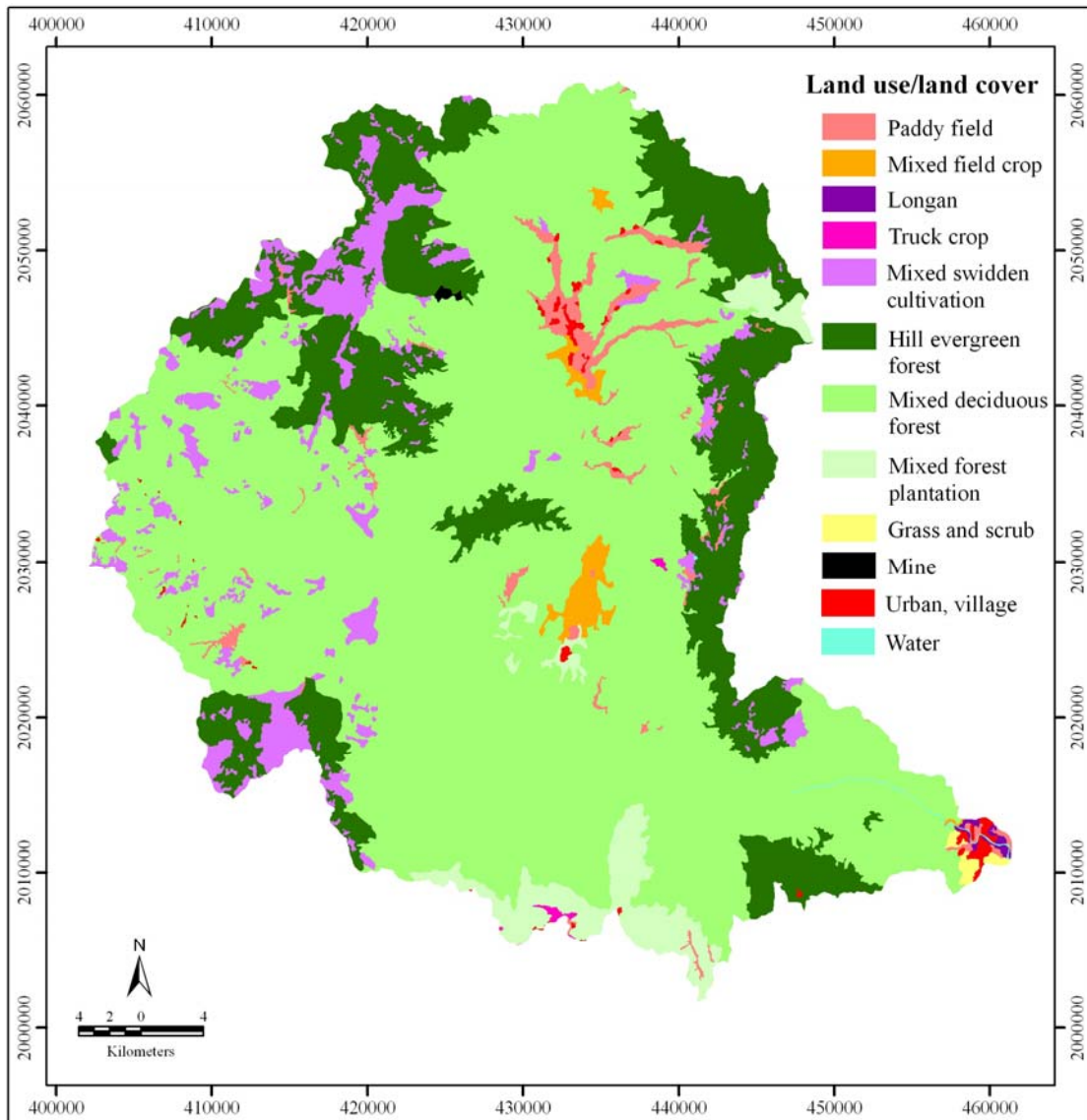


Figure 3.9 Land use/land cover map of the study area modified from Land Development Department, 2001, and based on unsupervised classification method (ISODATA) from Landsat-5 TM image, path 131/row 47, acquired on 12 February 2001, and field surveys (Source: Geo-Informatics and Space Technology Development Agency (Public Organization)).

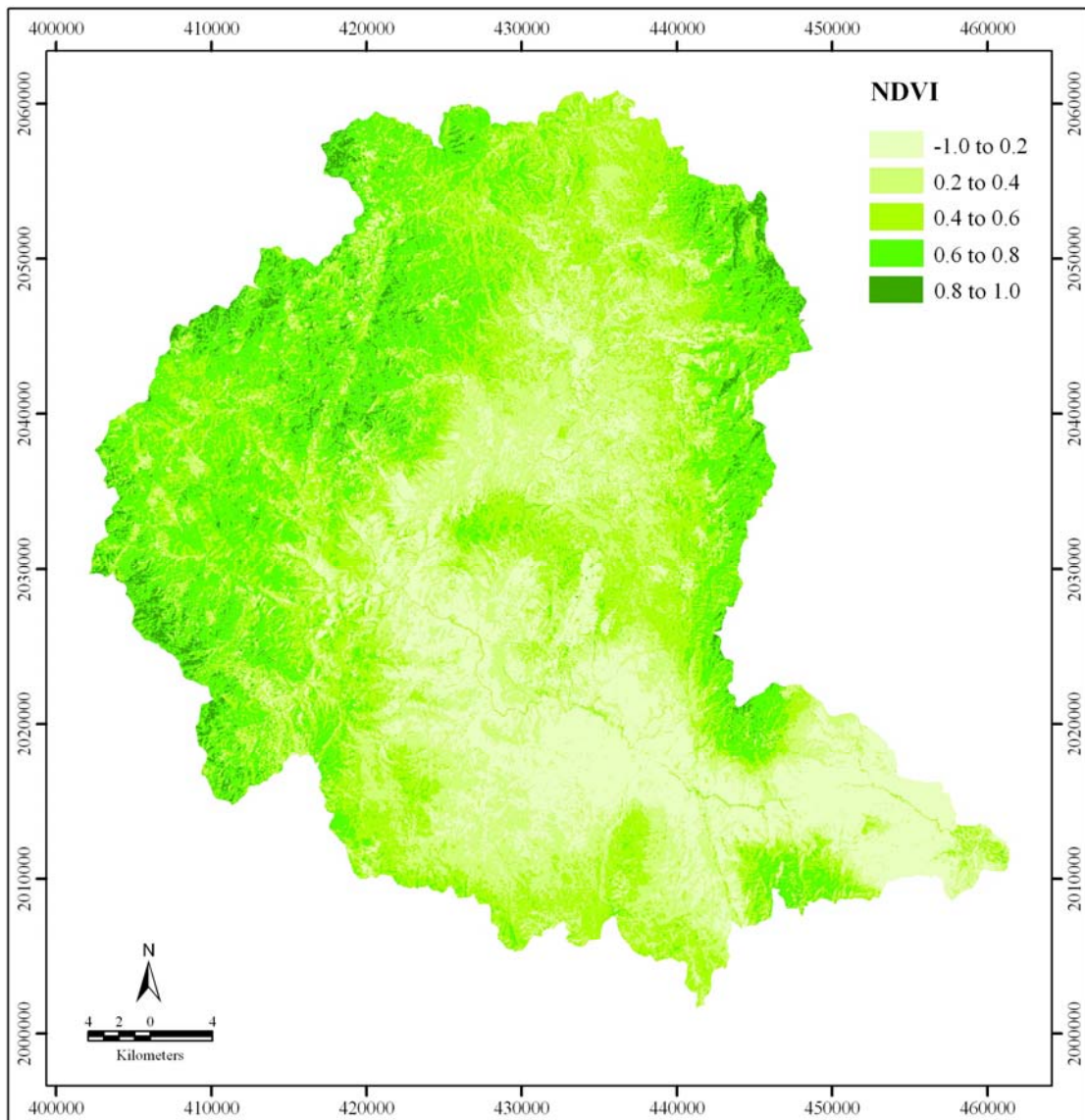


Figure 3.10 Normalized difference vegetation index (NDVI) map of the study area derived from Landsat-5 TM image, path 131/row 47, acquired on 12 February 2001 (Source: Geo-Informatics and Space Technology Development Agency (Public Organization)).

3.3 Landslide Location Detection

For landslide susceptibility analysis, accurate detection of the location of landslides is very important. The application of remote sensing methods, such as high resolution satellite images and aerial photographs were used to detect the landslide locations. In this study, the 1-m resolution IKONOS images were taken during the period of 2003 to 2007, and 1:4,000 scale aerial photographs were taken during the period of 2000 to 2002. These of remote sensing were used to detect the landslide locations, and the field surveys were used to verify the result of high resolution satellite images and aerial photographs interpretation (Figure 3.11).

The high resolution satellite images and aerial photographs were used to identify precise landslide locations and to find fine detail of the event. These landslides were observed in high resolution satellite images and aerial photographs by interpreting breaks in the forest canopy, bare soil, and other typical geomorphic characteristics of landslide scars. The landslide locations were also verified by fieldwork. Finally, a total of 101 landslides were mapped to assemble a database to be used in the study (Figure 3.12).

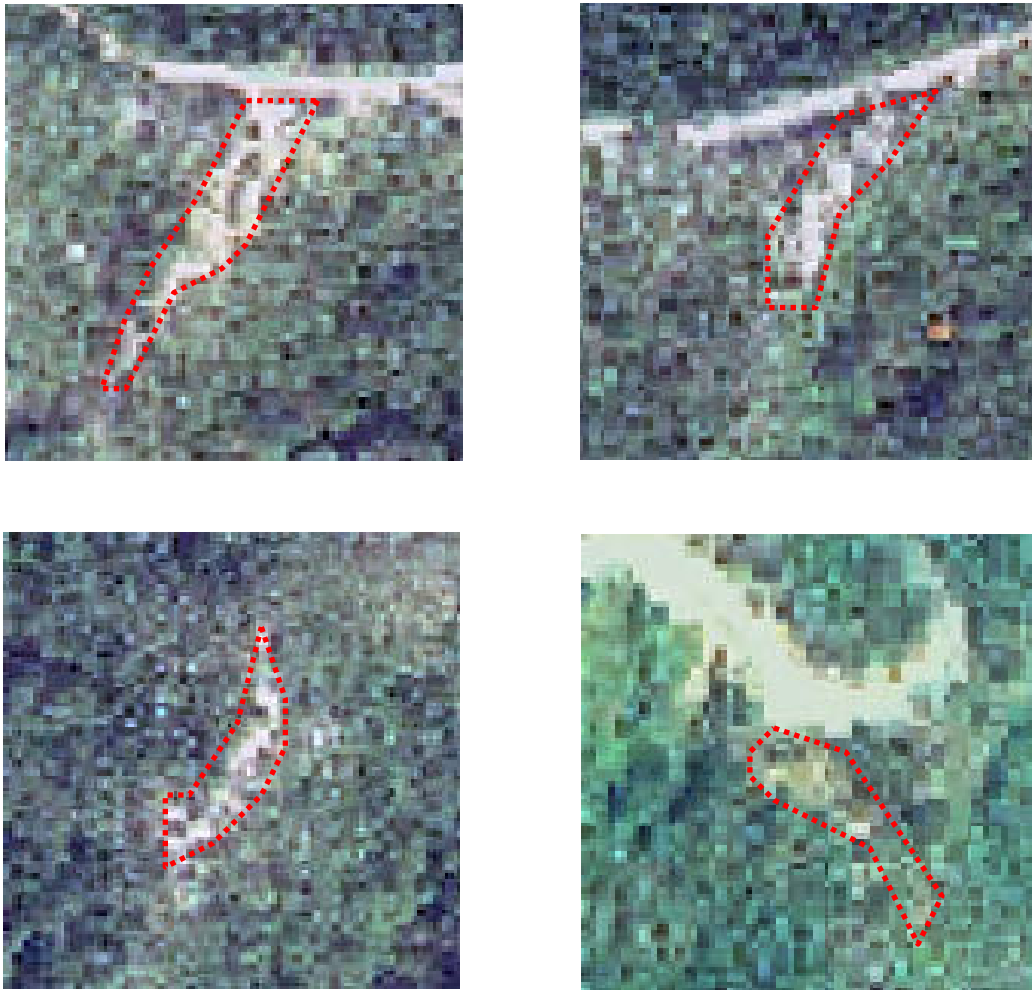


Figure 3.11 The high resolution satellite images (IKONOS) show landslide locations in the study area.

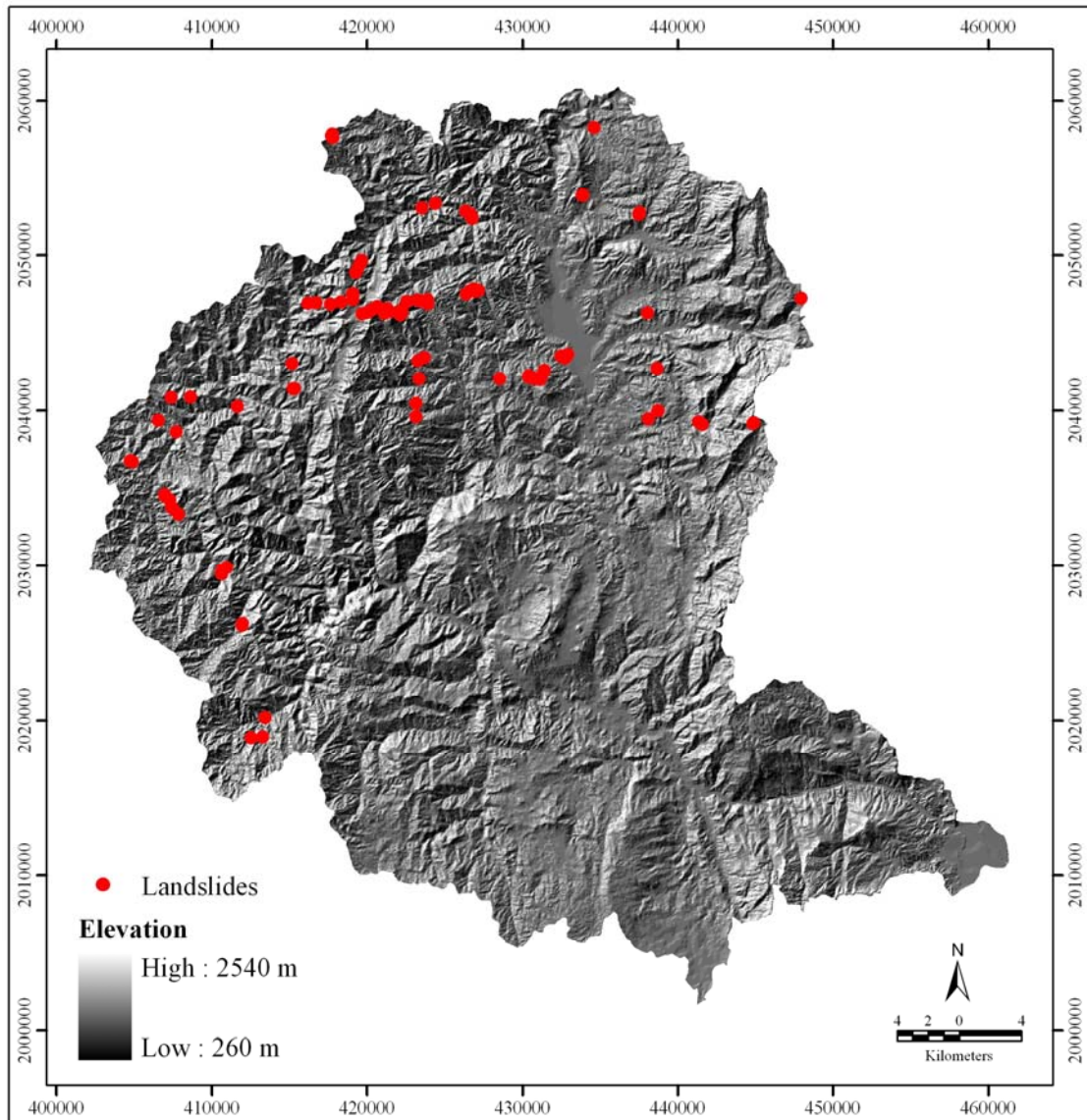


Figure 3.12 101 landslide locations with hill-shaded map in the study area.

3.4 Factors Influencing Landslides

The factors which determine the landslide hazard of an area can be divided into two groups: (i) the quasi-static variables, which contribute to landslide susceptibility, such as geology, slope gradient, slope aspect (i.e., orientation of slope face), elevation, geotechnical properties, and long-term drainage patterns; and (ii) the dynamic variables, which tend to trigger landslides in an area of given susceptibility, such as rainfall and earthquakes (Wu and Sidle, 1995; Atkinson and Massari, 1998). Obviously, the probability of a landslide depends on both the quasi-static and dynamic variables. However, the dynamic variables may change over a very short time span, and are thus very difficult to estimate. The spatial distribution of the quasi-static variables within a given area determines the spatial distribution of relative landslide susceptibility in that region (Carrara et al., 1995).

In this study, ten landslide affecting factors are selected and defined. They are elevation, slope aspect, slope angle, distance from drainage, lithology, distance from lineament, soil texture, precipitation, land use/land cover and NDVI. Each category is subdivided into different classes by its value or feature (Table 3.3 and Figures 3.1-3.10, 3.13).

Table 3.3 Distribution of landslide occurrence points for various data layers in the study area.

Factors	Class	Total number of pixels		Landslide occurrence point		Frequency ratio
		Number	%	Number	%	
Elevation	<600 m	558848	18.08	5	4.95	0.27
	600 m – 800 m	792967	25.65	20	19.80	0.77
	800 m – 1,000 m	782359	25.31	15	14.85	0.59
	1,000 m – 1,200 m	556841	18.01	24	23.76	1.32
	1,200 m – 1,400 m	280165	9.06	17	16.83	1.86
	1,400 m – 1,600 m	82504	2.67	16	15.84	5.93
	>1,600 m	37750	1.21	4	3.96	3.27
Slope aspect	Flat	161640	5.23	0	0	0
	North	349342	11.30	10	9.90	0.88
	Northeast	400242	12.95	13	12.87	0.99
	East	381664	12.35	12	11.88	0.96
	Southeast	367056	11.87	19	18.81	1.58
	South	340197	11.00	20	19.80	1.80
	Southwest	361455	11.69	6	5.94	0.51
	West	369212	11.94	11	10.89	0.91
	Northwest	360630	11.67	10	9.90	0.85
Slope angle	0° – 5°	611786	19.79	17	16.83	0.85
	5° – 10°	192901	6.24	0	0	0
	10° – 15°	435856	14.1	6	5.94	0.42
	15° – 20°	563190	18.22	24	23.76	1.30
	20° – 25°	490770	15.88	16	15.84	1.00
	25° – 30°	354860	11.48	18	17.82	1.55
	30° – 35°	214174	6.93	13	12.87	1.86
Drainage (Distance from drainage)	<500 m	1215767	39.32	34	33.66	0.86
	500 m – 1,000 m	831347	26.91	30	29.70	1.10
	1,000 m – 1,500 m	488601	15.80	18	17.82	1.13
	1,500 m – 2,000 m	246753	7.98	12	11.88	1.49
	2,000 m – 2,500 m	143219	4.63	4	3.96	0.86
	>2,500 m	165604	5.36	3	2.97	0.55
Lithology	Sandstone	177214	5.73	6	5.94	1.04
	Marble	27624	0.89	0	0	0
	Limestone, shale	331381	10.72	5	4.95	0.46
	Paragneiss	311446	10.07	9	8.91	0.88
	Alluvium	79856	2.59	1	0.99	0.38
	Shale, chert, and siltstone	378938	12.26	24	23.76	1.94
	Claystone and siltstone	47749	1.54	0	0	0
	Granite	858729	27.77	56	55.45	2.00
	Conglomerate, sandstone	1715	0.06	0	0	0
	Granodiorite porphyry	877139	28.37	0	0	0
	Lineament (Distance from lineament)	<500 m	316662	10.24	16	15.84
500 m – 1,000 m		293989	9.51	13	12.87	1.35
1,000 m – 2,000 m		542593	17.55	21	20.79	1.18
2,000 m – 3,000 m		435286	14.08	12	11.88	0.84
3,000 m – 4,000 m		333239	10.78	9	8.91	0.83
>4,000 m		1170022	37.84	30	29.70	0.78

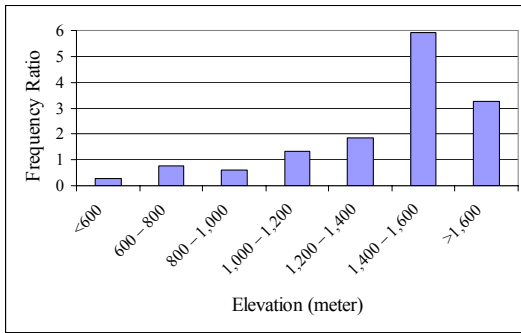
Table 3.3 Distribution of landslide occurrence points for various data layers in the study area (Continued).

Factors	Class	Total number of pixels		Landslide occurrence point		Frequency ratio
		Number	%	Number	%	
Soil texture	Clay	59053	1.9	0	0	0
	Loam	5896	0.19	0	0	0
	Sand	11151	0.36	0	0	0
	Sandy loam/sandy clay loam	6343	0.2	0	0	0
	Loam with gravel	207200	6.7	0	0	0
	Sandy loam with gravel	203365	6.57	2	1.98	0.30
	Clay/loam with rock	11651	0.37	0	0	0
	Slope complex area	2587132	83.68	99	98.02	1.17
Precipitation	<1,000 mm	820402	26.52	20	19.80	0.75
	1,000 mm – 1,200 mm	1160632	37.52	35	34.65	0.92
	1,200 mm – 1,400 mm	578674	18.71	24	23.76	1.27
	1,400 mm – 1,600 mm	350627	11.34	15	14.86	1.31
	1,600 mm – 1,800 mm	100290	3.24	4	3.96	1.22
	1,800 mm – 2,000 mm	47775	1.54	2	1.98	1.29
	>2,000 mm	34700	1.12	1	0.99	0.88
Land use/land cover	Paddy field	60629	1.96	0	0	0
	Mixed field crop	29575	0.96	4	3.96	4.13
	Longan	3258	0.11	0	0	0
	Truck crop	2528	0.08	0	0	0
	Mixed swidden cultivation	190965	6.18	17	16.83	2.72
	Hill evergreen forest	585675	18.94	28	27.72	1.46
	Mixed deciduous forest	2085444	67.45	52	51.49	0.76
	Mixed forest plantation	110816	3.58	0	0	0
	Grass and scrub	5803	0.19	0	0	0
	Mine	1520	0.05	0	0	0
	Urban, village	13443	0.43	0	0	0
NDVI	Water	2135	0.07	0	0	0
	-1.0 to 0.2	609023	19.69	4	3.96	0.20
	0.2 to 0.4	817512	26.44	28	27.72	1.05
	0.4 to 0.6	856906	27.72	30	29.70	1.07
	0.6 to 0.8	724519	23.43	36	35.64	1.52
	0.8 to 1.0	83831	2.71	3	2.97	1.10

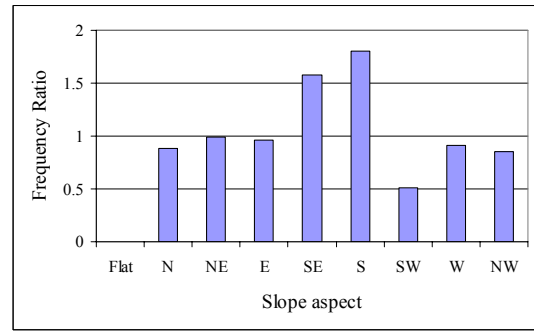
Total number of pixels in study area: 3,091,791.

Number of landslide occurrence points: 101.

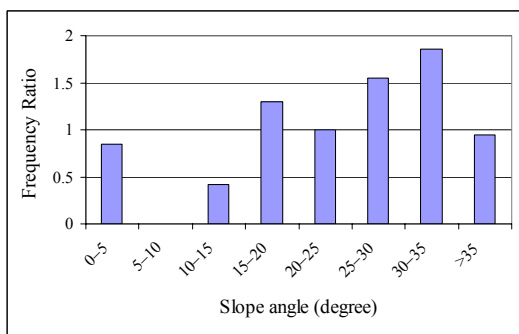
FR = % Landslide occurrence points / % number of pixels



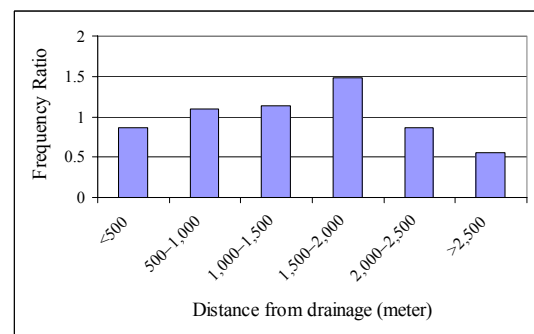
(a)



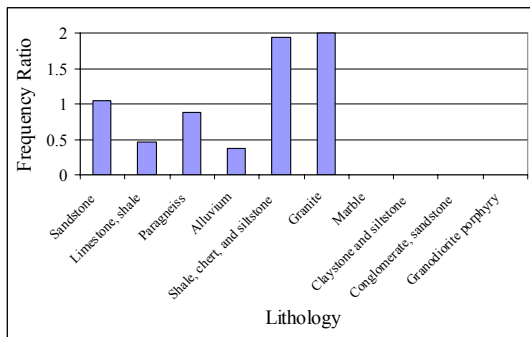
(b)



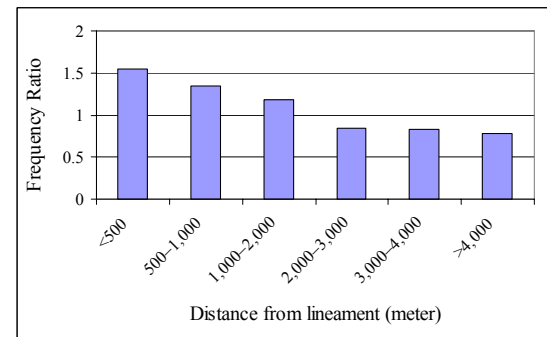
(c)



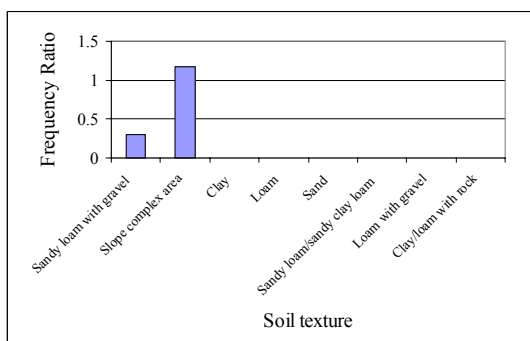
(d)



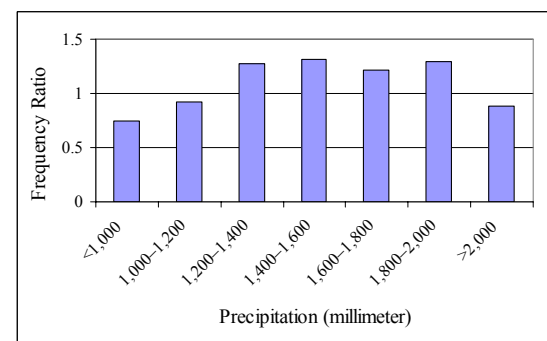
(e)



(f)



(g)



(h)

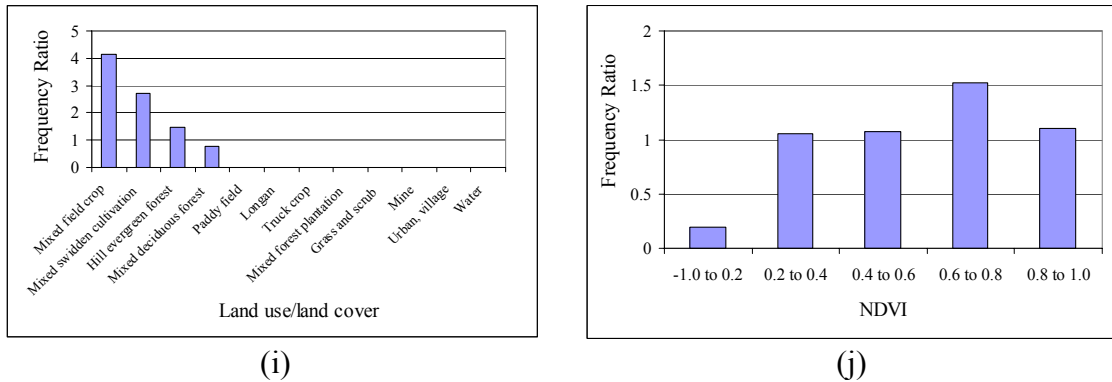


Figure 3.13 Histograms showing frequency ratio of landslide occurrence with (a) elevation; (b) slope aspect; (c) slope angle; (d) distance from drainage; (e) lithology; (f) distance from lineament; (g) soil texture; (h) precipitation; (i) land use/land cover; (j) NDVI.

3.4.1 Elevation

Although some researches have found that landslide activity, within a specific basin, occurs at certain elevations (Greenbaum et al., 1995; Jordan et al., 2000), the relationship between landslide activity and elevation is still unclear, hence it requires further studies. However, it is well known that elevation influences a large number of biophysical parameters and anthropogenic activities. In turn, these conditions are likely to affect slope stability and generate slope failure (Vivas, 1992). Elevation also affects soil characteristics significantly. In this study, the values of elevation were divided into seven classes: less than 600; 600–800; 800–1,000; 1,000–1,200; 1,200–1,400; 1,400–1,600; and more than 1,600 m (Figure 3.1).

3.4.2 Slope Aspect

Slope aspect is one of the important factors in preparing landslide susceptibility maps (Guzzetti et al., 1999; Nagarajan et al., 2000; Saha et al., 2002;

Cevik and Topal, 2003; Ercanoglu et al., 2004; Lee et al., 2004b; Lee, 2005). Slope aspect related parameters such as exposure to sunlight, drying winds, rainfall (degree of saturation), and discontinuities may control the occurrence of landslides (Dai et al., 2001; Cevik and Topal, 2003; Suzen and Doyuran, 2004; Komac, 2006). In this study, the slope aspect map of the study area was produced to show the relationship between slope aspect and landslide. The southwest and northeast parts of the study area are underlain by the monsoon and drying winds respectively that may control the occurrence of landslides. Slope aspect regions are classified according to the slope aspect class as flat (-1°); north ($337.5^\circ-360^\circ$, $0^\circ-22.5^\circ$); northeast ($22.5^\circ-67.5^\circ$); east ($67.5^\circ-112.5^\circ$); southeast ($112.5^\circ-157.5^\circ$); south ($157.5^\circ-202.5^\circ$); southwest ($202.5^\circ-247.5^\circ$); west ($247.5^\circ-292.5^\circ$); and northwest ($292.5^\circ-337.5^\circ$) (Figure 3.2). Some analyses were performed using slope aspect and the known landslide location map to determine the distribution of landslides, according to the slope aspect class, and the percentage of landslides which occurred in each slope aspect class (Table 3.3).

3.4.3 Slope Angle

The main parameter of the slope stability analysis is the slope angle (Lee and Min, 2001). Because the slope angle is directly related to the landslides, it is frequently used in preparing landslide susceptibility maps (Clerici et al., 2002; Saha et al., 2002; Cevik and Topal, 2003; Ercanoglu et al., 2004; Lee et al., 2004a; Lee, 2005; Yalcin, 2005). The slope angle map of the study area was divided into eight classes: $0^\circ-5^\circ$; $5^\circ-10^\circ$; $10^\circ-15^\circ$; $15^\circ-20^\circ$; $20^\circ-25^\circ$; $25^\circ-30^\circ$; $30^\circ-35^\circ$; and more than 35° (Figure 3.3). ArcGIS 9.0 analysis was performed to discover in which slope angle group the landslide happened and the rate of occurrence was observed. The landslide percentage

in each slope angle group class is presented in Table 3.3. This table indicates that most landslides occurred during 15° to 35° of slope angle.

3.4.4 Distance from Drainage

Many of the landslides in hilly areas occur due to the erosion activity associated with drainage. The distance from rivers is therefore considered one of the important factors in characterizing vulnerable terrain. Therefore, a drainage data layer has been prepared by digitizing the drainages from the topographic maps in a vector layer. An important parameter that controls the stability of a slope is the saturation degree of the material on the slope. The closeness of the slope to drainage structures is another important factor in terms of stability. Drainage may adversely affect stability by eroding the slopes or by saturating the lower part of material until resulting in water level increases (Gokceoglu and Aksoy, 1996; Dai et al., 2001; Saha et al., 2002; Cevik and Topal, 2003; Yalcin, 2005). A thorough field investigation should be carried out to determine the effects of drainage on the slope. Six different buffer areas were created within the study area to determine the degree to which the drainage affected the slopes. The landslide percentage in each drainage buffer zone is given in Figure 3.4 and Table 3.3, and shows that most of the landslides are closely located within the first 1,500 m buffer zone.

3.4.5 Lithology

Lithology is considered one of the most relevant parameters in landslide hazard in this area (Saha et al., 2002). Different rock types (or lithology) respond to erosion agents differently and conduct mass movement under differing natural conditions, and they have varied composition and structure, which contribute to the

strength of the material. The stronger rocks give more resistance to the driving forces as compared to the weaker rocks, and hence are less prone to landslides and vice versa. The bedrock geology of the Mae Cham watershed is mainly composed of rocks originated from Precambrian to Quaternary era (DMR, 2009). The ten rock types present in this data layer are sandstone; marble; limestone and shale; paragneiss; alluvium; shale, chert and siltstone; claystone and siltstone; granite; conglomerate and sandstone; and granodiorite porphyry (Figure 3.5). These lithologic groups are composed of rocks with similar lithologic properties and geological ages (Table 3.4).

Table 3.4 Lithologic groups and geological ages in the study area.

Lithologic group	Rock type	Rock group	Symbol	Age	Age (million year)
Sandstone	Sedimentary and Metamorphic rock	–	E	Cambrian	500–540
Marble	Sedimentary and Metamorphic rock	–	EO	Cambrian-Ordovician	470–520
Limestone and shale	Sedimentary and Metamorphic rock	Thung Song Group	O	Ordovician	440–500
Paragneiss	Sedimentary and Metamorphic rock	–	PE	Pre-Cambrian	540–2,500
Alluvium	Sedimentary and Metamorphic rock	–	Q	Quaternary	Present–1.8
Shale, chert and siltstone	Sedimentary and Metamorphic rock	Thong Pha Phum Group	SDCtp	Silurian-Devonian-Carboniferous	280–440
Claystone and siltstone	Sedimentary and Metamorphic rock	Mae Mah Group	Tmm	Tertiary	5–20
Granite	Igneous rock	–	Trgr	Triassic	200–250
Conglomerate, sandstone	Sedimentary and Metamorphic rock	–	TrJ	Triassic-Jurassic	180–220
Granodiorite porphyry	Igneous rock	–	Trm	Middle-Triassic	200–250

3.4.6 Distance from Lineament

Lineaments are the structural features which describe the zone/plane of weakness, fractures and faults along which landslide susceptibility is higher. It has generally been observed that the probability of landslide occurrence increases at sites close to lineaments, which not only affect the surface material structures but also make contribution to terrain permeability causing slope instability. In this study, the

landslide percentage in each lineament buffer zone is given in Figure 3.6 and Table 3.3 and shows that most of the landslides are closely located within the first 2,000 m buffer zone.

3.4.7 Soil Texture

The effects of soil on slope stability have been widely considered in landslide studies. Liener et al. (1996) use soil as one of the main inputs to locate landslide prone areas. The effects of the cohesiveness and thickness of the soil on landslide distribution are considered. It is also reported that difference between shallow and deep-seated landslide depends on the soil material and the thickness of the soil in steeper slopes. In this study, the soil texture was divided into eight units: clay; loam; sand; sandy loam/sandy clay loam; loam with gravel; sandy loam with gravel; clay/loam with rock; and slope complex area (Figure 3.7).

3.4.8 Precipitation

The effects of average annual precipitation have been widely recognized that hillslope instability can be caused by increased subsurface pore pressures during periods of intense rainfall (Anderson and Sitar, 1995; Iverson et al., 1997), which reduce the shear strength of hillslope materials (Keefer et al., 1984; Chen et al., 1995). A number of recent studies have demonstrated that rainfall-induced landslides can be transformed into debris flows as they move downslope (e.g., Fleming et al., 1989; Dai et al., 1999; Montgomery et al., 2000; Marchi et al., 2002; Guzzetti et al., 2004). In this study, the values of precipitation amount were divided into seven classes: less than 1,000; 1,000–1,200; 1,200–1,400; 1,400–1,600; 1,600–1,800; 1,800–2,000; and more than 2,000 mm (Figure 3.8).

3.4.9 Land Use/Land Cover

Land use/land cover is also a key factor responsible for landslide occurrences. The incidence of landslide is inversely related to the vegetation density. Hence, barren slopes are more prone to landslide activity as compared to the forest area. There are much conflicting evidences in the literature concerning the effects of vegetation on slope stability. Based on the examination of natural terrain, Franks (1999) reported that sparsely vegetated slopes are most susceptible to failure. However, Dai et al. (2001) found that the density of landslide on bare land is relatively low as compared with that on grassland. In this study, land use/land cover was divided into twelve classes: paddy field; mixed field crop; longan; truck crop; mixed swidden cultivation; hill evergreen forest; mixed deciduous forest; mixed forest plantation; grass and scrub; mine; urban; and water (Figure 3.9).

3.4.10 NDVI

The NDVI map is useful in delineating vegetation (Rouse et al., 1973). Vegetation Index has been considered to prepare a land use/land cover map in a multi-source classification process. The effect of vegetation on landslide has been studied in view of the slope inclination. As for example, steep slope (30° – 35°) with forest cover is assumed to have benefited from vegetation coverage but the same cannot be said for a very steep slope ($>35^{\circ}$). In the similar manner, the agriculture system (terraces) in the hilly areas is assumed to have relatively beneficial impacts on hill slope stability. In this study, the values of vegetation index were divided into five classes: -1.0 to 0.2; 0.2 to 0.4; 0.4 to 0.6; 0.6 to 0.8; and 0.8 to 1.0 (Figure 3.10).

3.5 Research Methodology

In this study, three different methods namely, analytical hierarchy process (AHP), frequency ratio (FR) model and integrated AHP and FR model, to produce landslide susceptibility map in lower Mae Chaem watershed, northern Thailand, and later compare three landslide susceptibility maps of the selected area. Relevant thematic layers pertaining the causative factors had been generated using remote sensing data, field surveys and geographic information system (GIS) tools.

Finally, landslide susceptibility mapping was produced by three methods namely; AHP, FR model, and integrated AHP and FR model. In conventional weighting system, weights and ratings to the causative factors and their categories are assigned based on the three different methods. To calculate the landslide susceptibility value, the landslide susceptibility index (LSI) was calculated by summation of each class's rating multiplied by the weight of each factor. Maps of these factors were made using the LSI value index, which is grouped into five classes with natural breaks algorithm. These are very high susceptibility (VHS), high susceptibility (HS), moderate susceptibility (MS), low susceptibility (LS) and very low susceptibility (VLS) zones. Finally, the three analytical results were verified using 25 known landslide locations that recorded by the local authorities in the last decade. The research procedure is schematically shown in Figure 3.14.

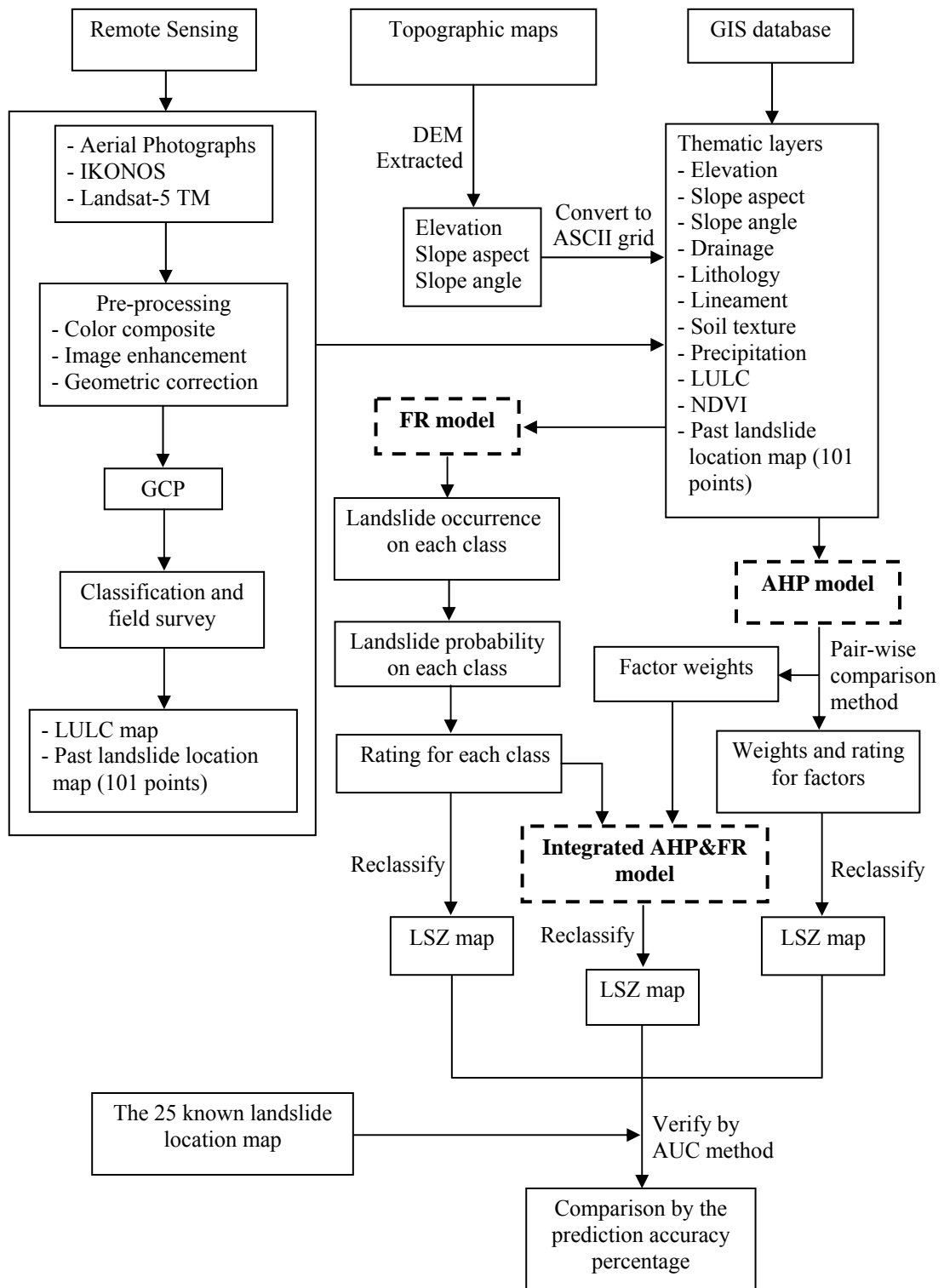


Figure 3.14 Flow diagram showing research procedure.

3.5.1 Analytical Hierarchy Process (AHP)

Analytical hierarchy process (AHP) is a semi-qualitative method, which involves a matrix-based pair-wise comparison of the contribution of different factors for landsliding. The AHP is a Multi-Criteria Decision Making (MCDM) tool at the core of which lies a method for converting subjective assessments of relative importance to a set of overall scores or weights.

AHP was developed by Saaty (1980). Factor weights for each criterion are determined by a pair-wise comparison matrix as described by Saaty (1990, 1994), and Saaty and Vargas (2001). To get factor weights in AHP, one has to build a pair-wise comparison matrix with scores given in Table 3.5. In the construction of a pair-wise comparison matrix, each factor is rated against every other factor by assigning a relative dominant value between 1 and 9 to the intersecting cell (Table 3.5). When the factor on the vertical axis is more important than the factor on the horizontal axis, this value varies between 1 and 9. Conversely, the value varies between the reciprocals $1/2$ and $1/9$. Since we have ten parameters, the comparison matrix has 100 boxes. However, because pair-wise comparison matrices are symmetrical in nature, only 55 values were needed to fill in the diagonal and the lower triangular half of the matrix. Then, in order to compute the principal eigenvector of the matrix and obtain a best-fit set of factor weights automatically in the way Saaty (1994) and Saaty and Vargas (2001) have described, raster maps produced by combining the parameters with landslide distribution were necessary.

In this study, AHP considers weighting and rating system developed by collecting questionnaires from expert opinions and the concerned organization research such as Department of Mineral Resources and Land Development

Department, and the selection of the appropriate criteria and scores were guided by 20 experts from various Thai government officials (Table A3 in Appendix A). The diagonal boxes of a pair-wise comparison matrix always take a value of 1. The boxes in the upper and lower halves are symmetrical with one another and the corresponding values are, therefore, reciprocal with each other. Once the matrix is constructed, weights whose sum equals one, will be obtained by computer based image processor with thematic layers of all causal factors categorized on the basis of class weights as inputs. But, when the parameters are few, weights can also be derived by a series of simple summation and division processes. The weights are then considered as the average of all possible ways of comparing the causal factors (Malczewski, 1999).

Table 3.5 Scale of preference between two parameters in AHP (Saaty, 2000).

Scales	Degree of preferences	Explanation
1	Equally	Two activities contribute equally to the objective.
3	Moderately	Experience and judgment slightly to moderately favor one activity over another.
5	Strongly	Experience and judgment strongly or essentially favor one activity over another.
7	Very strongly	An activity is strongly favored over another and its dominance is showed in practice.
9	Extremely	The evidence of favoring one activity over another is of the highest degree possible of an affirmation.
2, 4, 6, 8	Intermediate values	Used to represent compromises between the preferences in weights 1, 3, 5, 7 and 9.
Reciprocals	Opposites	Used for inverse comparison.

3.5.2 Probability Analysis–Frequency Ratio (FR) Model

The probability analysis–FR model is a quantitative method, which has comprised the analysis of the relationship between landslide occurrence and factor maps, and the calculation of frequency ratio. The spatial relationships between the landslide location and each landslide-related factor were analyzed by using the FR model. The frequency ratio, a ratio between the occurrence and absence of landslides

in each cell, was calculated for each factor's type (or range) that had been identified as significant with respect to causing landslides. An area ratio for each factor's type (or range) to the total area was calculated. Finally, frequency ratios for each factor's type (or range) were calculated by dividing the landslide occurrence ratio by the area ratio.

The frequency ratio is typically used as a guide to where further landslides are likely to occur. If the ratio is greater than 1, the relationship between landslides and the factor's type (or range) is higher and, if the ratio is less than 1, the relationship between landslide and each factor's type (or range) is lower. The ratios were used for calculating the landslide susceptibility index and mapping.

3.5.3 Integrated AHP and FR Model

The integrated AHP and FR model is a hybrid method between qualitative and quantitative methods. In this approach, the rating of each data class was determined using probability-frequency ratio (FR) model and the weight for each factor were given by AHP technique. The final step of this method is the combination of all weights and rating into a single map and the classification on the scores of this map into landslide susceptibility categories (Figure 3.15).

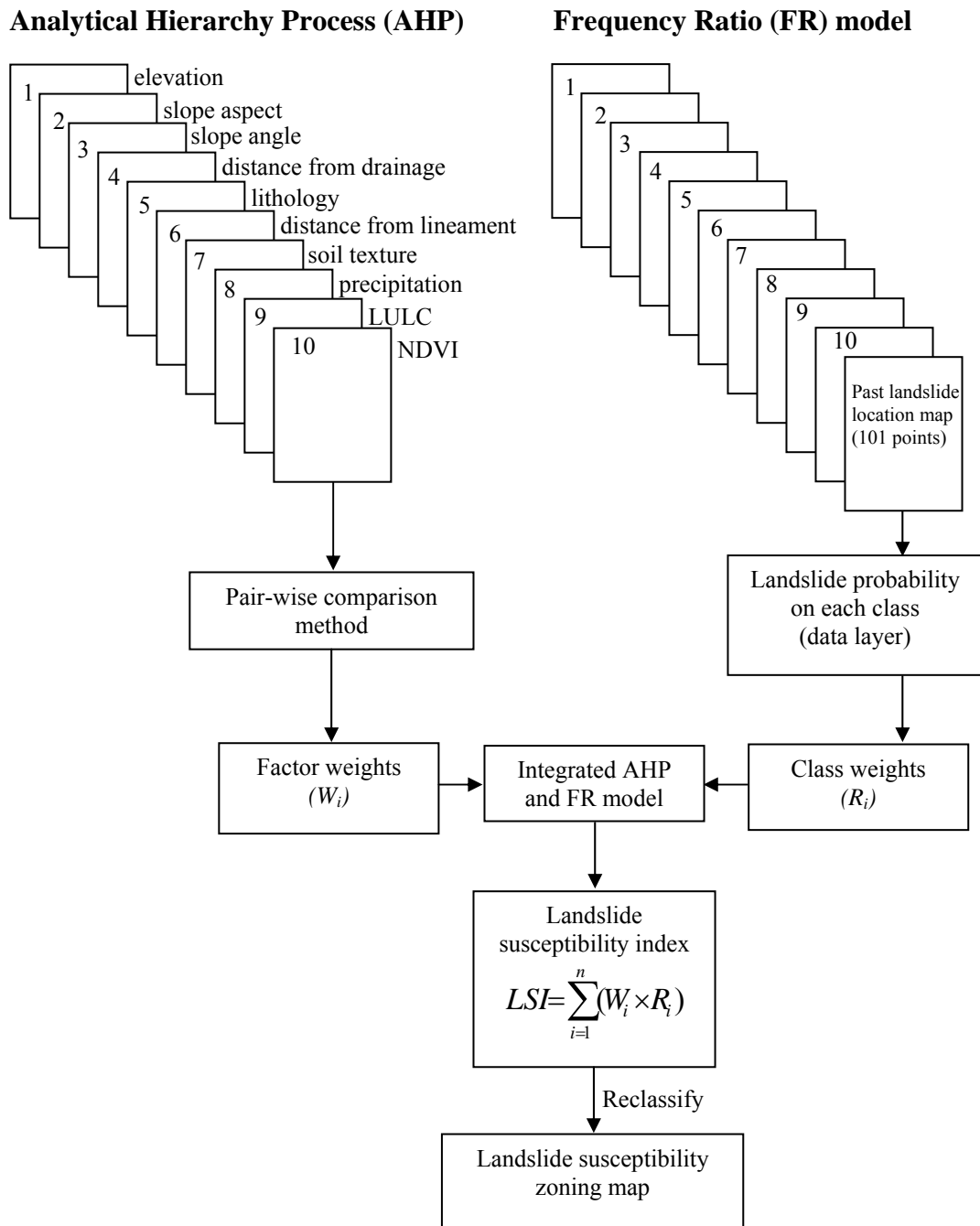


Figure 3.15 Flow chart of integrated AHP and FR model.

3.6 Area Under the Curve (AUC) Method

Finally, the susceptibility maps produced from AHP, FR model, and integrated AHP and FR model were verified using known landslide locations where the area under curve method (Lee et al., 2004a) was used. Verification was performed by comparing the 25 known landslide locations data with the landslide susceptibility map. Each factor was used and frequency ratios were compared. The rate curves were created and their areas under curve were calculated for all cases. The rate explains how well the model and factors predict the landslide occurrences. Therefore, the area under curve line can assess the prediction accuracy qualitatively. To obtain the relative ranks for each prediction pattern, the calculated index values of all cells in the study area were sorted in descending order. Then the ordered cell values were divided into 100 classes, with accumulated 1% intervals. The rate verification results appear as a line. To compare the quantitative result, the areas under curve (AUC) were re-calculated as the total area is 1, which means perfect prediction accuracy.

CHAPTER IV

RESULTS

4.1 Landslide Susceptibility Zoning Map

The preparation of landslide susceptibility zoning (LSZ) map is a major step forward in hazard management. In this study, factor maps can be prepared by GIS-based qualitative and quantitative techniques which useful to analyze the relationship between landslides and their influencing parameters. Remote sensing and GIS based methodology for LSZ maps are also presented in this study. The weight and rating system based on the relative importance of various causative factors as derived from remotely sensed data and other thematic maps was carried out (Saha et al., 2002).

A direct mapping approach will be used to establish the five different LSZ using classical overlay operations after having established maps representing major landslide influencing factors. The factors being used include elevation, slope aspect, slope angle, distance from drainage, lithology, distance from lineament, soil texture, precipitation, land use/land cover and NDVI. The different classes of thematic layers are assigned the corresponding weights and rating value as attribute information in the GIS and an “attribute map” is generated for each data layer. Summations of these attribute maps are then multiplied by the corresponding weights and rating to yield the landslide susceptibility index (LSI) for each grid cell.

The basic pre-requisite for landslide susceptibility zonation studies is the determination of weight and rating values representing the relative importance of

factors and their categories respectively for landslide occurrence. In this study, these weights and ratings are determined based on three different methods namely, analytical hierarchy process (AHP), frequency ratio (FR) model and integrated AHP and FR model, the weights and rating for each parameters were multiplied by the relevant parameter maps and then, all the weights and rating parameter maps were overlaid. In this way, a map having continuous scale of numerical values was obtained. The weight and rating were assigned to each attribute layer and their respective classes. A summation of these layers was carried out and the cumulative score was regrouped into five classes. A judicious way for this classification is to use the relative natural breaks algorithm to separate the landslide susceptibility index into landslide susceptibility classes level. In this study, five landslide susceptibility classes were identified which are very high susceptibility (VHS), high susceptibility (HS), moderate susceptibility (MS), low susceptibility (LS) and very low susceptibility (VLS) zones.

4.2 Application of AHP and Susceptibility Map

The final result consists of the factor weights and class weights, and a calculated consistency ratio (CR), as seen in Table 4.1 (For more details, see Appendices A–C). In AHP, the consistency used to build a matrix is checked by a consistency ratio, which depends on the number of parameters. For a 10×10 matrix, the CR must be less than 0.1 to accept the computed weights. The CR is a ratio between the matrix's consistency index and random index, and in general ranges from 0 to 1. The random index is the average consistence index obtained by generating

large numbers of random matrices. A CR close to 0 indicates the high probability that the weights were generated randomly (Saaty, 1980; 1994).

The models with a CR greater than 0.1 were automatically rejected, a CR less than 0.1 were often acceptable. With the AHP method, the values of spatial factors weights were defined. Using a weighted linear sum procedure (Voogd, 1983), the acquired weights were used to calculate the landslide susceptibility. In this study, the CR is 0.068, the ratio indicates a reasonable level of consistency in the pair-wise comparison, that good enough to recognize the factor weights. Consequently, the weight corresponding to precipitation is highest, whereas elevation is lowest (Table 4.1). For all cases of class weights, the CRs less than 0.1, the ratio indicates a reasonable level of consistency in the pair-wise comparison, that good enough to recognize the class weights.

Table 4.1 The pair-wise comparison matrix, factor weights, class weights (rating) and consistency ratio.

Factors	1	2	3	4	5	6	7	8	9	10	11	12	Rating
<i>Elevation (m)</i>													
(1) <600	1												0.027
(2) 600 – 800	2	1											0.037
(3) 800 – 1,000	3	2	1										0.059
(4) 1,000 – 1,200	4	3	2	1									0.087
(5) 1,200 – 1,400	5	4	3	2	1								0.126
(6) 1,400 – 1,600	7	6	5	4	3	1							0.239
(7) >1,600	9	8	7	6	5	3	1						0.426
Consistency ratio: 0.040													
<i>Slope aspect</i>													
(1) Flat	1												0.026
(2) North	3	1											0.071
(3) Northeast	5	3	1										0.189
(4) East	3	1	1/3	1									0.071
(5) Southeast	3	1	1/3	1	1								0.071
(6) South	3	1	1/3	1	1	1							0.071
(7) Southwest	7	5	3	5	5	5	1						0.354
(8) West	3	1	1/3	1	1	1	1/5	1					0.071
(9) Northwest	3	1	1/3	1	1	1	1/5	1	1				0.071
Consistency ratio: 0.008													

Table 4.1 The pair-wise comparison matrix, factor weights, class weights (rating) and consistency ratio (Continued).

Factors	1	2	3	4	5	6	7	8	9	10	11	12	Rating
Slope angle													
(1) 0° – 5°	1												0.024
(2) 5° – 10°	2	1											0.031
(3) 10° – 15°	3	2	1										0.048
(4) 15° – 20°	4	3	2	1									0.069
(5) 20° – 25°	5	4	3	2	1								0.103
(6) 25° – 30°	6	5	4	3	2	1							0.146
(7) 30° – 35°	7	6	5	4	3	2	1						0.205
(8) >35°	9	8	7	6	5	4	3	1					0.378
Consistency ratio: 0.037													
Drainage (m)													
(Distance from drainage)													
(1) <500	1												0.462
(2) 500 – 1,000	1/3	1											0.255
(3) 1,000 – 1,500	1/5	1/3	1										0.138
(4) 1,500 – 2,000	1/7	1/5	1/3	1									0.067
(5) 2,000 – 2,500	1/8	1/6	1/4	1/2	1								0.048
(6) >2,500	1/9	1/7	1/5	1/3	1/2	1							0.032
Consistency ratio: 0.045													
Lithology													
(1) Sandstone	1												0.124
(2) Marble	1/3	1											0.053
(3) Limestone, shale	1/3	1	1										0.053
(4) Paragneiss	1/2	2	2	1									0.083
(5) Alluvium	1/5	1/3	1/3	1/4	1								0.024
(6) Shale, chert, and siltstone	1/3	1	1	1/2	3	1							0.053
(7) Claystone and siltstone	1/4	1/2	1/2	1/3	2	1/2	1						0.031
(8) Granite	3	5	5	4	7	5	6	1					0.273
(9) Conglomerate, sandstone	1	3	3	2	5	3	4	1/3	1				0.124
(10) Granodiorite porphyry	2	4	4	3	6	4	5	1/2	2	1			0.187
Consistency ratio: 0.017													
Lineament (m)													
(Distance from lineament)													
(1) <500	1												0.293
(2) 500 – 1,000	1	1											0.293
(3) 1,000 – 2,000	1/2	1/2	1										0.177
(4) 2,000 – 3,000	1/3	1/3	1/2	1									0.107
(5) 3,000 – 4,000	1/4	1/4	1/3	1/2	1								0.067
(6) >4,000	1/4	1/4	1/3	1/2	1	1							0.067
Consistency ratio: 0.008													
Soil texture													
(1) Clay	1												0.019
(2) Loam	4	1											0.055
(3) Sand	8	5	1										0.238
(4) Sandy loam / sandy clay loam	7	4	1/2	1									0.169
(5) Loam with gravel	5	2	1/4	1/3	1								0.086
(6) Sandy loam with gravel	9	6	2	3	5	1							0.335
(7) Clay/loam with rock	3	1/2	1/6	1/5	1/3	1/7	1						0.039
(8) Slope complex area	4	1	1/5	1/4	1/2	1/6	2	1					0.055
Consistency ratio: 0.034													

Table 4.1 The pair-wise comparison matrix, factor weights, class weights (rating) and consistency ratio (Continued).

Factors	1	2	3	4	5	6	7	8	9	10	11	12	Rating
Precipitation (mm)													
(1) <1,000	1												0.027
(2) 1,000 – 1,200	2	1											0.036
(3) 1,200 – 1,400	3	2	1										0.053
(4) 1,400 – 1,600	5	4	3	1									0.103
(5) 1,600 – 1,800	6	5	4	2	1								0.143
(6) 1,800 – 2,000	8	7	6	4	3	1							0.266
(7) >2,000	9	8	7	5	4	2	1						0.376
Consistency ratio: 0.049													
Land use/land cover													
(1) Paddy field	1												0.137
(2) Mixed field crop	1/2	1											0.090
(3) Longan	1/3	1/2	1										0.063
(4) Truck crop	1/2	1	2	1									0.090
(5) Mixed swidden cultivation	1/2	1	2	1	1								0.090
(6) Hill evergreen forest	1/7	1/6	1/5	1/6	1/6	1							0.017
(7) Mixed deciduous forest	1/6	1/5	1/4	1/5	1/5	2	1						0.023
(8) Mixed forest plantation	1/5	1/4	1/3	1/4	1/4	3	2	1					0.033
(9) Grass and scrub	1/4	1/3	1/2	1/3	1/3	4	3	2	1				0.045
(10) Mine	2	3	4	3	3	8	7	6	5	1			0.200
(11) Urban, village	2	3	4	3	3	8	7	6	5	1	1		0.200
(12) Water	1/8	1/7	1/6	1/7	1/7	1/2	1/3	1/4	1/5	1/9	1/9	1	0.013
Consistency ratio: 0.039													
NDVI													
(1) -1.0 to 0.2	1												0.502
(2) 0.2 to 0.4	1/3	1											0.256
(3) 0.4 to 0.6	1/5	1/3	1										0.120
(4) 0.6 to 0.8	1/6	1/4	1/2	1									0.074
(5) 0.8 to 1.0	1/7	1/5	1/3	1/2	1								0.050
Consistency ratio: 0.031													
Data layers	1	2	3	4	5	6	7	8	9	10	11	12	Weights
Elevation	1												0.027
Slope aspect	1	1											0.030
Slope angle	5	4	1										0.165
Drainage	2	1/2	1/5	1									0.034
Lithology	5	5	2	3	1								0.170
Lineaments	3	5	1/2	4	1/2	1							0.121
Soil texture	2	3	1/5	3	1/2	1/3	1						0.054
Precipitation	5	6	2	5	3	3	5	1					0.259
Land use	4	4	1/3	3	1/4	1/3	3	1/5	1				0.082
NDVI	3	3	1/5	2	1/5	1/4	2	1/5	1/2	1			0.057
Consistency ratio: 0.068													

For landslide susceptibility analysis, using the factor weights and rating (Table 4.1) of AHP, the landslide susceptibility index (LSI) values were computed by summation of each factor's rating multiplied by the weight of each of the factors by using the following as Eq.(1).

$$LSI = \sum_{i=1}^n (W_i \times R_i) \dots\dots\dots (1)$$

Where LSI = Landslide susceptibility index

R_i = Ratings for the categories of the layers

W_i = Weights for the layers

From the calculation, it was found that the LSI had a minimum value of 0.04, and a maximum value of 0.28, with an average value of 0.11 and a standard deviation of 0.03. The LSI represents the relative susceptibility of a landslide occurrence. Therefore, the higher the index, the more susceptible the area is to landslide. If the LSI value is high, there is a higher susceptibility to landslides, a lower value indicates a lower susceptibility to landslides. These LSI values were divided into five classes based on the natural breaks range which represent five different zones in the landslide susceptibility map. These are very high susceptibility (VHS), high susceptibility (HS), moderate susceptibility (MS), low susceptibility (LS) and very low susceptibility (VLS) zones (Figure 4.1), and percentage covering areas of each susceptibility map are shown in Table 4.2.

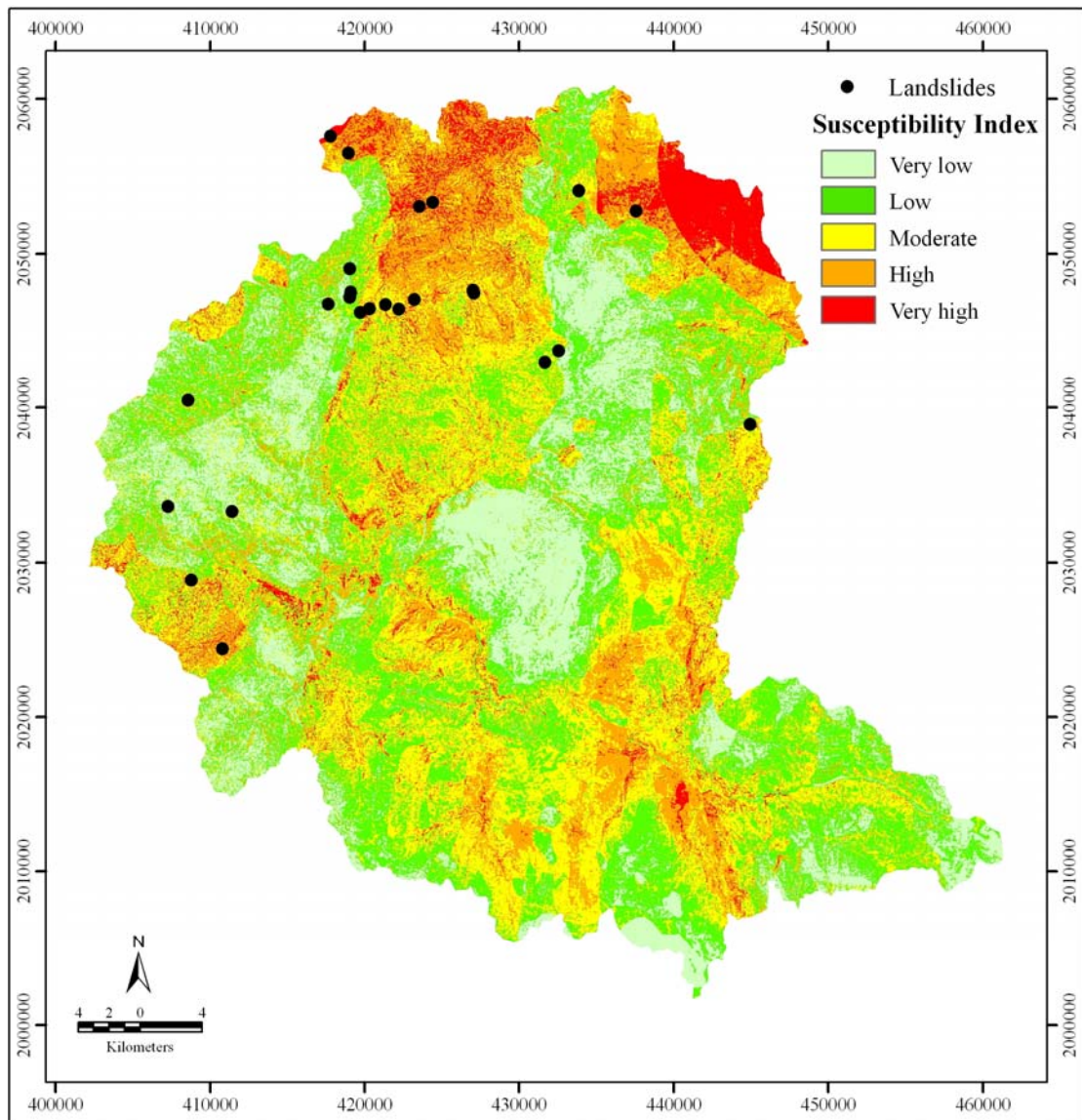


Figure 4.1 The landslide susceptibility map based on AHP with 25 known landslide locations on the basis of natural breaks classification.

Table 4.2 Landslide susceptibility classes, susceptibility index values and coverage percentage of the study area based on AHP.

Landslide Susceptibility Classes	Susceptibility index values	% of Area
Very low susceptibility (VLS)	0.04 – 0.08	18.86
Low susceptibility (LS)	0.08 – 0.11	29.32
Moderate susceptibility (MS)	0.11 – 0.13	28.47
High susceptibility (HS)	0.13 – 0.16	17.84
Very high susceptibility (VHS)	0.16 – 0.28	5.51

4.3 Application of Probability Analysis–Frequency Ratio (FR) Model and Susceptibility Map

4.3.1 Relationship between Landslides and Landslide Related Factors

The frequency ratios for all factors involved in the study are shown in Table 4.3. These FR values indicate level of correlation between locations of the landslide to these factors. The relationship between landslide occurrence and elevation shows that elevation below 1,000 m, the frequency ratio was lower than 1.0, which indicates a low landslide occurrence probability, and for elevation above 1,000 m, the frequency ratio was greater than 1.0, indicating a high landslide occurrence probability. This result means that the landslide probability increases with elevation.

In the case of slope aspect, landslides were most abundant on south-facing and southeast-facing slopes. Thus, slopes facing to the south and southeast are highly susceptible to landslides, whereas the frequency of landslide was lowest on southwest-facing slope.

In the case of slope angle, steeper slopes have greater landslide probabilities. Below a slope of 15° , the ratio was lower than 1.0, which indicates a very low probability of landslide occurrence. For slopes above 15° , the ratio was greater than 1.0, which indicates a high probability of landslide occurrence. This result means that the landslide probability increases with slope angle.

In the case of distance from drainage, from 0 to 2,000 m the ratio was greater than 1.0, indicating a high probability of landslide occurrence, and for distances above 2,000 m, the ratio was lower than 1.0, indicating a low probability. This result means that the landslide probability decreases with distance from drainage.

Table 4.3 Frequency ratio of landslide occurrence.

Factors	Class	Total number of pixels		Landslide occurrence point		Frequency ratio
		Number	%	Number	%	
Elevation	<600 m	558848	18.08	5	4.95	0.27
	600 m – 800 m	792967	25.65	20	19.80	0.77
	800 m – 1,000 m	782359	25.31	15	14.85	0.59
	1,000 m – 1,200 m	556841	18.01	24	23.76	1.32
	1,200 m – 1,400 m	280165	9.06	17	16.83	1.86
	1,400 m – 1,600 m	82504	2.67	16	15.84	5.93
	>1,600 m	37750	1.21	4	3.96	3.27
Slope aspect	Flat	161640	5.23	0	0	0
	North	349342	11.30	10	9.90	0.88
	Northeast	400242	12.95	13	12.87	0.99
	East	381664	12.35	12	11.88	0.96
	Southeast	367056	11.87	19	18.81	1.58
	South	340197	11.00	20	19.80	1.80
	Southwest	361455	11.69	6	5.94	0.51
	West	369212	11.94	11	10.89	0.91
	Northwest	360630	11.67	10	9.90	0.85
Slope angle	0° – 5°	611786	19.79	17	16.83	0.85
	5° – 10°	192901	6.24	0	0	0
	10° – 15°	435856	14.1	6	5.94	0.42
	15° – 20°	563190	18.22	24	23.76	1.30
	20° – 25°	490770	15.88	16	15.84	1.00
	25° – 30°	354860	11.48	18	17.82	1.55
	30° – 35°	214174	6.93	13	12.87	1.86
Drainage (Distance from drainage)	<500 m	1215767	39.32	34	33.66	0.86
	500 m – 1,000 m	831347	26.91	30	29.70	1.10
	1,000 m – 1,500 m	488601	15.80	18	17.82	1.13
	1,500 m – 2,000 m	246753	7.98	12	11.88	1.49
	2,000 m – 2,500 m	143219	4.63	4	3.96	0.86
	>2,500 m	165604	5.36	3	2.97	0.55
Lithology	Sandstone	177214	5.73	6	5.94	1.04
	Marble	27624	0.89	0	0	0
	Limestone, shale	331381	10.72	5	4.95	0.46
	Paragneiss	311446	10.07	9	8.91	0.88
	Alluvium	79856	2.59	1	0.99	0.38
	Shale, chert, and siltstone	378938	12.26	24	23.76	1.94
	Claystone and siltstone	47749	1.54	0	0	0
	Granite	858729	27.77	56	55.45	2.00
	Conglomerate, sandstone	1715	0.06	0	0	0
	Granodiorite porphyry	877139	28.37	0	0	0
Lineament (Distance from lineament)	<500 m	316662	10.24	16	15.84	1.55
	500 m – 1,000 m	293989	9.51	13	12.87	1.35
	1,000 m – 2,000 m	542593	17.55	21	20.79	1.18
	2,000 m – 3,000 m	435286	14.08	12	11.88	0.84
	3,000 m – 4,000 m	333239	10.78	9	8.91	0.83
>4,000 m	1170022	37.84	30	29.70	0.78	
Soil texture	Clay	59053	1.9	0	0	0
	Loam	5896	0.19	0	0	0
	Sand	11151	0.36	0	0	0
	Sandy loam/sandy clay loam	6343	0.2	0	0	0
	Loam with gravel	207200	6.7	0	0	0
	Sandy loam with gravel	203365	6.57	2	1.98	0.30
	Clay/loam with rock	11651	0.37	0	0	0
	Slope complex area	2587132	83.68	99	98.02	1.17

Table 4.3 Frequency ratio of landslide occurrence (Continued).

Factors	Class	Total number of pixels		Landslide occurrence point		Frequency ratio
		Number	%	Number	%	
Precipitation	<1,000 mm	820402	26.52	20	19.80	0.75
	1,000 mm – 1,200 mm	1160632	37.52	35	34.65	0.92
	1,200 mm – 1,400 mm	578674	18.71	24	23.76	1.27
	1,400 mm – 1,600 mm	350627	11.34	15	14.86	1.31
	1,600 mm – 1,800 mm	100290	3.24	4	3.96	1.22
	1,800 mm – 2,000 mm	47775	1.54	2	1.98	1.29
	>2,000 mm	34700	1.12	1	0.99	0.88
Land use/land cover	Paddy field	60629	1.96	0	0	0
	Mixed field crop	29575	0.96	4	3.96	4.13
	Longan	3258	0.11	0	0	0
	Truck crop	2528	0.08	0	0	0
	Mixed swidden cultivation	190965	6.18	17	16.83	2.72
	Hill evergreen forest	585675	18.94	28	27.72	1.46
	Mixed deciduous forest	2085444	67.45	52	51.49	0.76
	Mixed forest plantation	110816	3.58	0	0	0
	Grass and scrub	5803	0.19	0	0	0
	Mine	1520	0.05	0	0	0
	Urban, village	13443	0.43	0	0	0
	Water	2135	0.07	0	0	0
NDVI	-1.0 to 0.2	609023	19.69	4	3.96	0.20
	0.2 to 0.4	817512	26.44	28	27.72	1.05
	0.4 to 0.6	856906	27.72	30	29.70	1.07
	0.6 to 0.8	724519	23.43	36	35.64	1.52
	0.8 to 1.0	83831	2.71	3	2.97	1.10

Total number of pixels in study area: 3,091,791.

Number of landslide occurrence points: 101.

FR = % Landslide occurrence points / % number of pixels

In the case of lithology, the frequency ratio was highest in granite rock areas, and was lowest in alluvium areas. In the case of distance from lineament, for below a distance of 2,000 m, the ratio was greater than 1.0, indicating a high probability of landslide occurrence, and for distances above 2,000 m, the ratio was lower than 1.0, indicating a low probability. This result means that the landslide probability decreases with distance from lineament.

In the case of soil texture, the landslide occurrence probability value was higher in slope complex areas, and was lower in gravelly sandy loam.

In the case of precipitation, for a precipitation amount below 1,200 mm, the frequency ratio was lower than 1.0, which indicates a low landslide occurrence

probability, and for a precipitation amount above 1,200 mm, the frequency ratio was greater than 1.0, indicating a high landslide occurrence probability. This result means that the landslide probability increases with the precipitation amount.

In the case of land use/land cover, the landslide-occurrence values were higher in mixed field crop and mixed swidden cultivation areas, and lower in hill evergreen forest and mixed deciduous forest areas.

In the case of NDVI, for NDVI values below 0.2, the frequency ratio was lower than 1.0, which indicates a low landslide occurrence probability, and for NDVI values above 0.2, the frequency ratio was greater than 1.0, indicating a high landslide occurrence probability. This result means that the landslide probability increases with the vegetation index value. This could be due to more vegetation seen along structurally weaker zones.

4.3.2 Landslide Susceptibility Mapping

For FR model, the landslide susceptibility index (LSI) values were computed using Eq.(2) where the frequency ratios of each factor's type (or range) were summed to find its LSI:

$$LSI = \sum Fr \dots\dots\dots (2)$$

where Fr = the frequency ratio of each factor's type (or range).

Using the frequency ratio, the relationship was used as each factor's rating in the overlay analysis. From the calculation, it was found that the LSI had a minimum value of 3.17, and a maximum value of 20.63, with an average value of 9.96 and a standard deviation of 2.56. If the LSI value was high, there was a higher susceptibility to landslides, a lower value indicates a lower susceptibility to landslides. The

landslide susceptibility map calculated for FR model is shown in Figure 4.2, and percentage covering areas of each susceptibility map are shown in Table 4.4.

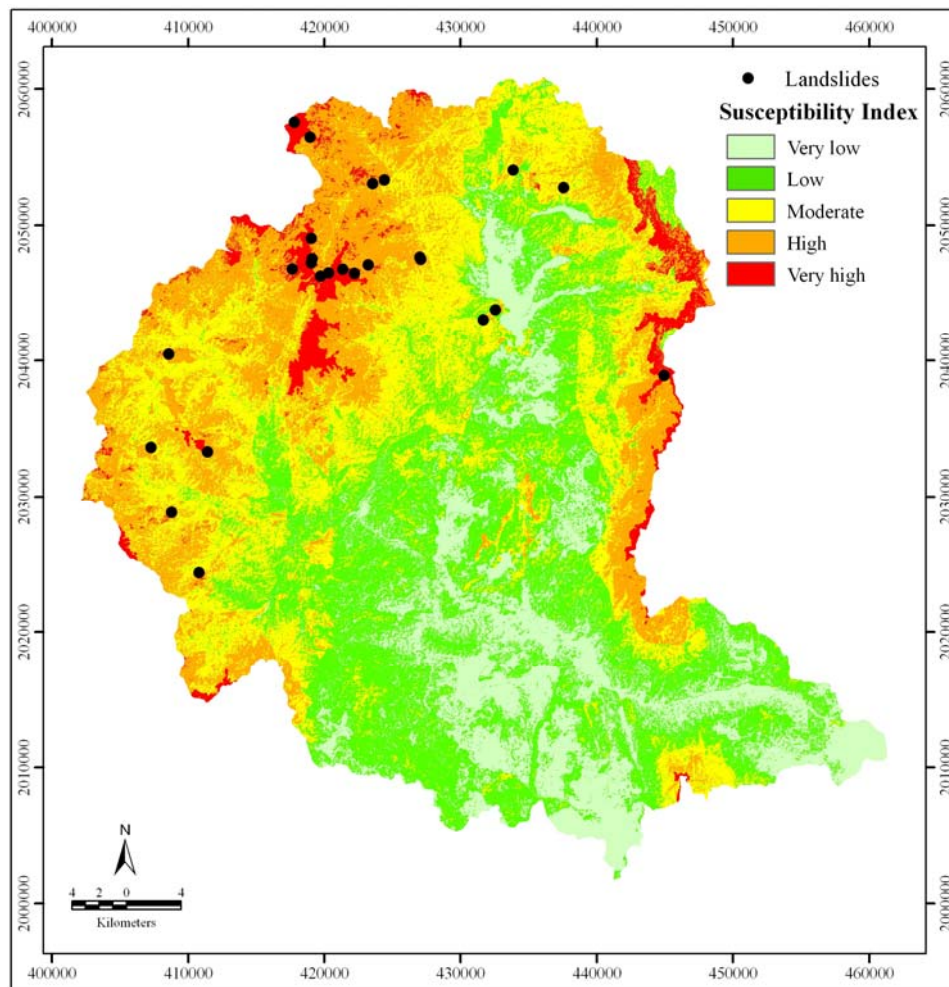


Figure 4.2 The landslide susceptibility map based on FR model with 25 known landslide locations on the basis of natural breaks classification.

Table 4.4 Landslide susceptibility classes, susceptibility index values and coverage percentage of the study area based on FR model.

Landslide Susceptibility Classes	susceptibility index values	% of Area
Very low susceptibility (VLS)	3.17 – 7.54	17.80
Low susceptibility (LS)	7.54 – 9.72	30.42
Moderate susceptibility (MS)	9.72 – 11.83	27.58
High susceptibility (HS)	11.83 – 14.56	20.49
Very high susceptibility (VHS)	14.56 – 20.63	3.71

4.4 Application of Integrated AHP and FR Model and Susceptibility

Map

The integration of 10 thematic layers representing the ratings for the categories (R_i) of the layers (obtained from FR) and weights for the layers (W_i) (obtained from AHP) was performed by using simple arithmetic overlay operation in GIS. Hence, this procedure has been named here as integrated AHP and FR model. The LSI for each pixel of the study area was thus obtained by using the following equation.

Using AHP and FR model were used to calculate the weights and rating for landslide susceptibility analysis (Table 4.5). To calculate the landslide susceptibility value, the landslide susceptibility index (LSI) was calculated by summation of each factor's rating multiplied by the weight of each of the factors, as per Eq.(3). The LSI represents the relative susceptibility of a landslide occurrence. Therefore, the higher the index, the more susceptible the area is to landslide. If the LSI value is high, there is a higher susceptibility to landslides, a lower value indicates a lower susceptibility to landslides.

$$LSI = \sum_{i=1}^n (W_i \times R_i) \dots\dots\dots (3)$$

Where LSI = Landslide susceptibility index

R_i = Ratings for the categories of the layers (obtained from FR)

W_i = Weights for the layers (obtained from AHP)

For each factor, the data layers of factors that affect the suitability of landslide occurrences for ten factors were then reclassified so that they could be used as rating maps required in the process. The calculated weight values are then transferred to the

ArcGIS 9.0, and it was found that the LSI had a minimum value of 0.35, and a maximum value of 1.77, with an average value of 1.00 and a standard deviation of 0.27. The LSI values were found to lie in the range from 0.35 to 1.77, and percentage area covering by different landslide susceptibility zones are shown in Table 4.6. The success rate curve approach was used to classify the LSI values into five different susceptibility zones to produce the landslide susceptibility map (Figure 4.3).

Table 4.5 Weights from integrated AHP and FR model.

Factors	Class	AHP's factor weights	FR's class weights	Integrated AHP and FR
Elevation	<600 m	0.027	0.27	0.007
	600 m – 800 m		0.77	0.021
	800 m – 1,000 m		0.59	0.016
	1,000 m – 1,200 m		1.32	0.036
	1,200 m – 1,400 m		1.86	0.050
	1,400 m – 1,600 m		5.93	0.160
	>1,600 m		3.27	0.088
Slope aspect	Flat	0.030	0	0
	North		0.88	0.026
	Northeast		0.99	0.030
	East		0.96	0.029
	Southeast		1.58	0.047
	South		1.80	0.054
	Southwest		0.51	0.015
	West		0.91	0.027
Slope angle	Northwest	0.165	0.85	0.026
	0° – 5°		0.85	0.140
	5° – 10°		0	0
	10° – 15°		0.42	0.069
	15° – 20°		1.30	0.215
	20° – 25°		1.00	0.165
	25° – 30°		1.55	0.256
	30° – 35°		1.86	0.307
Drainage (Distance from drainage)	>35°	0.034	0.94	0.155
	<500 m		0.86	0.029
	500 m – 1,000 m		1.10	0.037
	1,000 m – 1,500 m		1.13	0.038
	1,500 m – 2,000 m		1.49	0.051
	2,000 m – 2,500 m		0.86	0.029
>2,500 m	0.55	0.019		

Table 4.5 Weights from integrated AHP and FR model (Continued).

Factor	Class	AHP's factor weights	FR's class weights	Integrated AHP and FR
Lithology	Sandstone	0.170	1.04	0.177
	Marble		0	0
	Limestone, shale		0.46	0.078
	Paragneiss		0.88	0.150
	Alluvium		0.38	0.065
	Shale, chert, and siltstone		1.94	0.330
	Claystone and siltstone		0	0
	Granite		2.00	0.340
	Conglomerate, sandstone		0	0
	Granodiorite porphyry		0	0
Lineament (Distance from lineament)	<500 m	0.121	1.55	0.188
	500 m – 1,000 m		1.35	0.163
	1,000 m – 2,000 m		1.18	0.143
	2,000 m – 3,000 m		0.84	0.102
	3,000 m – 4,000 m		0.83	0.100
	>4,000 m		0.78	0.094
Soil texture	Clay	0.054	0	0
	Loam		0	0
	Sand		0	0
	Sandy loam/sandy clay loam		0	0
	Loam with gravel		0	0
	Sandy loam with gravel		0.30	0.016
	Clay/loam with rock		0	0
	Slope complex area		1.17	0.063
Precipitation	<1,000 mm	0.259	0.75	0.194
	1,000 mm – 1,200 mm		0.92	0.238
	1,200 mm – 1,400 mm		1.27	0.329
	1,400 mm – 1,600 mm		1.31	0.339
	1,600 mm – 1,800 mm		1.22	0.316
	1,800 mm – 2,000 mm		1.29	0.334
	>2,000 mm		0.88	0.228
Land use/ land cover	Paddy field	0.082	0	0
	Mixed field crop		4.13	0.339
	Longan		0	0
	Truck crop		0	0
	Mixed swidden cultivation		2.72	0.223
	Hill evergreen forest		1.46	0.120
	Mixed deciduous forest		0.76	0.062
	Mixed forest plantation		0	0
	Grass and scrub		0	0
	Mine		0	0
	Urban, village		0	0
	Water		0	0
NDVI	-1.0 to 0.2	0.057	0.20	0.011
	0.2 to 0.4		1.05	0.060
	0.4 to 0.6		1.07	0.061
	0.6 to 0.8		1.52	0.087
	0.8 to 1.0		1.10	0.063

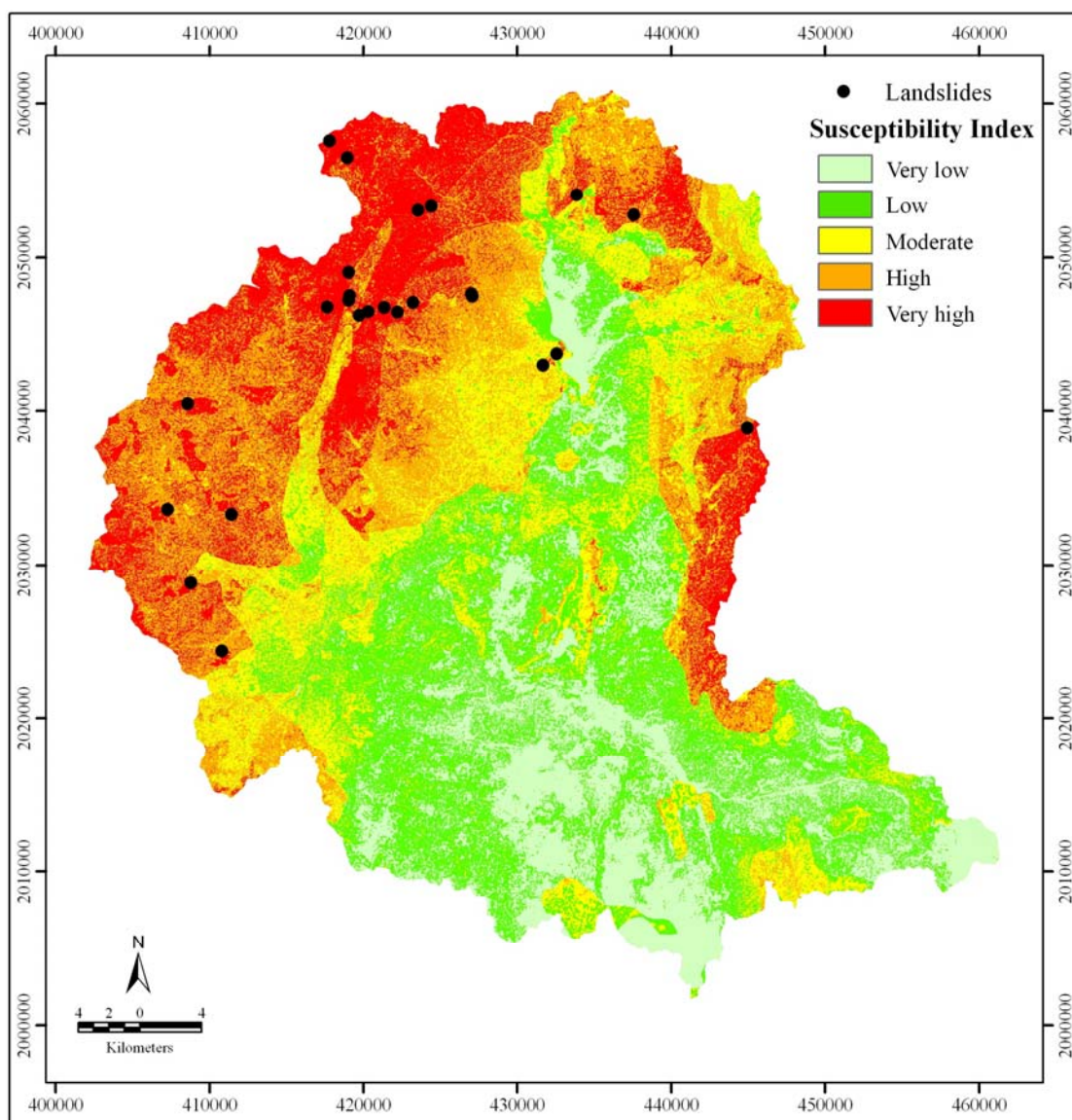


Figure 4.3 The landslide susceptibility map based on integrated AHP and FR model with 25 known landslide locations on the basis of natural breaks classification.

Table 4.6 Landslide susceptibility classes, susceptibility index values and coverage percentage of the study area based on integrated AHP and FR model.

Landslide Susceptibility Classes	susceptibility index values	% of Area
Very low susceptibility (VLS)	0.35 – 0.72	17.84
Low susceptibility (LS)	0.72 – 0.91	24.17
Moderate susceptibility (MS)	0.91 – 1.11	19.05
High susceptibility (HS)	1.11 – 1.30	22.57
Very high susceptibility (VHS)	1.30 – 1.77	16.37

Table 4.7 Compare percentage of area occupied by each landslide susceptibility class and the susceptibility index values between AHP, FR model and integrated AHP and FR model. The LSI ranges used in the classification were assigned using natural breaks algorithm.

Landslide Susceptibility Classes	AHP		FR model		Integrated AHP and FR model	
	LSI	% of Area	LSI	% of Area	LSI	% of Area
Very low susceptibility (VLS)	0.04 – 0.08	18.86	3.17 – 7.54	17.80	0.35 – 0.72	17.84
Low susceptibility (LS)	0.08 – 0.11	29.32	7.54 – 9.72	30.42	0.72 – 0.91	24.17
Moderate susceptibility (MS)	0.11 – 0.13	28.47	9.72 – 11.83	27.58	0.91 – 1.11	19.05
High susceptibility (HS)	0.13 – 0.16	17.84	11.83 – 14.56	20.49	1.11 – 1.30	22.57
Very high susceptibility (VHS)	0.16 – 0.28	5.51	14.56 – 20.63	3.71	1.30 – 1.77	16.37

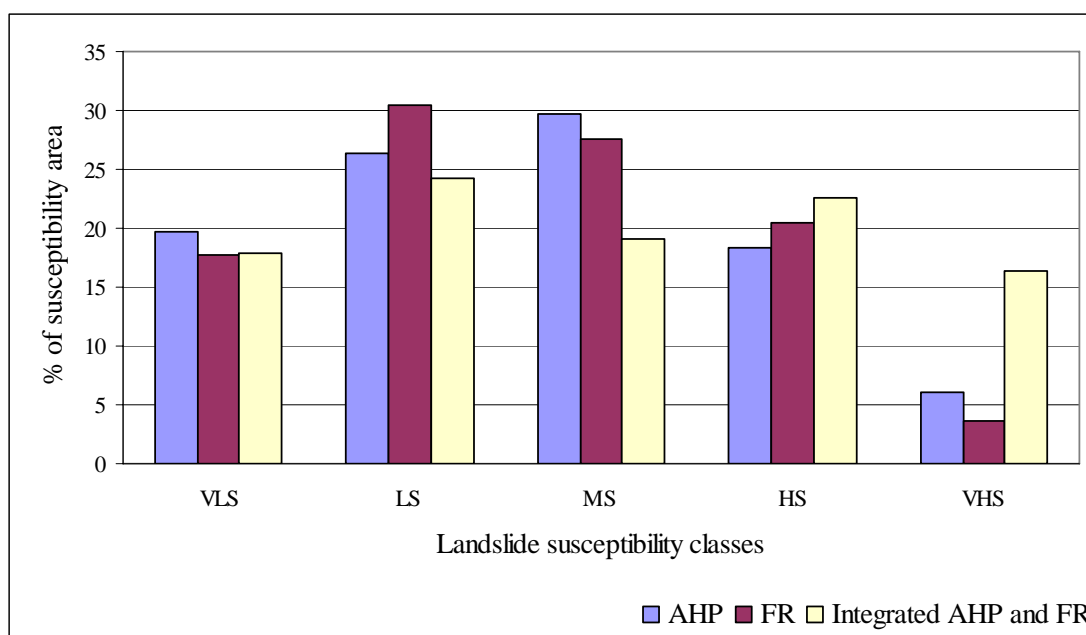


Figure 4.4 Histograms showing relative distribution of landslide susceptibility classes generated by AHP, FR model and integrated AHP and FR model.

4.5 Comparison and Verification of the Results

Finally, the susceptibility maps produced from AHP, FR model, and integrated AHP and FR model were verified using 25 known landslide locations where the area under curve (AUC) method (Lee et al., 2004a) was used.

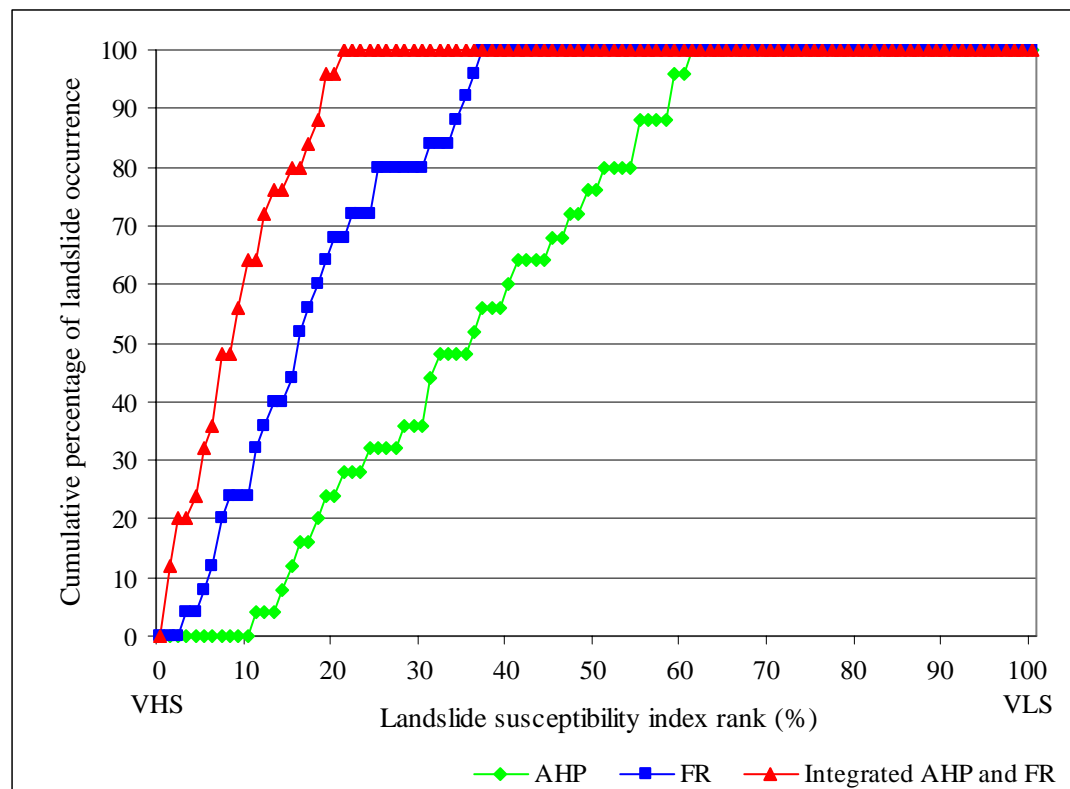


Figure 4.5 Illustration of cumulative frequency diagram showing landslide susceptibility index rank (x-axis) occurring in cumulative percent of landslide occurrence (y-axis).

The rate verification results appear as a line in Figure 4.5. For example, in case of AHP, 80–100% (20%) class of the study area where the landslide susceptibility index had a higher rank could explain 24% of all the landslides. In addition, the 70–100% (30%) class of the study area where the landslide susceptibility index had a higher rank could explain 36% of the landslides. In case of FR model, 90–

100% (10%) class of the study area where the landslide susceptibility index had a higher rank could explain 28% of all the landslides. In addition, the 80–100% (20%) class of the study area where the landslide susceptibility index had a higher rank could explain 68% of the landslides. In case of integrated AHP and FR model, 90–100% (10%) class of the study area where the landslide susceptibility index had a higher rank could explain 64% of all the landslides. In addition, the 80–100% (20%) class of the study area where the landslide susceptibility index had a higher rank could explain 96% of the landslides.

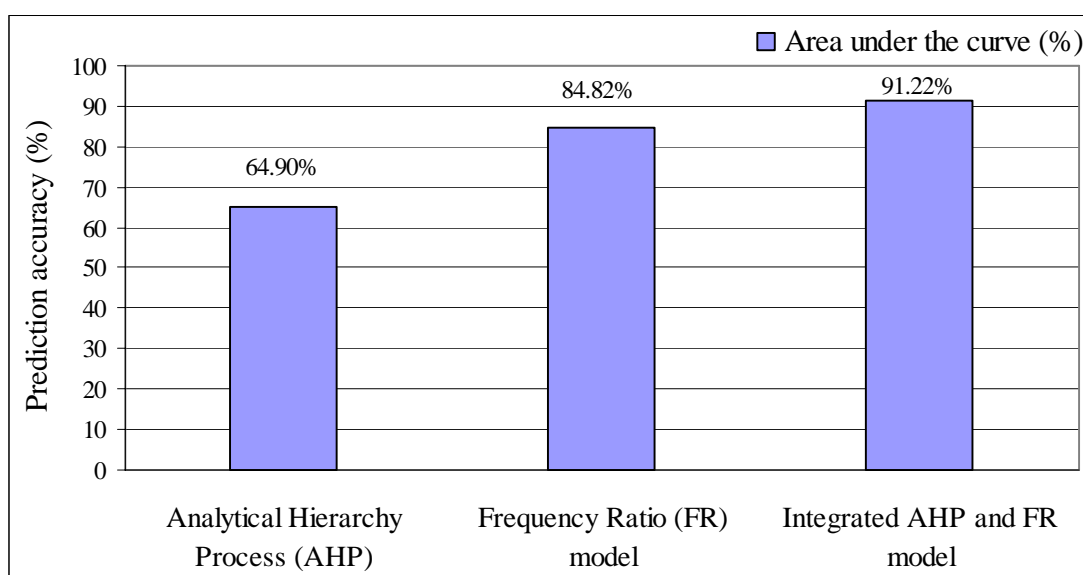


Figure 4.6 Histograms showing the percentage of prediction accuracy based on AUC method.

To compare the result quantitatively, the areas under curve line were re-calculated as the total area is 1 which means perfect prediction accuracy. So, the area under curve (AUC) can be used to assess the prediction accuracy qualitatively. The area under curve line is shown in Figure 4.5 and Figure 4.6. In the case of all factors, the case AHP used, the area ratio was 0.6490 and we could say the prediction

accuracy is 64.90%. In the case of FR model used, the area ratio was 0.8482 and we could say the prediction accuracy is 84.82%. In the case of integrated AHP and FR model used, the area ratio was 0.9122 and we could say the prediction accuracy is 91.22%.

CHAPTER V

CONCLUSIONS AND DISCUSSION

5.1 Conclusions

In this study, three different methods: the analytical hierarchy process (AHP), probability-frequency ratio (FR) model, and the integrated AHP and FR model were applied to develop landslide susceptibility maps for the lower Mae Chaem watershed located in northern Thailand. To achieve this objective, ten landslide inducing factors were taken into consideration which are elevation, slope aspect, slope angle, distance from drainage, lithology, distance from lineament, soil texture, precipitation, land use/land cover (LULC) and NDVI. The first eight parameters were extracted and calculated from their associated database while LULC and NDVI maps were derived from Landsat-5 TM satellite images. These factors were evaluated then factor weight and class weight were assigned to each associated factors based on the model used.

These given weights (for each unit area) were then assembled to create susceptibility maps as required (Figure 5.1a-c). From Table 4.7, about 23.35%, 24.20%, and 38.94% of the study area were classified to be in high or very high landslide risk zones according to the analysis by AHP, FR model, and integrated AHP and FR model, respectively.

Base on results of the pair-wise comparison of the AHP technique (Table 4.1), the three most influencing factors to induce landsliding activity (judged from its given weight) in the study area are precipitation (0.259), lithology (0.17), and slope angle

(0.165). And the three least influencing factors are elevation (0.027), slope aspect (0.03), and distance from drainage (0.034).

Based on the FR values seen in Table 4.3, areas notably vulnerable to the landslide activity are those located at altitudes greater than 1,400 m, areas that used for mixed field crop or mixed swidden cultivation, areas with slope angles of 25°-35°, and areas associated with granite or shale, chert, and siltstone terrains. In addition, there is no distinctive correlation seen for amount of rainfall classified and landslide occurrence probability which is rather contrast to result given by the AHP technique.

Output maps provided by the AHP, FR model, and integrated AHP and FR model were compared and their credibility was examined by the area under curve (AUC) method using 25 known landslide locations as reference. Results of the analysis indicate that maps produced from the AHP, FR model, and integrated AHP and FR model have achieved the accuracies of 64.90%, 84.82% and 91.22% respectively which are reasonably satisfied (except for the AHP technique). From these results, the integrated AHP and FR model has proved to be most effective in generating landslide susceptibility zonation map in the lower Mae Chaem watershed. These maps are very useful to the local authorities and responsible agencies because the data can help them in their decision-making and policy planning efforts in the near future.

5.2 Discussion

Though the FR model, and integrated AHP and FR model have been proved in this work to be an effective tool in the preparation of landslide susceptibility map at basin scale in local Thailand, but in theory, they still have some shortcomings in

themselves. For examples, it evaluates the importance of each used factor individually and ignores any spatial autocorrelation between them. As a result, some area might be overemphasized about the level of its proneness to landslide activity (with higher LSI values) if two or more important factors are highly correlated. Therefore, to reduce this problem, the selection of initial factors to be included in the analysis should be done carefully and this deficiency of the model should always be kept in mind.

In this work, detail of some factor like soil texture was not clearly identified by the available map as majority of the study area (about 83.68%) was simply classed as “slope complex area”. Therefore, it has only one highly dominant class existed for soil texture parameter. This is usually not appropriate for performing FR analysis as it should always have FR value close to unity for the dominant class and close to zero for all other classes. As a result, this kind of data can be omitted from the analysis without any serious consequences. It is also worth noting here that all factors included in the susceptibility must be static, or semi-static, parameters which means their given values are relatively constant (or change very slowly) over time. This is because the susceptibility analysis is typically having no “time-dimension” involved which makes its output maps valid for considerably long time. However, dynamic parameters, like earthquake and heavy rainfall can be included in the analysis as “triggering” factor of the landsliding activity and the new output map is generally called a “landslide hazard map” which also has time-dimension integrated (Chacon et al., 2006).

In addition, the FR-based model needs sufficient and well-distributed landslide data in order to determine the FR index properly (e.g. with less bias) which is still not satisfactory achieved in this thesis. However, by the advent of THEOS, the first earth observation satellite of Thailand (with 2-m spatial resolution in the panchromatic

mode) (GISTDA, 2009), the required data of future landslides that occur in the country should be more plausible. This will make the production of landslide susceptibility map in Thailand look more promising in the near future.

5.2.1 Landslide Occurrence in the Low Risk Zone

Though most of the observed landslide locations (that used as reference) were situated in the high or very high risk zones as expected but some of them (not many) were also found in the classified moderate or low risk zones (see Table 5.1 for detail). This unexpected result indicates limits of the model used (AHP in this case) that are difficult to avoid in this kind of study. This is because landsliding is a fairly complex phenomenon influenced by different factors in different places with different levels of the association. Therefore, every model must have some deficiencies in the simulating and predicting of landslide activity observed in the interested area.

Table 5.1 Allocation of the 25 referred landslide events to each susceptibility class defined by the AHP, FR model, and integrated AHP and FR model.

Landslide Susceptibility Classes	AHP		FR model		Integrated AHP and FR model	
	Number	%	Number	%	Number	%
Very high susceptibility (VHS)	6	24	17	68	24	96
High susceptibility (HS)	9	36	8	32	1	4
Moderate susceptibility (MS)	9	36	–	–	–	–
Low susceptibility (LS)	1	4	–	–	–	–
Very low susceptibility (VLS)	–	–	–	–	–	–
Total	25	100	25	100	25	100
Prediction accuracy (%)	64.90		84.82		91.22	

However, by having more specific details of the problematic landslide points (especially ones situated in the low or very low risk zones), we might be able to find

out limits or deficiencies of the used model in the study of landsliding mechanism and also have opportunities to improve its capability for any possible further use. In this work, we find that only AHP technique that is still not working satisfactory reflecting in its considerably low prediction accuracy (64.90%) and in the occurrences of some problematic points in low and moderate risk zones.

5.2.2 Comparison with the Susceptibility Maps Developed from Some Agencies

Recently, some state responsible agencies, e.g. Land Development Department (LDD), Department of Mineral Resources (DMR), and the Geo-Informatics and Space Technology Centre (Northern Region) at Chiang Mai University have developed the susceptibility maps at regional scale for general use by Thai public as seen in Figure 5.1d-f. Maps from LDD (2001) and DMR (2005) cover the whole country with three susceptibility classes identified (low, moderate, high) but map from the Chiang Mai University (2006) covers just only in northern part of the country in which three levels of the susceptible scale were identified (no risk, low, high).

Different factors and map producing techniques were used in the derivation of these susceptibility maps. For LDD (2001), the factors are geology, slope, LULC, soil characteristic, and precipitation and the used technique is weighted factor index method. For DMR (2005), the factors included are elevation, aspect, slope, flow accumulation and direction, LULC, soil characteristic, and wetness and the applied technique is landslide predictive model. For Chiang Mai University (2006), the chosen factors are rainfall, rock unit, slope, forest, buffer fault, windward, and altitude and the used technique is weighted factor index method.

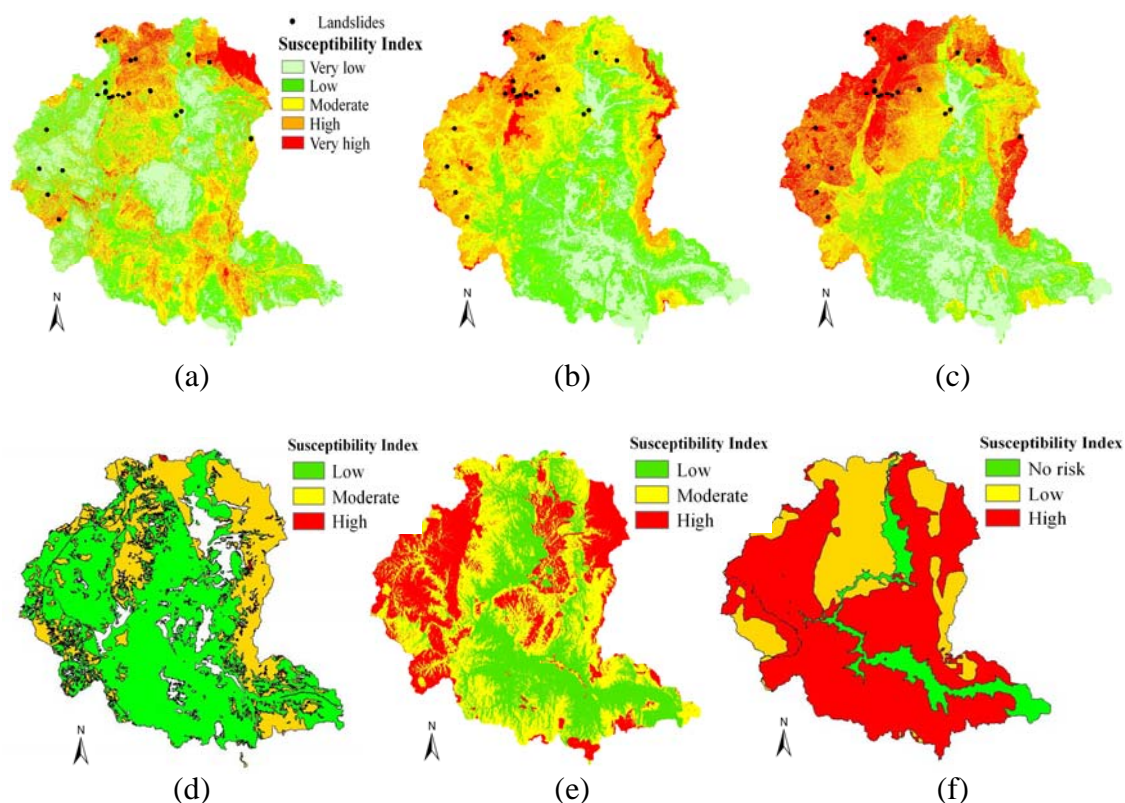


Figure 5.1 Susceptibility maps of the study area derived in this thesis and by different Thai agencies. (a) AHP; (b) FR model; (c) integrated AHP and FR model; (d) LDD (2001); (e) DMR (2005); (f) Chiang Mai University (2006).

When compared to the landslide susceptibility maps developed in this thesis (Figure 5.1a-c), several distinct discrepancies are obviously seen, especially on map from Chiang Mai University (2006). The differences may arise from several sources such as number, type, or scale of input data included, or technique used to determine landslide susceptibility zone, or number of susceptibility classes identified. However, several observed distinctions of these maps indicate that ones should be very cautious in using their given data and some kind of accuracy assessment should be performed beforehand to quantify the validation of the information provided.

REFERENCES

REFERENCES

- Abolmasov, B. and Obradovic, I. (1997). Evaluation of geological parameters for landslide hazard mapping by fuzzy logic. In: Marinou, P.G., Koukis, G.C., Tsiambaos, G.C., Stourna, G.C. (Eds.). **Engineering Geology and the Environment**. Balkema, Rotterdam. pp. 471–476.
- Akgun, A. and Bulut, F. (2007). GIS-based landslide susceptibility for Arsin-Yomra (Trabzon, North Turkey) region. **Environmental Geology**. 51(8): 1377–1387.
- Akgun, A., Dag, S. and Bulut, F. (2007). Landslide susceptibility mapping for a landslide-prone area (Findikli, NE of Turkey) by likelihood-frequency ratio and weighted linear combination models. **Environmental Geology**. Doi: 10.1007/s00254-007-0882-8.
- Akkrawintawong, K., Chotikasathien, W., Daorerk, V. and Charusiri, P. (2008). GIS Application for Landslide Hazard Mapping in Phang Nga Region, Southern Thailand. In **Proceedings of the International Symposia on Geoscience Resources and Environments of Asian Terranes (GREAT 2008)**, 4th IGCP 516, and 5th APSEG; November 24-26 (pp. 402–404). Bangkok, Thailand.
- Aleotti, P. and Chowdhury, R. (1999). Landslide hazard assessment: summary review and new perspectives. **Bulletin of Engineering Geology and the Environment**. 58: 21–44.
- Anbalagan, R. (1992). Landslide hazard evaluation and zonation mapping in mountainous terrain. **Engineering Geology**. 32: 269–277.

- Anderson, S.A. and Sitar, N. (1995). Analysis of rainfall-induced debris flows. **Journal of Geotechnical and Geoenvironmental Engineering**. 121: 544–552.
- Atkinson, P.M., Jiskoot, H., Massari, R. and Murray, T. (1998). Generalized linear modeling in geomorphology. **Earth Surface Processes and Landforms**. 23: 1185–1195.
- Atkinson, P. M. and Massari, R. (1998). Generalized linear modeling of susceptibility to landsliding in the central Apennines, Italy. **Computer & Geosciences**. 24: 373–385.
- Ayalew, L. and Yamagishi, H. (2004). Slope movements in the Blue Nile basin, as seen from landscape evolution perspective. **Geomorphology**. 57: 95–116.
- Ayalew, L., Yamagishi, H. and Ugawa, N. (2004). Landslide susceptibility mapping using GIS-based weighted linear combination, the case in Tsugawa area of Agano River, Niigata Prefecture, Japan. **Landslides**. 1: 73–81.
- Ayalew, L. and Yamagishi, H. (2005). The application of GIS-based logistic regression for landslide susceptibility mapping in the Kakuda-Yahiko mountains Central Japan. **Geomorphology**. 65: 15–31.
- Ayalew, L., Yamagishi, H., Marui, H. and Kanno, T. (2005). Landslide in Sado Island of Japan: part II. GIS-based susceptibility mapping with comparison of results from two methods and verifications. **Engineering Geology**. 81: 432–445.
- Baeza, C. and Corominas, J. (2001). Assessment of shallow landslide susceptibility by means of multivariate statistical techniques. **Earth Surface Processes and Landforms**. 26: 1251–1263.

- Barredol, J.I., Benavidesz, A., Herhl, J. and Van Westen, C.J. (2000). Comparing heuristic landslide hazard assessment techniques using GIS in the Tirajana basin, Gran Canaria Island, Spain. **International Journal of Applied Earth Observation and Geoinformation**. 2: 9–23.
- Binaghi, E., Luzi, L., Madella, P. and Rampini, A. (1998). Slope instability zonation: a comparison between certainty factor and fuzzy Dempster-Shafer approaches. **Natural Hazards**. 17: 77–97.
- Bonham-Carter, G.F. (1996). **Geographic information systems for geoscientists, modeling with GIS**. Pergamon Press, Oxford, 398 pp.
- Brabb, E.E. (1984). Innovative approaches to landslide hazard and risk mapping. In **Proceedings of the 4th international symposium on landslides, vol. 1** (pp. 307–324). Canadian Geotechnical Society, Toronto.
- Burrough, P.A. (1986). **Principals of geographical information systems and land resources assessment**. Clerandon Press, Oxford, England, 194 pp.
- Burrough, P.A.. and McDonnel, R. (1998). **Principles of geographical information Systems**. Oxford University Press, London.
- Carrara, A., Cardinali, M., Detti, R., Guzzetti, F., Pasqul, V. and Reichenbach, P. (1991). GIS techniques and statistical models in evaluating landslide hazard. **Earth Surface processes and Landforms**. 16: 427-445.
- Carrara, A., Cardinali, M., Guzzetti, F. and Reichenbach, P. (1995). GIS technology in mapping landslide hazard. In: Carrara, A., Guzzetti, F. (Eds.). **Geographical Information Systems in Assessing Natural Hazards**. Kluwer Academic Publisher, Dordrecht, The Netherlands. pp. 135–175.

- Carrara, A., Guzzetti, F., Cardinali, M. and Reichenbach, P. (1999). Use of GIS technology in the prediction and monitoring of landslide hazard. **Natural Hazards**. 20(2-3): 117–135.
- Carrara, A., Crosta, G. and Frattini, P. (2003). Geomorphological and historical data in assessing landslide hazard. **Earth Surface Processes and Landforms**. 28: 1125–1142.
- Carrara, A., Crosta, G. and Frattini, P. (2008). Comparing models of debris flow susceptibility in the alpine environment. **Geomorphology**. 94: 353–378.
- Cevik, E. and Topal, T. (2003). GIS-based landslide susceptibility mapping for a problematic segment of the natural gas pipeline, Hendek (Turkey). **Environmental Geology**. 44: 949–962.
- Chàcon, J., Irigaray, C., Fernández, T. and El Hamdouni, R. (2006). Engineering geology maps: landslides and geographical information systems. **Bulletin of Engineering Geology and the Environment**. 65: 341–411.
- Chen, R.H., Lin, M.L. and Chen, H. (1995). Mechanism of initiation of debris flow. In: Cheng, F.Y., Shew, F.S. (Eds.). **Urban Disaster Mitigation**. Elsevier, Oxford. pp. 231–243.
- Cheng, K., Wei, C. and Chang, S. (2004). Locating landslides using multitemporal satellite images. **Advances in Space Research**. 33: 296–301.
- Chiang Mai University (2006). **Application of remote sensing and geographic information system for landslide susceptibility zonation in northern, Thailand (in Thai)**. The Geo-Informatics and Space Technology Centre (Northern Region), Final Report, pp.1–53.

- Chung, C.F. and Fabbri, A.G. (2001). Prediction models for landslide hazard using fuzzy set approach. In: Marchetti, M., Rivas, V. (Eds.). **Geomorphology and Environmental Impact Assessment**. A.A. Balkema, Rotterdam. pp. 31–47.
- Chung, C.J. and Fabbri, A. (2003). Validation of Spatial Prediction Models for Landslide Hazard Mapping. **Natural Hazards**. 30: 451–472.
- Clerici, A., Perego, S., Tellini, C. and Vescovi, P. (2002). A procedure for landslide susceptibility zonation by the conditional analysis method. **Geomorphology**. 48: 349–364.
- Crozier, M.J. (1973). **Techniques for the morphometric analysis of landslips**. Zeitschrift fur Geomorphologie N.F. 17(1): 78-101.
- Crozier, M.J. (1986). **Landslides: causes, consequences & environment**. Croom Helm, London. 252 pp.
- Cruden, D.M. (1991). A simple definition of a landslide. **Bulletin of the international Association of Engineering Geology**. 43: 27-29.
- Cruden, D.M. (1993). **The Multilingual Landslide Glossary**. Bitech Publishers, Richmond., British Columbia, for the UNESCO working party on world landslide inventory in 1993.
- Cruden, D.M. and Varnes, D.J. (1996). Landslide types and processes. In landslides investigation and mitigation. Transportation Research Board, US National Research Council, Turner, A.K. and Schuster, R.L. (editors). **Special Report 247**. Washington, DC; 1996, Chapter 3, pp. 36–75.
- Cruden, D. and Fell, R. (eds) (1997). Landslide risk assessment. In **Proceedings of the workshop on landslide risk assessment** (384 pp.). Honolulu, Hawaii, USA, 19–21 February 1997. A.A. Balkema, Rotterdam & Brookfield.

- Dai, F.C., Lee, C.F. and Xu, Z.W. (2001). Assessment of landslide susceptibility on the natural terrain of Lantau Island, Hong Kong. **Environmental Geology**. 40(3): 381–391.
- Dai, F.C. and Lee, C.F. (2002). Landslide characteristics and slope instability modeling using GIS Lantau Island, Hong Kong. **Geomorphology**. 42: 213–238.
- Dai, F.C. and Lee, C.F. (2003). A spatiotemporal probabilistic modeling of storm-induced shallow landsliding using aerial photographs and logistic regression. **Earth Surface Processes and Landforms**. 28: 527–545.
- Dai, F., Lee, C.F. and Wang, S. (1999). Analysis of rainstorm-induced slide-debris flows on natural terrain of Lantau Island, Hong Kong. **Engineering Geology**. 51: 279–290.
- Dai, F., Lee, C. and Ngai, Y. (2002). Landslide risk assessment and management: An overview. **Engineering Geology**. 64: 65–87.
- Dairaku, K., Kuraji, K., Suzuki, M., Tangtham, N., Jirasuktaveekul, W. and Punyatrong, K. (2000). The effect of rainfall duration and intensity on orographic rainfall enhancement in a mountainous area: a case study in the Mae Chaem watershed, Thailand. **Journal of the Japan Society of Hydrology and Water Resources**. 13(1): 57–68.
- DOE (1990). (Department of the Environment). **Government accepts NRPB recommendations to reduce action level for radon**. London, Department of the Environment, Press Release, 19 January 1990.

- Donati, L. and Turrini, M.C. (2002). An objective method to rank the importance of the factors predisposing to landslides with the GIS methodology: application to an area of the Apennines (Valnerina; Perugia, Italy). **Engineering Geology**. 63: 277–289.
- DMR (2005). **Landslide susceptibility mapping in Thailand (in Thai)**. Department of Mineral Resources (DMR) Thailand [On-line]. Available: <http://www.dmr.go.th>
- DMR (2009). **Geology of Northern and Upper-Western Thailand (in Thai)**. Department of Mineral Resources (DMR) Thailand [On-line]. Available: <http://www.dmr.go.th>
- Ercanoglu, M. and Gokceoglu, C. (2002). Assessment of landslide susceptibility for a landslide-prone area (north of Yenice, NW Turkey) by fuzzy approach. **Environmental Geology**. 41: 720–730.
- Ercanoglu, M. and Gokceoglu, C. (2004). Use of fuzzy relations to produce landslide susceptibility map of a landslide prone area (West Black Sea Region, Turkey). **Engineering Geology**. 75: 229–250.
- Ercanoglu, M., Gokceoglu, C. and Van Asch, T.H.W.J. (2004). Landslide susceptibility zoning north of Yenice (NW Turkey) by multivariate statistical techniques. **Natural Hazards**. 32: 1–23.
- Ermini, L., Catani, F. and Casagli, N. (2005). Artificial Neural Networks applied to landslide susceptibility assessment. **Geomorphology**. 66: 327–343.
- Fleming, R.W., Ellen, S.D. and Albus, M.A. (1989). Transformation of dilative and contractive landslide debris into debris flows an example from Marin County, California. **Engineering Geology**. 27: 201–223.

- Franks, C.A.M. (1999). Characteristics of some rainfall-induced landslides on natural slopes, Lantau Island, Hong Kong. **The Quarterly Journal of Engineering Geology and Hydrogeology**. 32(3): 247–259.
- Frost, J.D., Carroll, D.P. and Rochaway, T.D. (1997). Spatial liquefaction analysis, Spatial analysis in soil dynamics and earthquake engineering. ASCE, Reston, Va. **Geotechnical Special Publication No. 67**, Geo Institute, ASCE, pp. 70–86.
- GISTDA (2009). **Thailand's first Observation Satellite, THEOS (in Thai)**. Geoinformatics and Space Technology Development Agency (Public Organization): GISTDA [On-line]. Available: <http://theos.gistda.or.th>
- Gokceoglu, C. and Aksoy, H. (1996). Landslide susceptibility mapping of the slopes in the residual soils of the Mengen region (Turkey) by deterministic stability analyses and image processing techniques. **Engineering Geology**. 44: 147–161.
- Go´mez, H. and Kavzoglu, T. (2005). Assessment of shallow landslide susceptibility using artificial neural networks in Jabonosa River Basin, Venezuela. **Engineering Geology**. 78: 11–27.
- Greenbaum, D., Tutton, M., Bowker, M., Browne, T., Buleka, J., Grealley, K., Kuna, G., McDonald, A., Marsh, S., O’Connor, E. and Tragheim, D. (1995). Rapid Methods of Landslide Hazard Mapping: Papua New Guinea Case Study. British Geological Survey. **Technical Report WC/95/27**.
- Guzzetti, F., Carrarra, A., Cardinali, M. and Reichenbach, P. (1999). Landslide hazard evaluation: a review of current techniques and their application in a multi-scale study, Central Italy. **Geomorphology**. 31: 181–216.

- Guzzetti, F. (2000). Landslide fatalities and the evaluation of landslide risk in Italy. **Engineering Geology**. 58(2): 89–107.
- Guzzetti, F., Cardinali, M., Reichenbach, P., Cipolla, F., Sebastiani, C., Galli, M. and Salvati, P. (2004). Landslides triggered by the 23 November 2000 rainfall event in the Imperia Province, Western Liguria, Italy. **Engineering Geology**. 73: 229–245.
- Hansen, A. (1984). **Landslide hazard analysis**. Slope instability: edited by D. Brunsten and D. B. Prior. (n.p.):John Wiley& Sons. pp. 523–601.
- Hansen, P.K. (2001). Environmental variability and agro-ecological stratification in a watershed in northern Thailand. Capacity Building in Biodiversity Project. **Technical paper no. 2**.
- Hartlen, J. and Viberg, L. (1988). General report: evaluation of landslide hazard. In **Proceedings of the 5th International Symposium in Landslides** (pp. 3–35). Vol.1 (C. Bonnard ed.), Lausanne, A.A. Balkema, Rotterdam, Netherlands.
- He, Y., Xie, H., Cui, P., Wei, F., Zhong, D. and Gardner, J. (2003). GIS-based hazard mapping and zonation of debris flows in Xiaojiang Basin, southwestern China. **Environmental Geology**. 45: 285–293.
- Irigaray, C., Fernández, T. and Chacón, J. (1996). Comparative analysis of methods for landslide susceptibility mapping. In: Chacón, J., Irigaray, C. and Fernández, T. (Eds), A.A. Balkema, Rotterdam. **Landslides**. pp. 373–384.
- Irigaray, C., Fernandez, T.F., Hamdouni, R.E. and Chacon, J.C. (1999). Verification of landslide susceptibility mapping: a case study. **Earth Surface Processes and Landforms**. 24: 537–544.

- Iverson, R.M., Reid, M.E. and LaHusen, R.G. (1997). Debris flow mobilization from landslides. *Annu. Rev. Earth and Planetary Sciences*. 25: 85–138.
- Jackson, R.D., Slater, P.N. and Pinter, P.J. (1983). Discrimination of growth and water stress in wheat by various vegetation indices through clear and turbid atmospheres. *Remote Sensing of the Environment*. 15: 187–208.
- Jibson, W.R., Edwin, L.H. and John, A.M. (2000). A method for producing digital frequency seismic landslide hazard maps. *Engineering Geology*. 58: 271–289.
- Jordan, C., O'Connor, E., Marchant, A., Northmore, A., Greenbaum, D., McDonald, A., Kovacic, M. and Ahmed, R. (2000). Rapid landslide susceptibility mapping using remote sensing and GIS modelling. In **Proceedings of the 14th International Conference on Applied Geologic Remote Sensing** (pp. 113–120). Las Vegas.
- Kanungo, D.P., Arora, M.K., Sarkar, S. and Gupta, R.P. (2006). A comparative study of conventional, ANN black box, fuzzy and combined neural and fuzzy weighting procedures for landslide susceptibility zonation in Darjeeling Himalayas. *Engineering Geology*. 85: 347–366.
- Keefer, D.K., Wilson, R.C., Mark, R.K., Brabb, E.E., Brown III, W.M., Ellen, S.D., Harp, E.L., Wieczorek, G.F., Alger, C.S and Zatkan, R.S. (1984). Real-time landslide warning during heavy rainfall. *Science*. 238: 921–925.
- Komac, M. (2006). A landslide susceptibility model using the Analytical Hierarchy Process method and multivariate statistics in perialpine Slovenia. *Geomorphology*. 74: 17–28.

- Kuraji, K., Punyatrong, K. and Suzuki, M. (2001). Altitudinal increase in rainfall in the Mae Chaem watershed, Thailand. **Journal of the Meteorological Society of Japan**. 79(1B): 353–363.
- LDD (2001). **Landslide susceptibility mapping in Thailand (in Thai)**. Land Development Department (LDD) Thailand [On-line]. Available: <http://www.ddd.go.th>
- Lee, E.M. and Jones, D.K.C. (2004). **Landslide risk assessment**. Thomas Telford, London, p. 454.
- Lee, S. (2005). Application of logistic regression model and its validation for landslide susceptibility mapping using GIS and remote sensing data. **International Journal of Remote Sensing**. 26: 1477–1491.
- Lee, S. (2007a). Application and verification of fuzzy algebraic operators to landslide susceptibility mapping. **Environmental Geology**. 52(4): 615–623.
- Lee, S. (2007b). Comparison of landslide susceptibility maps generated through multiple logistic regression for three test areas in Korea. **Earth Surface Processes and Landforms**. 32: 2133–2148.
- Lee, S. and Choi, U. (2003). Development of GIS based geological hazard information system and its application for landslide analysis in Korea. **Geosciences Journal**. 7: 243–252.
- Lee, S. and Dan, N.T. (2005). Probabilistic landslide susceptibility mapping in the Lai Chau province of Vietnam: focus on the relationship between tectonic fractures and landslides. **Environmental Geology**. 48: 778–787.

- Lee, S. and Lee, M.J. (2006). Detecting landslide location using KOMPSAT-1 and its application to landslide susceptibility mapping at the Gangneung area, Korea. **Advances in Space Research**. 38: 2261–2271.
- Lee, S. and Min, K. (2001). Statistical analysis of landslide susceptibility at Yongin, Korea. **Environmental Geology**. 40: 1095–1113.
- Lee, S. and Pradhan, B. (2006a). Landslide hazard assessment at Cameron Highland Malaysia using frequency ratio and logistic regression models. **Geophysical Research Abstracts**. 8: SRef-ID: 1607–7962/gra/EGU06-A-03241.
- Lee, S. and Pradhan, B. (2006b). Probabilistic landslide hazards and risk mapping on Penang Island, Malaysia. **Journal of Earth System Science**. 115: 661–672.
- Lee, S. and Pradhan, B. (2007). Landslide hazard mapping at Selangor, Malaysia using frequency ratio and logistic regression models. **Landslides**. 4(1): 33–41.
- Lee, S. and Sambath, T. (2006). Landslide susceptibility mapping in the Damrei Romel area, Cambodia using frequency ratio and logistic regression models. **Environmental Geology**. 50: 847–855.
- Lee, S. and Talib, J.A. (2005). Probabilistic landslide susceptibility and factor effect analysis. **Environmental Geology**. 47: 982–990.
- Lee, S., Choi, J. and Min, K. (2002). Landslide susceptibility analysis and verification using the Bayesian probability model. **Environmental Geology**. 43: 120–131.
- Lee, S., Ryu, J.H., Lee, M.J. and Won, J.S. (2003a). Landslide susceptibility analysis using artificial neural network at Boeun, Korea. **Environmental Geology**. 44: 820–833.

- Lee, S., Ryu, J.H., Min, K.D. and Won, J.S. (2003b). Landslide susceptibility analysis using GIS and artificial neural network. **Earth Surface Processes and Landforms**. 27: 1361–1376.
- Lee, S., Choi, J. and Min, K. (2004a). Probabilistic landslide hazard mapping using GIS and remote sensing data at Boun, Korea. **International Journal of Remote Sensing**. 25: 2037–2052.
- Lee, S., Ryu, J.H., Won, J.S. and Park, H.J. (2004b). Determination and application of the weights for landslide susceptibility mapping using an artificial neural network. **Engineering Geology**. 71: 289–302.
- Liener, S., Kienholz, H., Liniger, M. and Krummenacher, B. (1996). SLIDISP—A procedure to locate landslide prone areas. Landslides Glissements de Terrain. In **Proceedings of the 7th International Symposium on Landslides**. Trondheim, Norway.
- Liu, C.N. and Wu, C.C. (2008). Integrating GIS and stress transfer mechanism in mapping rainfall-triggered landslide susceptibility. **Engineering Geology**. 101: 60–74.
- Luzi, L., Pergalani, F. and Terlien, M.T.J. (2000). Slope vulnerability to earthquakes at sub-regional scale, using frequency techniques and geographic information systems. **Engineering Geology**. 58: 313–336.
- Malczewski, J. (1999). **GIS and Multi-Criteria Decision Analysis**. John Wiley and Sons, New York. 392 pp.
- Marchi, L., Arattano, M. and Deganutti, A.M. (2002). Ten years of debris flow monitoring in the Moscardo Torrent (Italian Alps). **Geomorphology**. 46: 1–17.

- Miles, S.B. and Ho, C.L. (1999). Applications and issues of GIS as tool for civil engineering modeling. **Journal of computing in civil engineering**. ASCE, 13(3): 144–161.
- Montavani, F., Soeters, R. and Westen, V. (1996). Remote sensing techniques for landslide studies and hazard zonation in Europe. **Journal of Geomorphology**. 15: 213–225.
- Montgomery, D.R., Schmidt, K.M., Greenberg, H.M. and Dietrich, W.E. (2000). Forest clearing and regional landsliding. **Geology**. 28: 311–314.
- Mwasi, B. (2001). Land use conflicts resolution in a fragile ecosystem using Multi-Criteria Evaluation (MCE) and a GIS-based Decision Support System (DSS). In **Proceedings of the international Conference on Spatial Information for Sustainable Development** (11 pp.). Nairobi, Kenya, FIG — International Federation of Surveyors.
- Nagarajan, R., Mukherjee, A., Roy, A. and Khire, M.V. (1998). Temporal remote sensing data and GIS application in landslide hazard zonation of part of Western Ghat, India. **International Journal of Remote Sensing**. 19: 573–585.
- Naramngam, S. and Tangtham, N. (1997). Application of GIS and factor of safety in determining landslide hazardous area in Tapi watershed, Changwat Nakhon Si Thammarat. **Thai Journal of Forestry**. 16: 106-119.

- Nie, H.F., Diao, S.J., Liu, J.X. and Huang, H. (2001). The application of remote sensing technique and AHP-fuzzy method in comprehensive analysis and assessment for regional stability of Chongqing City, China. In **Proceedings of the 22nd international Asian Conference. on Remote Sensing, Vol. 1** (pp. 660–665). University of Singapore, Singapore.
- Nielsen, T.H., Wrigth, R.h., Vlastic, T.C. and Spangle, W.E. (1979). Relative slope stability and land-use planning in the San Francisco Bay region, California. **US Geological Survey Professional Paper 944**.
- Oh, H.J., Lee, S., Chotikasathein, W., Kim, C.H. and Kwon, J.H. (2008). Predictive landslide susceptibility mapping using spatial information in the Pechabun area of Thailand. **Environmental Geology**. 43: 120–131.
- Ohlmacher, G.C. and Davis, J.C. (2003). Using multiple logistic regression and GIS technology to predict landslide hazard in northeast Kansas, USA. **Engineering Geology**. 69: 331–343.
- Okimura, T. and Kawatani, T. (1987). Mapping of the potential surface-failure sites on granite slopes. In: Gardiner, E. (Ed.). **International Geomorphology**. Part I. Wiley, Chichester. pp. 121–138.
- Revellino, P., Hungr, O., Guadagno, F.M. and Evans, S.G. (2004). Velocity and runout simulation of destructive debris flows and debris avalanches in pyroclastic deposits, Campania region, Italy. **Environmental Geology**. 45: 295–311.

- Rouse Jr., J.W., Haas, R.H., Schell, J.A. and Deering, D.W. (1973). Monitoring vegetation systems in the Great Plains with ERTS. In **Proceedings of the 1st Earth Resources Technology Satellite-1 Symposium** (pp. 309–317). Goddard Space Flight Cent., Washington, DC.
- Saaty, T.L. (1980). **The Analytical Hierarchy Process**. McGraw Hill, New York. 350 pp.
- Saaty, T.L. (1990). **The analytic hierarchy process: planning, priority setting, resource allocation**. RWS Publications, Pittsburgh. 502 pp.
- Saaty, T.L. (1994). **Fundamentals of decision making and priority theory with analytic hierarchy process**. RWS Publications, Pittsburgh. 527 pp.
- Saaty, T.L. (2000). **The fundamentals of decision making and priority theory with the Analytic Hierarchy Process**. RWS Publications, Pittsburgh, 2nd ed., 6: 478 pp.
- Saha, A.K., Gupta, R.P. and Arora, M.K. (2002). GIS-based landslide hazard zonation in the Bhagirathi (Ganga) valley, Himalayas. **International Journal of Remote Sensing**. 23(2): 357–369.
- Sgzen, M.L. (2002). **Data driven landslide hazard assessment using geographic information systems and remote sensing**. Ph.D. Dissertation. Department of geological engineer, School of Natural and Applied Sciences of the Middle East Technical University: 196 pp.
- Soeters, R. and Van Westen, C.J. (1996). Slope stability: recognition, analysis and zonation. In: A.K., Turner and R.L., Shuster (editor) “Landslides: investigation and mitigation”. Transportation research Board–National Research Council. **Special Report 247**. pp. 129–177.

- Soralump, S. (2007). Corporation of geotechnical engineering data for landslide hazard map in Thailand. In **Proceedings of EIT-JSCE Joint seminar on Rock Engineering**. Bangkok, Thailand.
- Suzen, M.L. and Doyuran, V. (2003). A comparison of the GIS based landslide susceptibility assessment methods: multivariate versus bivariate. **Environmental Geology**. 45: 665–679.
- Suzen, M.L. and Doyuran, V. (2004). Data driven bivariate landslide susceptibility assessment using geographical information systems: a method and application to Asarsuyu catchment, Turkey. **Engineering Geology**. 71(3–4): 303–321.
- Thomas, D., Preechapanya, P. and Saipothong, P. (2002). Landscape agroforestry in upper tributary watersheds of northern Thailand. **Journal of Agriculture (Thailand)**. 18(1): S255–S302.
- Tomlin, C.D. (1990). **Geographic information systems and cartographic modeling**. Prentice Hall, Englewood Cliffs.
- Tucker, C.J., Newcomb, W.W., Los, S.O. and Prince, S.D. (1991). Mean and inter-year variation of growing-season normalized difference vegetation index for the Sahel 1981–1989. **International Journal of Remote Sensing**. 12: 1113–1115.
- USGS (2004). **Landslide Types and Processes**. United States Geological Survey (USGS) [On-line]. Available: <http://pubs.usgs.gov/fs/2004/3072/fs-2004-3072.html>

- Van Beek, R. (2002). Assessment of the influence of changes in climate and land use on landslide activity in a Mediterranean environment. **Netherlands Geographical Studies no. 294**. KNAG, Faculty of Geosciences, Utrecht University, p 366.
- Varnes, D.J. (1978). Slope movement types and processes. In landslide analysis and control. **Special Report 176** (Washington, DC: transportation Research Board, 1978). pp. 12–33.
- Varnes, D.J. (1984). Landslide hazard zonation: a review of principles and practice. **Natural Hazards**. No. 3. UNESCO, Paris, France.
- Van Westen, C.J., Soeters, R. and Sijmons, K. (2000). Digital Geomorphological landslide hazard mapping of the Alpage area, Italy. **International Journal of Applied Earth Observation and Geoinformation**. 2(1): 51–59.
- Van Westen, C.J. and Getahun, F. (2003). Analyzing the evolution of the Tessina landslide using aerial photographs and digital elevation models. **Geomorphology**. 54: 77–89.
- Van Westen, C.J., Van Asch, T.W.J. and Soeters, R. (2006). Landslide hazard and risk zonation—why is it still so difficult? **Bulletin of Engineering Geology and the Environment**. 65: 167–184. Doi: 10.1007/s10064-005-0023-0.
- Vijith, H. and Madhu, G. (2008). Estimating potential landslide sites of an upland sub-watershed in Western Ghat's of Kerala (India) through frequency ratio and GIS. **Environmental Geology**. 55: 1397–1405.
- Vivas, L. (1992). **Los Andes Venezolanos**. Academia Nacional de la Historia, Caracas.

- Voogd, H. (1983). **Multicriteria Evaluation for Urban and Regional Planning**. Pion Ltd., London.
- Walker, A. (2002). Forests and water in northern Thailand. Resource Management in Asia-Pacific. **Working Paper no. 37**. Resource Management in Asia-Pacific Program. The Australian National University, Canberra, Australia.
- Walker, A. (2003). Agricultural transformation and the politics of hydrology in northern Thailand. **Development and Change**. 34(5): 941–964.
- Wieczorek, G. (1984). Preparing a detailed landslide-inventory map for hazard evaluation and reduction. **Bulletin of the Association of Engineering Geologists**. 21(3): 337–342.
- Wu, W. and Sidle, R.C. (1995). A distributed slope stability model for steep forested basins. **Water Resources Research**. 31: 2097–2110.
- Yagi, H. (2003). Development of assessment method for landslide hazardness by AHP. **Abstract Volume of the 42nd Annual Meeting of the Japan Landslide Society**. pp. 209–212.
- Yalcin, A. (2005). **An investigation on Ardesen (Rize) region on the basis of landslide susceptibility**. Ph.D. Dissertation. Karadeniz Technical University, Trabzon, Turkey (in Turkish).
- Yalcin, A., (2008). GIS-based landslide susceptibility mapping using analytical hierarchy process and bivariate statistics in Ardesen (Turkey): Comparisons of results and confirmations. **Catena**. 72: 1–12.
- Yesilnacar, E. and Topal, T. (2005). Landslide susceptibility mapping: A comparison of logistic regression and neural networks methods in a medium scale study, Hendek region (Turkey). **Engineering Geology**. 79: 251–266.

- Yin, K.L. and Yan, T.Z. (1988). Statistical prediction model for slope instability of metamorphosed rocks. In: Bonnard, C. (Ed.), In **Proceedings of the 5th International Symposium on Landslides** (pp. 1269–1272). Lausanne. Balkema, Rotterdam.
- Yumuang, S. (2006). 2001 debris flow and debris flood in Nam Ko area, Phetchabun province, central Thailand. **Environmental Geology**. 51: 545–564.
- Zezere, J.L., Reis, E., Garcia, R., Oliveira, S., Rodrigues, M.L., Vieira, G. and Ferreira, A.B. (2004). Integration of spatial and temporal data for the definition of different landslide hazard scenarios in the area north of Lisbon (Portugal). **Natural Hazards and Earth System Science**. 4: 133–146.
- Zhou, C., Lee, C., Li, J. and Xu, Z. (2002). On the spatial relationship between landslides and causative factors on Lantau Island, Hong Kong. **Geomorphology**. 43: 197–207.

APPENDICES

APPENDIX A

QUESTIONNAIRE AND LIST OF EXPERTS

QUESTIONNAIRE

Introduction to this research

The part of this research used analytical hierarchy process (AHP), which is a semi-qualitative method, which involves a matrix-based pair-wise comparison of the contribution of different factors for landslide. The analytical hierarchy process (AHP) is a Multi-Criteria Decision Making (MCDM) tool at the core of which lies a method for converting subjective assessments of relative importance to a set of overall scores or weights.

Analytical hierarchy process (AHP) was developed by Saaty (1980). To get factor weights in AHP, one has to build a pair-wise comparison matrix with scores. In this study, there are ten landslide inducing parameters which are considered for landslide susceptibility analysis. These parameters are elevation, slope aspect, slope angle, distance from drainage, lithology, distance from lineament, soil texture, precipitation, land use/land cover and NDVI.

Table A1 Scale of preference between two parameters in AHP (Saaty, 2000).

Scales	Degree of preferences	Explanation
1	Equally	Two activities contribute equally to the objective.
3	Moderately	Experience and judgment slightly to moderately favor one activity over another.
5	Strongly	Experience and judgment strongly or essentially favor one activity over another.
7	Very strongly	An activity is strongly favored over another and its dominance is showed in practice.
9	Extremely	The evidence of favoring one activity over another is of the highest degree possible of an affirmation.
2, 4, 6, 8	Intermediate values	Used to represent compromises between the preferences in weights 1, 3, 5, 7 and 9.
Reciprocals	Opposites	Used for inverse comparison.

Explanation

1. Please input scale with values from 1 to 9 to rate the relative preferences for two criteria (see Table A1).

2. Please select one criteria by circle that your experience and judgment favor one criteria over another.

For example

No.	Criteria 1	Criteria 2	Degree of preferences (scale 1-9)
1	Elevation	Elevation	1
2	Elevation	Slope aspect	3
3	Elevation	Slope angle	9

Table A2 Questionnaire.

No.	Criteria 1	Criteria 2	Degree of preferences (scale 1-9)
1	Elevation	Elevation	1
2	Elevation	Slope aspect	
3	Elevation	Slope angle	
4	Elevation	Drainage	
5	Elevation	Lithology	
6	Elevation	Lineament	
7	Elevation	Soil texture	
8	Elevation	Precipitation	
9	Elevation	Land use/land cover	
10	Elevation	NDVI	
11	Slope aspect	Slope aspect	1
12	Slope aspect	Slope angle	
13	Slope aspect	Drainage	
14	Slope aspect	Lithology	
15	Slope aspect	Lineament	

Table A2 Questionnaire (Continued).

No.	Criteria 1	Criteria 2	Degree of preferences (scale 1-9)
16	Slope aspect	Soil texture	
17	Slope aspect	Precipitation	
18	Slope aspect	Land use/land cover	
19	Slope aspect	NDVI	
20	Slope angle	Slope angle	1
21	Slope angle	Drainage	
22	Slope angle	Lithology	
23	Slope angle	Lineament	
24	Slope angle	Soil texture	
25	Slope angle	Precipitation	
26	Slope angle	Land use/land cover	
27	Slope angle	NDVI	
28	Drainage	Drainage	1
29	Drainage	Lithology	
30	Drainage	Lineament	
31	Drainage	Soil texture	
32	Drainage	Precipitation	
33	Drainage	Land use/land cover	
34	Drainage	NDVI	
35	Lithology	Lithology	1
36	Lithology	Lineament	
37	Lithology	Soil texture	
38	Lithology	Precipitation	
39	Lithology	Land use/land cover	
40	Lithology	NDVI	
41	Lineament	Lineament	1
42	Lineament	Soil texture	
43	Lineament	Precipitation	

Table A2 Questionnaire (Continued).

No.	Criteria 1	Criteria 2	Degree of preferences (scale 1-9)
44	Lineament	Land use/land cover	
45	Lineament	NDVI	
46	Soil texture	Soil texture	1
47	Soil texture	Precipitation	
48	Soil texture	Land use/land cover	
49	Soil texture	NDVI	
50	Precipitation	Precipitation	1
51	Precipitation	Land use/land cover	
52	Precipitation	NDVI	
53	Land use/land cover	Land use/land cover	1
54	Land use/land cover	NDVI	
55	NDVI	NDVI	1

Remark: The evaluation scale must be 1, representing equally preferred criteria when comparing anything to itself.

Comments and suggestions:.....

.....

Signature of expert

PERSONAL DETAILS

1. Name - Surname:

(in Thai).....

(in English).....

2. Education Degree:.....

3. Occupation:.....Position:.....

4. Organization:.....

5. Contact Address:.....

6. Telephone:.....Fax:.....

7. E-mail:.....

Thank you for taking time to share your opinions. Researcher would very much appreciate your valuable feedbacks. Please contact researcher, if you have doubtfulness about questionnaire or need more explanation.

For any details, please contact researcher: Miss Narumon Intarawichian, Tel. 086-6051820.

Table A3 List of experts.

No.	Name	Position	Office
1	Assoc. Prof. Dr. Charlie Navanugraha	Lecturer	Faculty of Environment and Resource Studies, Mahidol University
2	Mr. Chira Prangkio	Director	Geo-Informatics and Space Technology Centre (Northern Region), Chiang Mai University
3	Mr. Chayakrit Malumpong	Lecturer	Department of Geography, Faculty of Social Sciences, Chiang Mai University
4	Asst. Prof. Surachai Sompadung	Lecturer	
5	Dr. Thanuchai Silaratana	Lecturer	
6	Mr. Winit Youngme	Lecturer	
7	Assoc. Prof. Ladda Wannakao	Lecturer	Department of Geotechnology, faculty of technology, Khon Kaen University
8	Mr. Thanit Intarat	Lecturer	
9	Mr. Rangsaridh Boonsin	Director	Department of Geography, Faculty of Humanities and Social Sciences, Burapha University
10	Miss Pratumporn Funnpheng	Soil Surveyor	Office of Information and Communication Technology, Land Development Department
11	Mrs. Nongyow Deetae	Soil Surveyor	
12	Mr. Somjai Yensabai	Geologist	Office of Soil Survey and Land Use Planning, Land Development Department
13	Mr. Pradit Nulay	Geologist	
14	Mr. Tinnakorn Tatong	Geologist	
15	Mr. Krittapob Akkrawintawong	Geologist	
16	Miss Namphon Khampilang	Geologist	
17	Miss Sasiwimol Nawawitphisit	Geologist	
18	Mrs. Suree Teerarungsigul	Geologist	Environmental Geology Division, Department of Mineral Resources
19	Mr. Pairat Sakpisuthipong	Geologist	
20	Mr. Patiwet Chalermpong	Geo-Informatics academic	
			Geo-Informatics and Space Technology Development Agency (Public Organization)

APPENDIX B

THE PAIR-WISE COMPARISON METHOD:

AHP'S FACTOR WEIGHTS

Table B1 Factor weights from questionnaires.

No.	Criteria 1	Criteria 2	Expert																				Weight
			1	2	3	4	5	6	7	8	9	10	11	12	13	14	15	16	17	18	19	20	
1	EL	EL	1	1	1	1	1	1	1	1	1	1	1	1	1	1	1	1	1	1	1	1	1
2	EL	SAS	1	1	3	6	1/2	1	1/3	1	4	5	1/5	1/5	6	1/3	5	1/3	7	1	1/3	1	1
3	EL	SAN	1/5	1/5	3	1/8	1/5	1/5	1/3	1/3	4	1/5	1/7	1/9	2	1/5	8	1/5	1/7	1/5	1/2	1/3	1/5
4	EL	DD	1/5	1/2	1/5	6	1/2	2	1/2	1/2	1/2	1/6	1/2	1/7	4	1/2	7	2	7	7	2	1/6	1/2
5	EL	LT	1/7	1/5	1/9	6	1/2	1/5	1/5	1/3	4	1/5	1/7	1/5	2	1/3	2	1/5	7	1/9	2	1/3	1/5
6	EL	DL	1/5	1/4	3	1/3	1/2	3	1/5	1/3	1/2	1/7	1/7	1/9	2	1/3	7	1/3	1/5	1/3	2	1/3	1/3
7	EL	ST	1/2	1/7	3	6	1/2	1/3	1/5	1/2	4	1/5	1/7	4	5	1/2	9	1/3	1/2	9	2	1/6	1/2
8	EL	PC	1/7	1/8	1/5	1/9	1/4	1/5	1/5	1/4	1/3	1/6	1/7	3	1/2	1/5	9	1/3	1/9	3	1/2	1/5	1/5
9	EL	LULC	1/4	1/6	1/5	6	1/4	3	1/3	1/4	4	1/8	1/6	1/5	1/4	1/3	1/9	1/4	5	7	2	4	1/4
10	EL	NDVI	1/5	1/2	1/3	6	1/3	3	1/3	1/3	4	1/6	1/6	1/3	6	5	1/3	1/2	5	7	2	1/2	1/3
11	SAS	SAS	1	1	1	1	1	1	1	1	1	1	1	1	1	1	1	1	1	1	1	1	1
12	SAS	SAN	1/7	1/8	3	1/4	1/4	1/4	3	1/3	1/4	1/4	1/4	2	1/3	1/2	5	1/7	1/4	1/4	1/2	1/4	1/4
13	SAS	DD	1/5	1/3	1/5	1	1/5	2	5	2	4	1/6	4	1/7	2	2	5	2	1/7	1/7	2	2	2
14	SAS	LT	1/7	1/6	1/7	1/3	1/5	1/5	5	1/3	3	1/5	1/5	1/5	1/4	1/5	1/2	1/5	1/5	1/5	3	1/9	1/5
15	SAS	DL	1/5	1/5	1/5	1/7	1/5	1/5	3	1/3	1/3	1/9	1/5	1/5	1/4	1/6	3	1/5	1/7	1/9	1/5	1/4	1/5
16	SAS	ST	1/3	1/8	3	1/3	1/4	1/2	3	1/3	1/3	1/7	1/6	4	1/3	1/3	7	3	5	1/7	1/3	1/3	1/3
17	SAS	PC	1/6	1/6	1/9	1/9	1/6	1/6	1/5	1/4	1/6	1/6	1/4	5	1/6	1/3	5	3	1/7	3	3	1/6	1/6
18	SAS	LULC	1/5	1/7	1/4	1/4	1/4	3	4	1/4	1/4	1/9	5	1/4	1/4	1/2	5	4	1/7	1/4	3	1/4	1/4
19	SAS	NDVI	1/3	1/3	1/3	1/5	1/7	4	4	1/3	1/3	1/2	1/3	1/6	1/3	5	7	3	1/7	1/8	1/3	1/4	1/3
20	SAN	SAN	1	1	1	1	1	1	1	1	1	1	1	1	1	1	1	1	1	1	1	1	1
21	SAN	DD	3	5	3	8	5	5	5	6	5	5	7	1/6	5	2	5	5	5	5	5	2	5
22	SAN	LT	1/2	3	1/2	8	4	1/2	1	3	1/5	1/2	3	1/2	1/2	1/2	1/5	1/7	5	9	4	1/2	1/2
23	SAN	DL	5	4	1/5	8	5	2	2	2	1/6	1/3	3	1/7	2	2	1/3	1/5	1/5	1/9	2	2	2
24	SAN	ST	3	2	1	8	5	6	1	5	1/3	7	3	6	7	1/4	7	5	5	5	3	5	5
25	SAN	PC	1/2	1/2	1/9	1/9	5	1/2	1/6	1/2	1/6	7	1/5	4	1/4	1/3	5	1/2	1/7	2	5	1/2	1/2
26	SAN	LULC	3	3	1/7	3	7	5	5	2	3	2	7	3	4	2	7	5	5	3	5	3	3
27	SAN	NDVI	1/3	5	5	8	5	5	1/6	4	3	5	5	1/6	5	5	5	5	5	3	2	4	5
28	DD	DD	1	1	1	1	1	1	1	1	1	1	1	1	1	1	1	1	1	1	1	1	1
29	DD	LT	1/3	1/4	1/7	1/3	1/3	1/3	1/3	1/3	1/3	1/3	1/5	4	1/3	1/3	1/7	1/5	1/5	1/9	1/3	1/3	1/3
30	DD	DL	1/3	1/4	5	1/7	1/4	1/2	1/4	1/3	1/4	1/3	1/5	1/5	1/4	1/4	1/4	1/5	1/5	1/9	1/2	1/4	1/4
31	DD	ST	1/7	1/3	5	1/3	1/3	1/5	1/3	2	4	1/3	1/3	6	1/3	1/3	2	1/3	5	1/7	1/3	4	1/3
32	DD	PC	1/7	1/5	1/9	1/9	1/3	1/5	1/4	1/3	1/6	1/2	1/5	2	1/5	1/3	3	1/5	1/7	1/8	1/5	1/3	1/5

Table B1 Factor weights from questionnaires (Continued).

No.	Criteria 1	Criteria 2	Expert																				Weight
			1	2	3	4	5	6	7	8	9	10	11	12	13	14	15	16	17	18	19	20	
33	DD	LULC	1/3	1/3	3	1/3	1/2	2	1/3	1/3	3	1/4	4	4	1/4	4	2	1/3	5	7	4	6	1/3
34	DD	NDVI	1/5	1/2	1/2	1/5	1/2	4	1/3	1/2	1/4	6	4	5	1/2	5	1/2	1/3	7	6	3	1/2	1/2
35	LT	LT	1	1	1	1	1	1	1	1	1	1	1	1	1	1	1	1	1	1	1	1	1
36	LT	DL	2	2	5	1/7	1/2	2	1/4	2	1/4	2	2	1/8	2	1/2	7	5	1/5	1/9	2	6	2
37	LT	ST	1	2	7	1	2	2	1/4	2	5	2	2	9	5	2	9	5	2	9	1/3	2	2
38	LT	PC	1/3	1/3	1/7	1/9	1/3	1/5	1/4	1/2	1/6	7	2	5	1/3	1/3	9	5	1/3	7	1/3	1/4	1/3
39	LT	LULC	5	1/2	5	4	1/2	5	3	1/3	1/3	6	4	4	2	4	7	5	7	4	2	4	4
40	LT	NDVI	5	3	5	5	1/2	5	3	1/2	3	8	5	6	4	6	7	5	7	6	2	7	5
41	DL	DL	1	1	1	1	1	1	1	1	1	1	1	1	1	1	1	1	1	1	1	1	1
42	DL	ST	1/5	1/2	5	7	3	2	1/4	3	3	5	2	8	3	3	3	3	5	9	3	7	3
43	DL	PC	1/7	1/3	1/9	1/9	1/3	1/5	1/3	1/3	1/3	5	2	6	1/3	1/2	5	1/3	1/7	1/9	1/3	1/4	1/3
44	DL	LULC	1/5	1/2	3	7	1/3	5	3	1/3	6	3	5	7	4	3	5	3	7	8	2	3	3
45	DL	NDVI	1/5	4	1/3	7	1/3	3	4	1/2	6	6	4	4	6	7	4	3	7	7	2	4	4
46	ST	ST	1	1	1	1	1	1	1	1	1	1	1	1	1	1	1	1	1	1	1	1	1
47	ST	PC	1/7	1/2	1/9	1/9	1/5	1/5	1	1/3	1/5	2	1/5	2	1/5	1/5	3	1/5	1/5	1/9	1/4	1/3	1/5
48	ST	LULC	1/3	1/3	1/7	1/4	1/3	3	3	1/3	1/3	1/3	5	1/3	1/4	1/3	2	1/3	5	1/7	3	1/3	1/3
49	ST	NDVI	1/2	4	1/2	1/5	1/3	4	3	1/2	1/3	7	5	1/2	1/4	4	2	1/2	1/3	8	3	1/2	1/2
50	PC	PC	1	1	1	1	1	1	1	1	1	1	1	1	1	1	1	1	1	1	1	1	1
51	PC	LULC	5	3	9	9	3	5	6	5	3	1/6	7	1/3	5	5	2	5	5	7	4	5	5
52	PC	NDVI	5	5	9	9	3	5	7	5	5	3	5	1/3	5	7	2	5	9	7	3	5	5
53	LULC	LULC	1	1	1	1	1	1	1	1	1	1	1	1	1	1	1	1	1	1	1	1	1
54	LULC	NDVI	1	2	5	1/5	1/2	2	2	2	1/3	3	2	2	1/3	2	2	5	2	8	2	2	2
55	NDVI	NDVI	1	1	1	1	1	1	1	1	1	1	1	1	1	1	1	1	1	1	1	1	1

Remark: EL = Elevation SAS = Slope aspect SAN = Slope angle DD = Distance from Drainage LT = Lithology DL = Distance from lineament

ST = Soil texture PC = Precipitation LULC = Land use/Land cover NDVI = Normalized Difference Vegetation Index

THE PROCEDURE CONSISTS OF THREE MAJOR STEPS FOR EACH FACTOR

Table B2 Step I: Generation of the pair-wise comparison matrix for each factor.

Criterion	Elevation	Slope aspect	Slope angle	Drainage	Lithology	Lineament	Soil texture	Precipitation	LULC	NDVI
Elevation	1.00	1.00	0.20	0.50	0.20	0.33	0.50	0.20	0.25	0.33
Slope aspect	1.00	1.00	0.25	2.00	0.20	0.20	0.33	0.17	0.25	0.33
Slope angle	5.00	4.00	1.00	5.00	0.50	2.00	5.00	0.50	3.00	5.00
Drainage	2.00	0.50	0.20	1.00	0.33	0.25	0.33	0.20	0.33	0.50
Lithology	5.00	5.00	2.00	3.00	1.00	2.00	2.00	0.33	4.00	5.00
Lineament	3.00	5.00	0.50	4.00	0.50	1.00	3.00	0.33	3.00	4.00
Soil texture	2.00	3.00	0.20	3.00	0.50	0.33	1.00	0.20	0.33	0.50
Precipitation	5.00	6.00	2.00	5.00	3.00	3.00	5.00	1.00	5.00	5.00
LULC	4.00	4.00	0.33	3.00	0.25	0.33	3.00	0.20	1.00	2.00
NDVI	3.00	3.00	0.20	2.00	0.20	0.25	2.00	0.20	0.50	1.00
Total	31.00	32.50	6.88	28.50	6.68	9.69	22.16	3.33	17.66	23.66

Table B3 Step II: Computation of the criterion weights for each factor.

Criterion	Elevation	Slope aspect	Slope angle	Drainage	Lithology	Lineament	Soil texture	Precipitation	LULC	NDVI	Total	Weight	Weight (%)
Elevation	0.03	0.03	0.03	0.02	0.03	0.03	0.02	0.06	0.01	0.01	0.27	0.027	2.70
Slope aspect	0.03	0.03	0.04	0.07	0.03	0.02	0.01	0.05	0.01	0.01	0.30	0.030	3.00
Slope angle	0.16	0.12	0.15	0.18	0.07	0.21	0.23	0.15	0.17	0.21	1.65	0.165	16.50
Drainage	0.06	0.02	0.03	0.04	0.05	0.03	0.01	0.06	0.02	0.02	0.34	0.034	3.40
Lithology	0.16	0.15	0.29	0.11	0.15	0.21	0.09	0.10	0.23	0.21	1.70	0.170	17.00
Lineament	0.10	0.15	0.07	0.14	0.07	0.10	0.14	0.10	0.17	0.17	1.21	0.121	12.10
Soil texture	0.06	0.09	0.03	0.11	0.07	0.03	0.05	0.06	0.02	0.02	0.54	0.054	5.40
Precipitation	0.16	0.18	0.29	0.18	0.45	0.31	0.23	0.30	0.28	0.21	2.59	0.259	2.59
LULC	0.13	0.12	0.05	0.11	0.04	0.03	0.14	0.06	0.06	0.08	0.82	0.082	8.20
NDVI	0.10	0.09	0.03	0.07	0.03	0.03	0.09	0.06	0.03	0.04	0.57	0.057	5.70
Total	1.00	1.00	1.00	1.00	1.00	1.00	1.00	1.00	1.00	1.00	-	1.000	100

Table B4 Step III: Estimation of the consistency ratio for each factor.

Criterion	Elevation	Slope aspect	Slope angle	Drainage	Lithology	Lineament	Soil texture	Precipitation	LULC	NDVI	Weighted Sum Vector	weight	Consistency Vector
Elevation	0.03	0.03	0.03	0.02	0.03	0.04	0.03	0.05	0.02	0.02	0.30	0.03	10.00
Slope aspect	0.03	0.03	0.04	0.06	0.03	0.02	0.02	0.04	0.02	0.02	0.32	0.03	10.67
Slope angle	0.15	0.12	0.17	0.15	0.09	0.24	0.25	0.13	0.24	0.3	1.84	0.17	10.82
Drainage	0.06	0.02	0.03	0.03	0.06	0.03	0.02	0.05	0.03	0.03	0.35	0.03	11.67
Lithology	0.15	0.15	0.34	0.09	0.17	0.24	0.1	0.09	0.32	0.3	1.95	0.17	11.47
Lineament	0.09	0.15	0.09	0.12	0.09	0.12	0.15	0.09	0.24	0.24	1.37	0.12	11.42
Soil texture	0.06	0.09	0.03	0.09	0.09	0.04	0.05	0.05	0.03	0.03	0.56	0.05	11.20
Precipitation	0.15	0.18	0.34	0.15	0.51	0.36	0.25	0.26	0.4	0.3	2.90	0.26	11.15
LULC	0.12	0.12	0.06	0.09	0.04	0.04	0.15	0.05	0.08	0.12	0.87	0.08	10.88
NDVI	0.09	0.09	0.03	0.06	0.03	0.03	0.1	0.05	0.04	0.06	0.59	0.06	9.83
Total													109.11

Number of criteria (n) = 10

$$\text{Lambda } (\lambda) = \frac{109.11}{10} = 10.91$$

$$\text{Consistency Index (CI)} = \frac{\lambda - n}{n - 1} = \frac{10.91 - 10}{10 - 1} = 0.101$$

Random Index (RI) for $n = 10$ is 1.49

$$\text{Consistency Ratio (CR)} = \frac{CI}{RI} = \frac{0.101}{1.49} = 0.068$$

$CR < 0.10$, this ratio indicates a reasonable level of consistency in the pair-wise comparisons.

APPENDIX C

THE PAIR-WISE COMPARISON METHOD:

AHP'S CLASS WEIGHTS

THE PROCEDURE CONSISTS OF THREE MAJOR STEPS FOR EACH CLASS

Normally, the determination of the values of the parameters relative to each class is a situation that depends on the choices of the decision-maker. However, in this study, both the comparison of the parameters relative to each class and the determination of the decision alternatives, namely the effect values of the class weights of the parameters (rating) were based on organization research such as Department of Mineral Resources and Land Development Department and information of interviewed their researcher.

1. Elevation

Table C1 Step I: Generation of the pair-wise comparison matrix for each elevation's class.

Class	<600 m	600 m – 800 m	800 m – 1,000 m	1,000 m – 1,200 m	1,200 m – 1,400 m	1,400 m – 1,600 m	>1,600 m
<600 m	1.00	0.50	0.33	0.25	0.20	0.14	0.11
600 m – 800 m	2.00	1.00	0.50	0.33	0.25	0.17	0.13
800 m – 1,000 m	3.00	2.00	1.00	0.50	0.33	0.20	0.14
1,000 m – 1,200 m	4.00	3.00	2.00	1.00	0.50	0.25	0.17
1,200 m – 1,400 m	5.00	4.00	3.00	2.00	1.00	0.33	0.20
1,400 m – 1,600 m	7.00	6.00	5.00	4.00	3.00	1.00	0.33
>1,600 m	9.00	8.00	7.00	6.00	5.00	3.00	1.00
Total	31.00	24.50	18.83	14.08	10.28	5.09	2.08

Table C2 Step II: Computation of the criterion weights for each elevation's class.

Class	<600 m	600 m – 800 m	800 m – 1,000 m	1,000 m – 1,200 m	1,200 m – 1,400 m	1,400 m – 1,600 m	>1,600 m	Total	Weight	Weight (%)
<600 m	0.03	0.02	0.02	0.02	0.02	0.03	0.05	0.19	0.027	2.71
600 m – 800 m	0.06	0.04	0.03	0.02	0.02	0.03	0.06	0.26	0.037	3.71
800 m – 1,000 m	0.10	0.08	0.05	0.04	0.03	0.04	0.07	0.41	0.059	5.86
1,000 m – 1,200 m	0.13	0.12	0.11	0.07	0.05	0.05	0.08	0.61	0.087	8.71
1,200 m – 1,400 m	0.16	0.16	0.16	0.14	0.10	0.06	0.10	0.88	0.126	12.57
1,400 m – 1,600 m	0.23	0.24	0.27	0.28	0.29	0.20	0.16	1.67	0.239	23.86
>1,600 m	0.29	0.33	0.37	0.43	0.49	0.59	0.48	2.98	0.426	42.57
Total	1.00	1.00	1.00	1.00	1.00	1.00	1.00	-	1.000	100.00

Table C3 Step III: Estimation of the consistency ratio for each elevation's class.

Class	<600 m	600 m – 800 m	800 m – 1,000 m	1,000 m – 1,200 m	1,200 m – 1,400 m	1,400 m – 1,600 m	>1,600 m	Weighted Sum Vector	weight	Consistency Vector
<600 m	0.03	0.02	0.02	0.02	0.03	0.03	0.05	0.20	0.03	6.64
600 m – 800 m	0.06	0.04	0.03	0.03	0.03	0.04	0.06	0.29	0.04	7.22
800 m – 1,000 m	0.09	0.08	0.06	0.05	0.04	0.05	0.06	0.43	0.06	7.10
1,000 m – 1,200 m	0.12	0.12	0.12	0.09	0.07	0.06	0.07	0.65	0.09	7.20
1,200 m – 1,400 m	0.15	0.16	0.18	0.18	0.13	0.08	0.09	0.97	0.13	7.42
1,400 m – 1,600 m	0.21	0.24	0.30	0.36	0.39	0.24	0.14	1.88	0.24	7.84
>1,600 m	0.27	0.32	0.42	0.54	0.65	0.72	0.43	3.35	0.43	7.79
Total	-	-	-	-	-	-	-	-	-	51.22

Number of class (n) = 7

$$\text{Lambda } (\lambda) = \frac{51.22}{7} = 7.32$$

$$\text{Consistency Index (CI)} = \frac{\lambda - n}{n - 1} = \frac{7.32 - 7}{7 - 1} = 0.05$$

Random Index (RI) for $n = 7$ is 1.32

$$\text{Consistency Ratio (CR)} = \frac{CI}{RI} = \frac{0.05}{1.32} = 0.040$$

CR<0.10, this ratio indicates a reasonable level of consistency in the pair-wise comparisons.

2. Slope aspect

Table C4 Step I: Generation of the pair-wise comparison matrix for each slope aspect's class.

Class	Flat	North	Northeast	East	Southeast	South	Southwest	West	Northwest
Flat	1.00	0.33	0.20	0.33	0.33	0.33	0.14	0.33	0.33
North	3.00	1.00	0.33	1.00	1.00	1.00	0.20	1.00	1.00
Northeast	5.00	3.00	1.00	3.00	3.00	3.00	0.33	3.00	3.00
East	3.00	1.00	0.33	1.00	1.00	1.00	0.20	1.00	1.00
Southeast	3.00	1.00	0.33	1.00	1.00	1.00	0.20	1.00	1.00
South	3.00	1.00	0.33	1.00	1.00	1.00	0.20	1.00	1.00
Southwest	7.00	5.00	3.00	5.00	5.00	5.00	1.00	5.00	5.00
West	3.00	1.00	0.33	1.00	1.00	1.00	0.20	1.00	1.00
Northwest	3.00	1.00	0.33	1.00	1.00	1.00	0.20	1.00	1.00
Total	31.00	14.33	6.18	14.33	14.33	14.33	2.67	14.33	14.33

Table C5 Step II: Computation of the criterion weights for each slope aspect's class.

Class	Flat	North	Northeast	East	Southeast	South	Southwest	West	Northwest	Total	Weight	Weight (%)
Flat	0.03	0.02	0.03	0.02	0.02	0.02	0.05	0.02	0.02	0.23	0.026	2.56
North	0.10	0.07	0.05	0.07	0.07	0.07	0.07	0.07	0.07	0.64	0.071	7.11
Northeast	0.16	0.21	0.16	0.21	0.21	0.21	0.12	0.21	0.21	1.70	0.189	18.89
East	0.10	0.07	0.05	0.07	0.07	0.07	0.07	0.07	0.07	0.64	0.071	7.11
Southeast	0.10	0.07	0.05	0.07	0.07	0.07	0.07	0.07	0.07	0.64	0.071	7.11
South	0.10	0.07	0.05	0.07	0.07	0.07	0.07	0.07	0.07	0.64	0.071	7.11
Southwest	0.23	0.35	0.49	0.35	0.35	0.35	0.37	0.35	0.35	3.19	0.354	35.44
West	0.10	0.07	0.05	0.07	0.07	0.07	0.07	0.07	0.07	0.64	0.071	7.11
Northwest	0.10	0.07	0.05	0.07	0.07	0.07	0.07	0.07	0.07	0.64	0.071	7.11
Total	1.00	1.00	1.00	1.00	1.00	1.00	1.00	1.00	1.00	-	1.000	100.00

Table C6 Step III: Estimation of the consistency ratio for each slope aspect's class.

Class	Flat	North	Northeast	East	Southeast	South	Southwest	West	Northwest	Weighted Sum Vector	weight	Consistency Vector
Flat	0.03	0.02	0.04	0.02	0.02	0.02	0.05	0.02	0.02	0.26	0.03	8.52
North	0.09	0.07	0.06	0.07	0.07	0.07	0.07	0.07	0.07	0.64	0.07	9.18
Northeast	0.15	0.21	0.19	0.21	0.21	0.21	0.12	0.21	0.21	1.72	0.19	9.03
East	0.09	0.07	0.06	0.07	0.07	0.07	0.07	0.07	0.07	0.64	0.07	9.18
Southeast	0.09	0.07	0.06	0.07	0.07	0.07	0.07	0.07	0.07	0.64	0.07	9.18
South	0.09	0.07	0.06	0.07	0.07	0.07	0.07	0.07	0.07	0.64	0.07	9.18
Southwest	0.21	0.35	0.57	0.35	0.35	0.35	0.35	0.35	0.35	3.23	0.35	9.23
West	0.09	0.07	0.06	0.07	0.07	0.07	0.07	0.07	0.07	0.64	0.07	9.18
Northwest	0.09	0.07	0.06	0.07	0.07	0.07	0.07	0.07	0.07	0.64	0.07	9.18
Total	-	-	-	-	-	-	-	-	-	-	-	81.87

Number of class (n) = 9

$$\text{Lambda } (\lambda) = \frac{81.87}{9} = 9.10$$

$$\text{Consistency Index (CI)} = \frac{\lambda - n}{n - 1} = \frac{9.10 - 9}{9 - 1} = 0.01$$

Random Index (RI) for $n = 9$ is 1.45

$$\text{Consistency Ratio (CR)} = \frac{CI}{RI} = \frac{0.01}{1.45} = 0.008$$

$CR < 0.10$, this ratio indicates a reasonable level of consistency in the pair-wise comparisons.

3. Slope angle

Table C7 Step I: Generation of the pair-wise comparison matrix for each slope angle's class.

Class	0° – 5°	5° – 10°	10° – 15°	15° – 20°	20° – 25°	25° – 30°	30° – 35°	>35°
0° – 5°	1.00	0.50	0.33	0.25	0.20	0.17	0.14	0.11
5° – 10°	2.00	1.00	0.50	0.33	0.25	0.20	0.17	0.13
10° – 15°	3.00	2.00	1.00	0.50	0.33	0.25	0.20	0.14
15° – 20°	4.00	3.00	2.00	1.00	0.50	0.33	0.25	0.17
20° – 25°	5.00	4.00	3.00	2.00	1.00	0.50	0.33	0.20
25° – 30°	6.00	5.00	4.00	3.00	2.00	1.00	0.50	0.25
30° – 35°	7.00	6.00	5.00	4.00	3.00	2.00	1.00	0.33
>35°	9.00	8.00	7.00	6.00	5.00	4.00	3.00	1.00
Total	37.00	29.50	22.83	17.08	12.28	8.45	5.59	2.33

Table C8 Step II: Computation of the criterion weights for each slope angle's class.

Class	0° – 5°	5° – 10°	10° – 15°	15° – 20°	20° – 25°	25° – 30°	30° – 35°	>35°	Total	Weight	Weight (%)
0° – 5°	0.03	0.02	0.01	0.01	0.02	0.02	0.03	0.05	0.19	0.024	2.38
5° – 10°	0.05	0.03	0.02	0.02	0.02	0.02	0.03	0.06	0.25	0.031	3.13
10° – 15°	0.08	0.07	0.04	0.03	0.03	0.03	0.04	0.06	0.38	0.048	4.75
15° – 20°	0.11	0.10	0.09	0.06	0.04	0.04	0.04	0.07	0.55	0.069	6.88
20° – 25°	0.14	0.14	0.13	0.12	0.08	0.06	0.06	0.09	0.82	0.103	10.25
25° – 30°	0.16	0.17	0.18	0.18	0.16	0.12	0.09	0.11	1.17	0.146	14.63
30° – 35°	0.19	0.20	0.22	0.23	0.24	0.24	0.18	0.14	1.64	0.205	20.50
>35°	0.24	0.27	0.31	0.35	0.41	0.47	0.54	0.43	3.02	0.378	37.75
Total	1.00	1.00	1.00	1.00	1.00	1.00	1.00	1.00	-	1.000	100.00

Table C9 Step III: Estimation of the consistency ratio for each slope angle's class.

Class	0° – 5°	5° – 10°	10° – 15°	15° – 20°	20° – 25°	25° – 30°	30° – 35°	>35°	Weighted Sum Vector	weight	Consistency Vector
0° – 5°	0.02	0.02	0.02	0.02	0.02	0.03	0.03	0.04	0.19	0.02	9.29
5° – 10°	0.04	0.03	0.03	0.02	0.03	0.03	0.04	0.05	0.26	0.03	8.61
10° – 15°	0.06	0.06	0.05	0.04	0.03	0.04	0.04	0.05	0.37	0.05	7.41
15° – 20°	0.08	0.09	0.10	0.07	0.05	0.05	0.05	0.06	0.56	0.07	7.95
20° – 25°	0.10	0.12	0.15	0.14	0.10	0.08	0.07	0.08	0.83	0.10	8.30
25° – 30°	0.12	0.15	0.20	0.21	0.20	0.15	0.11	0.10	1.23	0.15	8.20
30° – 35°	0.14	0.18	0.25	0.28	0.30	0.30	0.21	0.13	1.79	0.21	8.50
>35°	0.18	0.24	0.35	0.42	0.50	0.60	0.63	0.38	3.30	0.38	8.68
Total	-	-	-	-	-	-	-	-	-	-	66.95

Number of class (n) = 8

$$\text{Lambda } (\lambda) = \frac{66.95}{8} = 8.37$$

$$\text{Consistency Index (CI)} = \frac{\lambda - n}{n - 1} = \frac{8.37 - 8}{8 - 1} = 0.05$$

Random Index (RI) for $n = 8$ is 1.41

$$\text{Consistency Ratio (CR)} = \frac{CI}{RI} = \frac{0.05}{1.41} = 0.037$$

CR < 0.10, this ratio indicates a reasonable level of consistency in the pair-wise comparisons.

4. Distance from drainage

Table C10 Step I: Generation of the pair-wise comparison matrix for each distance from drainage's class.

Class	<500 m	500 m – 1,000 m	1,000 m – 1,500 m	1,500 m – 2,000 m	2,000 m – 2,500 m	>2,500 m
<500 m	1.00	3.00	5.00	7.00	8.00	9.00
500 m – 1,000 m	0.33	1.00	3.00	5.00	6.00	7.00
1,000 m – 1,500 m	0.20	0.33	1.00	3.00	4.00	5.00
1,500 m – 2,000 m	0.14	0.20	0.33	1.00	2.00	3.00
2,000 m – 2,500 m	0.13	0.17	0.25	0.50	1.00	2.00
>2,500 m	0.11	0.14	0.20	0.33	0.50	1.00
Total	1.91	4.84	9.78	16.83	21.50	27.00

Table C11 Step II: Computation of the criterion weights for each distance from drainage's class.

Class	<500 m	500 m – 1,000 m	1,000 m – 1,500 m	1,500 m – 2,000 m	2,000 m – 2,500 m	>2,500 m	Total	Weight	Weight (%)
<500 m	0.52	0.62	0.51	0.42	0.37	0.33	2.77	0.462	46.17
500 m – 1,000 m	0.17	0.21	0.31	0.30	0.28	0.26	1.53	0.255	25.50
1,000 m – 1,500 m	0.10	0.07	0.10	0.18	0.19	0.19	0.83	0.138	13.83
1,500 m – 2,000 m	0.07	0.04	0.03	0.06	0.09	0.11	0.40	0.067	6.67
2,000 m – 2,500 m	0.07	0.04	0.03	0.03	0.05	0.07	0.29	0.048	4.83
>2,500 m	0.06	0.03	0.02	0.02	0.02	0.04	0.19	0.032	3.17
Total	1.00	1.00	1.00	1.00	1.00	1.00	-	1.000	100.00

Table C12 Step III: Estimation of the consistency ratio for each distance from drainage's class.

Class	<500 m	500 m – 1,000 m	1,000 m – 1,500 m	1,500 m – 2,000 m	2,000 m – 2,500 m	>2,500 m	Weighted Sum Vector	weight	Consistency Vector
<500 m	0.46	0.78	0.70	0.49	0.40	0.27	3.10	0.46	6.74
500 m – 1,000 m	0.15	0.26	0.42	0.35	0.30	0.21	1.69	0.26	6.51
1,000 m – 1,500 m	0.09	0.09	0.14	0.21	0.20	0.15	0.88	0.14	6.27
1,500 m – 2,000 m	0.06	0.05	0.05	0.07	0.10	0.09	0.42	0.07	6.04
2,000 m – 2,500 m	0.06	0.04	0.04	0.04	0.05	0.06	0.28	0.05	5.68
>2,500 m	0.05	0.04	0.03	0.02	0.03	0.03	0.19	0.03	6.44
Total	-	-	-	-	-	-	-	-	37.67

Number of class (n) = 6

$$\text{Lambda } (\lambda) = \frac{37.67}{6} = 6.28$$

$$\text{Consistency Index (CI)} = \frac{\lambda - n}{n - 1} = \frac{6.28 - 6}{6 - 1} = 0.06$$

Random Index (RI) for $n = 6$ is 1.24

$$\text{Consistency Ratio (CR)} = \frac{CI}{RI} = \frac{0.06}{1.24} = 0.045$$

CR < 0.10, this ratio indicates a reasonable level of consistency in the pair-wise comparisons.

5. Lithology

Table C13 Step I: Generation of the pair-wise comparison matrix for each lithology's class.

Class	Sandstone	Marble	Limestone, shale	Paragneiss	Alluvium	Shale, chert, and siltstone	Claystone and siltstone	Granite	Conglomerate, sandstone	Granodiorite porphyry
Sandstone	1.00	3.00	3.00	2.00	5.00	3.00	4.00	0.33	1.00	0.50
Marble	0.33	1.00	1.00	0.50	3.00	1.00	2.00	0.20	0.33	0.25
Limestone, shale	0.33	1.00	1.00	0.50	3.00	1.00	2.00	0.20	0.33	0.25
Paragneiss	0.50	2.00	2.00	1.00	4.00	2.00	3.00	0.25	0.50	0.33
Alluvium	0.20	0.33	0.33	0.25	1.00	0.33	0.50	0.14	0.20	0.17
Shale, chert, and siltstone	0.33	1.00	1.00	0.50	3.00	1.00	2.00	0.20	0.33	0.25
Claystone and siltstone	0.25	0.50	0.50	0.33	2.00	0.50	1.00	0.17	0.25	0.20
Granite	3.00	5.00	5.00	4.00	7.00	5.00	6.00	1.00	3.00	2.00
Conglomerate, sandstone	1.00	3.00	3.00	2.00	5.00	3.00	4.00	0.33	1.00	0.50
Granodiorite porphyry	2.00	4.00	4.00	3.00	6.00	4.00	5.00	0.50	2.00	1.00
Total	8.94	20.83	20.83	14.08	39.00	20.83	29.50	3.32	8.94	5.45

Table C14 Step II: Computation of the criterion weights for each lithology's class.

Class	Sandstone	Marble	Limestone, shale	Paragneiss	Alluvium	Shale, chert, and siltstone	Claystone and siltstone	Granite	Conglomerate, sandstone	Granodiorite porphyry	Total	Weight	Weight (%)
Sandstone	0.11	0.14	0.14	0.14	0.13	0.14	0.14	0.10	0.11	0.09	1.24	0.124	12.40
Marble	0.04	0.05	0.05	0.04	0.08	0.05	0.07	0.06	0.04	0.05	0.53	0.053	5.30
Limestone, shale	0.04	0.05	0.05	0.04	0.08	0.05	0.07	0.06	0.04	0.05	0.53	0.053	5.30
Paragneiss	0.06	0.10	0.10	0.07	0.10	0.10	0.10	0.08	0.06	0.06	0.83	0.083	8.30
Alluvium	0.02	0.02	0.02	0.02	0.03	0.02	0.02	0.04	0.02	0.03	0.24	0.024	2.40
Shale, chert, and siltstone	0.04	0.05	0.05	0.04	0.08	0.05	0.07	0.06	0.04	0.05	0.53	0.053	5.30
Claystone and siltstone	0.03	0.02	0.02	0.02	0.05	0.02	0.03	0.05	0.03	0.04	0.31	0.031	3.10
Granite	0.34	0.24	0.24	0.28	0.18	0.24	0.20	0.30	0.34	0.37	2.73	0.273	27.30
Conglomerate, sandstone	0.11	0.14	0.14	0.14	0.13	0.14	0.14	0.10	0.11	0.09	1.24	0.124	12.40
Granodiorite porphyry	0.22	0.19	0.19	0.21	0.15	0.19	0.17	0.15	0.22	0.18	1.87	0.187	18.70
Total	1.00	1.00	1.00	1.00	1.00	1.00	1.00	1.00	1.00	1.00	-	1.000	100.00

Table C15 Step III: Estimation of the consistency ratio for each lithology's class.

Class	Sandstone	Marble	Limestone, shale	Paragneiss	Alluvium	Shale, chert, and siltstone	Claystone and siltstone	Granite	Conglomerate, sandstone	Granodiorite porphyry	Weighted Sum Vector	weight	Consistency Vector
Sandstone	0.12	0.15	0.15	0.16	0.10	0.15	0.12	0.09	0.12	0.10	1.25	0.12	10.45
Marble	0.04	0.05	0.05	0.04	0.06	0.05	0.06	0.05	0.04	0.05	0.49	0.05	9.81
Limestone, shale	0.04	0.05	0.05	0.04	0.06	0.05	0.06	0.05	0.04	0.05	0.49	0.05	9.81
Paragneiss	0.06	0.10	0.10	0.08	0.08	0.10	0.09	0.07	0.06	0.06	0.80	0.08	10.00
Alluvium	0.02	0.02	0.02	0.02	0.02	0.02	0.02	0.04	0.02	0.03	0.22	0.02	11.13
Shale, chert, and siltstone	0.04	0.05	0.05	0.04	0.06	0.05	0.06	0.05	0.04	0.05	0.49	0.05	9.81
Claystone and siltstone	0.03	0.03	0.03	0.03	0.04	0.03	0.03	0.05	0.03	0.04	0.32	0.03	10.51
Granite	0.36	0.25	0.25	0.32	0.14	0.25	0.18	0.27	0.36	0.38	2.76	0.27	10.22
Conglomerate, sandstone	0.12	0.15	0.15	0.16	0.10	0.15	0.12	0.09	0.12	0.10	1.25	0.12	10.45
Granodiorite porphyry	0.24	0.20	0.20	0.24	0.12	0.20	0.15	0.14	0.24	0.19	1.92	0.19	10.08
Total	-	-	-	-	-	-	-	-	-	-	-	-	102.29

Number of class (n) = 10

$$\text{Lambda } (\lambda) = \frac{102.29}{10} = 10.23$$

$$\text{Consistency Index (CI)} = \frac{\lambda - n}{n - 1} = \frac{10.23 - 10}{10 - 1} = 0.03$$

Random Index (RI) for $n = 10$ is 1.49

$$\text{Consistency Ratio (CR)} = \frac{CI}{RI} = \frac{0.03}{1.49} = 0.017$$

$CR < 0.10$, this ratio indicates a reasonable level of consistency in the pair-wise comparisons.

6. Distance from lineament

Table C16 Step I: Generation of the pair-wise comparison matrix for each distance from lineament's class.

Class	<500m	500 m – 1,000 m	1,000 m – 2,000 m	2,000 m – 3,000 m	3,000 m – 4,000 m	>4,000 m
<500m	1.00	1.00	2.00	3.00	4.00	4.00
500 m – 1,000 m	1.00	1.00	2.00	3.00	4.00	4.00
1,000 m – 2,000 m	0.50	0.50	1.00	2.00	3.00	3.00
2,000 m – 3,000 m	0.33	0.33	0.50	1.00	2.00	2.00
3,000 m – 4,000 m	0.25	0.25	0.33	0.50	1.00	1.00
>4,000 m	0.25	0.25	0.33	0.50	1.00	1.00
Total	3.33	3.33	6.16	10.00	15.00	15.00

Table C17 Step II: Computation of the criterion weights for each distance from lineament's class.

Class	<500m	500 m – 1,000 m	1,000 m – 2,000 m	2,000 m – 3,000 m	3,000 m – 4,000 m	>4,000 m	Total	Weight	Weight (%)
<500m	0.30	0.30	0.32	0.30	0.27	0.27	1.76	0.293	29.33
500 m – 1,000 m	0.30	0.30	0.32	0.30	0.27	0.27	1.76	0.293	29.33
1,000 m – 2,000 m	0.15	0.15	0.16	0.20	0.20	0.20	1.06	0.177	17.67
2,000 m – 3,000 m	0.10	0.10	0.08	0.10	0.13	0.13	0.64	0.107	10.67
3,000 m – 4,000 m	0.08	0.08	0.05	0.05	0.07	0.07	0.40	0.067	6.67
>4,000 m	0.08	0.08	0.05	0.05	0.07	0.07	0.40	0.067	6.67
Total	1.00	1.00	1.00	1.00	1.00	1.00	-	1.000	100.00

Table C18 Step III: Estimation of the consistency ratio for each distance from lineament's class.

Class	<500m	500 m – 1,000 m	1,000 m – 2,000 m	2,000 m – 3,000 m	3,000 m – 4,000 m	>4,000 m	Weighted Sum Vector	weight	Consistency Vector
<500m	0.29	0.29	0.36	0.33	0.28	0.28	1.83	0.29	6.31
500 m – 1,000 m	0.29	0.29	0.36	0.33	0.28	0.28	1.83	0.29	6.31
1,000 m – 2,000 m	0.15	0.15	0.18	0.22	0.21	0.21	1.11	0.18	6.17
2,000 m – 3,000 m	0.10	0.10	0.09	0.11	0.14	0.14	0.67	0.11	6.10
3,000 m – 4,000 m	0.07	0.07	0.06	0.06	0.07	0.07	0.40	0.07	5.71
>4,000 m	0.07	0.07	0.06	0.06	0.07	0.07	0.40	0.07	5.71
Total	-	-	-	-	-	-	-	-	36.30

Number of class (n) = 6

$$\text{Lambda } (\lambda) = \frac{36.30}{6} = 6.05$$

$$\text{Consistency Index (CI)} = \frac{\lambda - n}{n - 1} = \frac{6.05 - 6}{6 - 1} = 0.01$$

Random Index (RI) for $n = 6$ is 1.24

$$\text{Consistency Ratio (CR)} = \frac{CI}{RI} = \frac{0.01}{1.24} = 0.008$$

CR < 0.10, this ratio indicates a reasonable level of consistency in the pair-wise comparisons.

7. Soil texture

Table C19 Step I: Generation of the pair-wise comparison matrix for each soil texture's class.

Class	Clay	Loam	Sand	Sandy loam/ sandy clay loam	Loam with gravel	Sandy loam with gravel	Clay/loam with rock	Slope complex area
Clay	1.00	0.25	0.13	0.14	0.20	0.11	0.33	0.25
Loam	4.00	1.00	0.20	0.25	0.50	0.17	2.00	1.00
Sand	8.00	5.00	1.00	2.00	4.00	0.50	6.00	5.00
Sandy loam/sandy clay loam	7.00	4.00	0.50	1.00	3.00	0.33	5.00	4.00
Loam with gravel	5.00	2.00	0.25	0.33	1.00	0.20	3.00	2.00
Sandy loam with gravel	9.00	6.00	2.00	3.00	5.00	1.00	7.00	6.00
Clay/loam with rock	3.00	0.50	0.17	0.20	0.33	0.14	1.00	0.50
Slope complex area	4.00	1.00	0.20	0.25	0.50	0.17	2.00	1.00
Total	41.00	19.75	4.45	7.17	14.53	2.62	26.33	19.75

Table C20 Step II: Computation of the criterion weights for each soil texture's class.

Class	Clay	Loam	Sand	Sandy loam/ sandy clay loam	Loam with gravel	Sandy loam with gravel	Clay/loam with rock	Slope complex area	Total	Weight	Weight (%)
Clay	0.02	0.01	0.03	0.02	0.01	0.04	0.01	0.01	0.15	0.019	1.88
Loam	0.10	0.05	0.04	0.03	0.03	0.06	0.08	0.05	0.44	0.055	5.50
Sand	0.20	0.25	0.22	0.28	0.28	0.19	0.23	0.25	1.90	0.238	23.75
Sandy loam/sandy clay loam	0.17	0.20	0.11	0.14	0.21	0.13	0.19	0.20	1.35	0.169	16.88
Loam with gravel	0.12	0.10	0.06	0.05	0.07	0.08	0.11	0.10	0.69	0.086	8.63
Sandy loam with gravel	0.22	0.30	0.45	0.42	0.34	0.38	0.27	0.30	2.68	0.335	33.50
Clay/loam with rock	0.07	0.03	0.04	0.03	0.02	0.05	0.04	0.03	0.31	0.039	3.88
Slope complex area	0.10	0.05	0.04	0.03	0.03	0.06	0.08	0.05	0.44	0.055	5.50
Total	1.00	1.00	1.00	1.00	1.00	1.00	1.00	1.00	-	1.000	100.00

Table C21 Step III: Estimation of the consistency ratio for each soil texture's class.

Class	Clay	Loam	Sand	Sandy loam/ sandy clay loam	Loam with gravel	Sandy loam with gravel	Clay/loam with rock	Slope complex area	Weighted Sum Vector	weight	Consistency Vector
Clay	0.02	0.02	0.03	0.02	0.02	0.04	0.01	0.02	0.17	0.02	8.68
Loam	0.08	0.06	0.05	0.04	0.05	0.06	0.08	0.06	0.47	0.06	7.89
Sand	0.16	0.30	0.24	0.34	0.36	0.17	0.24	0.30	2.11	0.24	8.79
Sandy loam/sandy clay loam	0.14	0.24	0.12	0.17	0.27	0.11	0.20	0.24	1.49	0.17	8.78
Loam with gravel	0.10	0.12	0.06	0.06	0.09	0.07	0.12	0.12	0.73	0.09	8.16
Sandy loam with gravel	0.18	0.36	0.48	0.51	0.45	0.34	0.28	0.36	2.96	0.34	8.71
Clay/loam with rock	0.06	0.03	0.04	0.03	0.03	0.05	0.04	0.03	0.31	0.04	7.80
Slope complex area	0.08	0.06	0.05	0.04	0.05	0.06	0.08	0.06	0.47	0.06	7.89
Total	-	-	-	-	-	-	-	-	-	-	66.69

Number of class (n) = 8

$$\text{Lambda } (\lambda) = \frac{66.69}{8} = 8.34$$

$$\text{Consistency Index (CI)} = \frac{\lambda - n}{n - 1} = \frac{8.34 - 8}{8 - 1} = 0.05$$

Random Index (RI) for $n = 8$ is 1.41

$$\text{Consistency Ratio (CR)} = \frac{CI}{RI} = \frac{0.05}{1.41} = 0.034$$

$CR < 0.10$, this ratio indicates a reasonable level of consistency in the pair-wise comparisons.

8. Precipitation

Table C22 Step I: Generation of the pair-wise comparison matrix for each precipitation's class.

Class	<1,000 mm	1,000 mm – 1,200 mm	1,200 mm – 1,400 mm	1,400 mm – 1,600 mm	1,600 mm – 1,800 mm	1,800 mm – 2,000 mm	>2,000 mm
<1,000 mm	1.00	0.50	0.33	0.20	0.17	0.13	0.11
1,000 mm – 1,200 mm	2.00	1.00	0.50	0.25	0.20	0.14	0.13
1,200 mm – 1,400 mm	3.00	2.00	1.00	0.33	0.25	0.17	0.14
1,400 mm – 1,600 mm	5.00	4.00	3.00	1.00	0.50	0.25	0.20
1,600 mm – 1,800 mm	6.00	5.00	4.00	2.00	1.00	0.33	0.25
1,800 mm – 2,000 mm	8.00	7.00	6.00	4.00	3.00	1.00	0.50
>2,000 mm	9.00	8.00	7.00	5.00	4.00	2.00	1.00
Total	34.00	27.50	21.83	12.78	9.12	4.02	2.33

Table C23 Step II: Computation of the criterion weights for each precipitation's class.

Class	<1,000 mm	1,000 mm – 1,200 mm	1,200 mm – 1,400 mm	1,400 mm – 1,600 mm	1,600 mm – 1,800 mm	1,800 mm – 2,000 mm	>2,000 mm	Total	Weight	Weight (%)
<1,000 mm	0.03	0.02	0.02	0.02	0.02	0.03	0.05	0.19	0.027	2.71
1,000 mm – 1,200 mm	0.06	0.04	0.02	0.02	0.02	0.03	0.06	0.25	0.036	3.57
1,200 mm – 1,400 mm	0.09	0.07	0.05	0.03	0.03	0.04	0.06	0.37	0.053	5.29
1,400 mm – 1,600 mm	0.15	0.15	0.14	0.08	0.05	0.06	0.09	0.72	0.103	10.29
1,600 mm – 1,800 mm	0.18	0.18	0.18	0.16	0.11	0.08	0.11	1.00	0.143	14.29
1,800 mm – 2,000 mm	0.24	0.25	0.27	0.31	0.33	0.25	0.21	1.86	0.266	26.57
>2,000 mm	0.26	0.29	0.32	0.39	0.44	0.50	0.43	2.63	0.376	37.57
Total	1.00	1.00	1.00	1.00	1.00	1.00	1.00	-	1.000	100.00

Table C24 Step III: Estimation of the consistency ratio for each precipitation's class.

Class	<1,000 mm	1,000 mm – 1,200 mm	1,200 mm – 1,400 mm	1,400 mm – 1,600 mm	1,600 mm – 1,800 mm	1,800 mm – 2,000 mm	>2,000 mm	Weighted Sum Vector	weight	Consistency Vector
<1,000 mm	0.03	0.02	0.02	0.02	0.02	0.04	0.04	0.19	0.03	6.24
1,000 mm – 1,200 mm	0.06	0.04	0.03	0.03	0.03	0.04	0.05	0.27	0.04	6.63
1,200 mm – 1,400 mm	0.09	0.08	0.05	0.03	0.04	0.05	0.05	0.39	0.05	7.74
1,400 mm – 1,600 mm	0.15	0.16	0.15	0.10	0.07	0.07	0.08	0.77	0.10	7.74
1,600 mm – 1,800 mm	0.18	0.20	0.20	0.20	0.14	0.09	0.10	1.10	0.14	7.89
1,800 mm – 2,000 mm	0.24	0.28	0.30	0.40	0.42	0.27	0.19	2.10	0.27	7.78
>2,000 mm	0.27	0.32	0.35	0.50	0.56	0.54	0.38	2.92	0.38	7.68
Total	-	-	-	-	-	-	-	-	-	51.70

Number of class (n) = 7

$$\text{Lambda } (\lambda) = \frac{51.70}{7} = 7.39$$

$$\text{Consistency Index (CI)} = \frac{\lambda - n}{n - 1} = \frac{7.39 - 7}{7 - 1} = 0.06$$

Random Index (RI) for $n = 7$ is 1.32

$$\text{Consistency Ratio (CR)} = \frac{CI}{RI} = \frac{0.06}{1.32} = 0.049$$

CR < 0.10, this ratio indicates a reasonable level of consistency in the pair-wise comparisons.

9. Land use/land cover

Table C25 Step I: Generation of the pair-wise comparison matrix for each land use/land cover's class.

Class	Paddy field	Mixed field crop	Longan	Truck crop	Mixed swidden cultivation	Hill evergreen forest	Mixed deciduous forest	Mixed forest plantation	Grass and scrub	Mine	Urban, village	Water
Paddy field	1.00	2.00	3.00	2.00	2.00	7.00	6.00	5.00	4.00	0.50	0.50	8.00
Mixed field crop	0.50	1.00	2.00	1.00	1.00	6.00	5.00	4.00	3.00	0.33	0.33	7.00
Longan	0.33	0.50	1.00	0.50	0.50	5.00	4.00	3.00	2.00	0.25	0.25	6.00
Truck crop	0.50	1.00	2.00	1.00	1.00	6.00	5.00	4.00	3.00	0.33	0.33	7.00
Mixed swidden cultivation	0.50	1.00	2.00	1.00	1.00	6.00	5.00	4.00	3.00	0.33	0.33	7.00
Hill evergreen forest	0.14	0.17	0.20	0.17	0.17	1.00	0.50	0.33	0.25	0.13	0.13	2.00
Mixed deciduous forest	0.17	0.20	0.25	0.20	0.20	2.00	1.00	0.50	0.33	0.14	0.14	3.00
Mixed forest plantation	0.20	0.25	0.33	0.25	0.25	3.00	2.00	1.00	0.50	0.17	0.17	4.00
Grass and scrub	0.25	0.33	0.50	0.33	0.33	4.00	3.00	2.00	1.00	0.20	0.20	5.00
Mine	2.00	3.00	4.00	3.00	3.00	8.00	7.00	6.00	5.00	1.00	1.00	9.00
Urban, village	2.00	3.00	4.00	3.00	3.00	8.00	7.00	6.00	5.00	1.00	1.00	9.00
Water	0.13	0.14	0.17	0.14	0.14	0.50	0.33	0.25	0.20	0.11	0.11	1.00
Total	7.72	12.59	19.45	12.59	12.59	56.50	45.83	36.08	27.28	4.49	4.49	68.00

Table C26 Step II: Computation of the criterion weights for each land use/land cover's class.

Class	Paddy field	Mixed field crop	Longan	Truck crop	Mixed swidden cultivation	Hill evergreen forest	Mixed deciduous forest	Mixed forest plantation	Grass and scrub	Mine	Urban, village	Water	Total	Weight	Weight (%)
Paddy field	0.13	0.16	0.15	0.16	0.16	0.12	0.13	0.14	0.15	0.11	0.11	0.12	1.64	0.137	13.67
Mixed field crop	0.06	0.08	0.10	0.08	0.08	0.11	0.11	0.11	0.11	0.07	0.07	0.10	1.08	0.090	9.00
Longan	0.04	0.04	0.05	0.04	0.04	0.09	0.09	0.08	0.07	0.06	0.06	0.09	0.75	0.063	6.25
Truck crop	0.06	0.08	0.10	0.08	0.08	0.11	0.11	0.11	0.11	0.07	0.07	0.10	1.08	0.090	9.00
Mixed swidden cultivation	0.06	0.08	0.10	0.08	0.08	0.11	0.11	0.11	0.11	0.07	0.07	0.10	1.08	0.090	9.00
Hill evergreen forest	0.02	0.01	0.01	0.01	0.01	0.02	0.01	0.01	0.01	0.03	0.03	0.03	0.20	0.017	1.67
Mixed deciduous forest	0.02	0.02	0.01	0.02	0.02	0.04	0.02	0.01	0.01	0.03	0.03	0.04	0.27	0.023	2.25
Mixed forest plantation	0.03	0.02	0.02	0.02	0.02	0.05	0.04	0.03	0.02	0.04	0.04	0.06	0.39	0.033	3.25
Grass and scrub	0.03	0.03	0.03	0.03	0.03	0.07	0.07	0.06	0.04	0.04	0.04	0.07	0.54	0.045	4.50
Mine	0.26	0.24	0.21	0.24	0.24	0.14	0.15	0.17	0.18	0.22	0.22	0.13	2.40	0.200	20.00
Urban, village	0.26	0.24	0.21	0.24	0.24	0.14	0.15	0.17	0.18	0.22	0.22	0.13	2.40	0.200	20.00
Water	0.02	0.01	0.01	0.01	0.01	0.01	0.01	0.01	0.01	0.02	0.02	0.01	0.15	0.013	1.25
Total	1.00	1.00	1.00	1.00	1.00	1.00	1.00	1.00	1.00	1.00	1.00	1.00	-	1.000	100.00

Table C27 Step III: Estimation of the consistency ratio for each land use/land cover's class.

Class	Paddy field	Mixed field crop	Longan	Truck crop	Mixed swidden cultivation	Hill evergreen forest	Mixed deciduous forest	Mixed forest plantation	Grass and scrub	Mine	Urban, village	Water	Weighted Sum Vector	weight	Consistency Vector
Paddy field	0.14	0.18	0.18	0.18	0.18	0.14	0.12	0.15	0.20	0.10	0.10	0.08	1.75	0.14	12.50
Mixed field crop	0.07	0.09	0.12	0.09	0.09	0.12	0.10	0.12	0.15	0.07	0.07	0.07	1.15	0.09	12.80
Longan	0.05	0.05	0.06	0.05	0.05	0.10	0.08	0.09	0.10	0.05	0.05	0.06	0.77	0.06	12.85
Truck crop	0.07	0.09	0.12	0.09	0.09	0.12	0.10	0.12	0.15	0.07	0.07	0.07	1.15	0.09	12.80
Mixed swidden cultivation	0.07	0.09	0.12	0.09	0.09	0.12	0.10	0.12	0.15	0.07	0.07	0.07	1.15	0.09	12.80
Hill evergreen forest	0.02	0.02	0.01	0.02	0.02	0.02	0.01	0.01	0.01	0.03	0.03	0.02	0.20	0.02	10.10
Mixed deciduous forest	0.02	0.02	0.02	0.02	0.02	0.04	0.02	0.02	0.02	0.03	0.03	0.03	0.27	0.02	13.52
Mixed forest plantation	0.03	0.02	0.02	0.02	0.02	0.06	0.04	0.03	0.03	0.03	0.03	0.04	0.38	0.03	12.61
Grass and scrub	0.04	0.03	0.03	0.03	0.03	0.08	0.06	0.06	0.05	0.04	0.04	0.05	0.53	0.05	10.68
Mine	0.28	0.27	0.24	0.27	0.27	0.16	0.14	0.18	0.25	0.20	0.20	0.09	2.55	0.20	12.75
Urban, village	0.28	0.27	0.24	0.27	0.27	0.16	0.14	0.18	0.25	0.20	0.20	0.09	2.55	0.20	12.75
Water	0.02	0.01	0.01	0.01	0.01	0.01	0.01	0.01	0.01	0.02	0.02	0.01	0.15	0.01	15.43
Total	-	-	-	-	-	-	-	-	-	-	-	-	-	-	151.59

Number of class (n) = 12

$$\text{Lambda } (\lambda) = \frac{151.59}{12} = 12.63$$

$$\text{Consistency Index (CI)} = \frac{\lambda - n}{n - 1} = \frac{12.63 - 12}{12 - 1} = 0.06$$

Random Index (RI) for $n = 12$ is 1.48

$$\text{Consistency Ratio (CR)} = \frac{CI}{RI} = \frac{0.06}{1.48} = 0.039$$

$CR < 0.10$, this ratio indicates a reasonable level of consistency in the pair-wise comparisons.

10. NDVI

Table C28 Step I: Generation of the pair-wise comparison matrix for each NDVI's class.

Class	-1.0 to 0.2	0.2 to 0.4	0.4 to 0.6	0.6 to 0.8	0.8 to 1.0
-1.0 to 0.2	1.00	3.00	5.00	6.00	7.00
0.2 to 0.4	0.33	1.00	3.00	4.00	5.00
0.4 to 0.6	0.20	0.33	1.00	2.00	3.00
0.6 to 0.8	0.17	0.25	0.50	1.00	2.00
0.8 to 1.0	0.14	0.20	0.33	0.50	1.00
Total	1.84	4.78	9.83	13.50	18.00

Table C29 Step II: Computation of the criterion weights for each NDVI's class.

Class	-1.0 to 0.2	0.2 to 0.4	0.4 to 0.6	0.6 to 0.8	0.8 to 1.0	Total	Weight	Weight (%)
-1.0 to 0.2	0.54	0.63	0.51	0.44	0.39	2.51	0.502	50.20
0.2 to 0.4	0.18	0.21	0.31	0.30	0.28	1.28	0.256	25.60
0.4 to 0.6	0.11	0.07	0.10	0.15	0.17	0.60	0.120	12.00
0.6 to 0.8	0.09	0.05	0.05	0.07	0.11	0.37	0.074	7.40
0.8 to 1.0	0.08	0.04	0.03	0.04	0.06	0.25	0.050	5.00
Total	1.00	1.00	1.00	1.00	1.00	-	1.000	100.00

Table C30 Step III: Estimation of the consistency ratio for each NDVI's class.

Class	-1.0 to 0.2	0.2 to 0.4	0.4 to 0.6	0.6 to 0.8	0.8 to 1.0	Weighted Sum Vector	weight	Consistency Vector
-1.0 to 0.2	0.50	0.78	0.60	0.42	0.35	2.65	0.50	5.30
0.2 to 0.4	0.17	0.26	0.36	0.28	0.25	1.32	0.26	5.06
0.4 to 0.6	0.10	0.09	0.12	0.14	0.15	0.60	0.12	4.97
0.6 to 0.8	0.09	0.07	0.06	0.07	0.10	0.38	0.07	5.43
0.8 to 1.0	0.07	0.05	0.04	0.04	0.05	0.25	0.05	4.93
Total	-	-	-	-	-	-	-	25.68

Number of class (n) = 5

$$\text{Lambda } (\lambda) = \frac{25.68 - 5}{5} = 5.14$$

$$\text{Consistency Index (CI)} = \frac{\lambda - n}{n - 1} = \frac{5.14 - 5}{5 - 1} = 0.03$$

Random Index (RI) for $n = 5$ is 1.12

$$\text{Consistency Ratio (CR)} = \frac{CI}{RI} = \frac{0.03}{1.12} = 0.031$$

$CR < 0.10$, this ratio indicates a reasonable level of consistency in the pair-wise comparisons.

APPENDIX D

AVERAGE ANNUAL RAINFALL DATA AND STATION

Table D1 Average annual rainfall data are available from 1996 to 2005.

No.	Province	Station	ID	Latitude (N)	Longitude (E)	Elevation (m)	Rainfall (mm)
1	Mae Hong Son	Khun Yuam	300001	18°50'00"	97°56'00"	140.00	1,285.60
2	Mae Hong Son	Mae La Noi	300003	18°20'00"	97°58'00"	320.00	1,487.30
3	Mae Hong Son	Pang Ma Pha Highland Rice & Field Crop Station	300004	19°32'00"	98°13'00"	660.00	1,274.60
4	Mae Hong Son	Muang Mae Hong Son	300201	19°18'00"	97°50'00"	267.74	1,333.40
5	Mae Hong Son	Mae Sariang	300202	18°10'00"	97°56'00"	211.04	1,174.20
6	Chiang Mai	Fang	327001	19°55'00"	99°14'00"	460.00	1,333.30
7	Chiang Mai	Chom Thong	327003	18°25'00"	98°40'00"	280.00	915.30
8	Chiang Mai	Doi Saket	327004	18°52'00"	99°12'00"	320.00	1,096.70
9	Chiang Mai	Mae Taeng	327005	19°07'15"	98°56'49"	330.00	1,159.80
10	Chiang Mai	Phrao	327006	19°22'00"	99°10'00"	440.00	1,142.90
11	Chiang Mai	Mae Chaem	327007	18°30'00"	98°22'00"	480.00	884.00
12	Chiang Mai	Omkoi	327008	17°48'00"	98°22'00"	820.00	1,014.90
13	Chiang Mai	Sa Moeng	327009	18°49'00"	98°46'00"	530.00	1,192.90
14	Chiang Mai	Hot	327010	18°08'00"	98°38'00"	270.00	1,007.20
15	Chiang Mai	Saraphi	327011	18°43'00"	99°03'00"	300.00	1,147.70
16	Chiang Mai	San Sai	327012	18°51'00"	99°03'00"	300.00	855.90
17	Chiang Mai	Hang Dong	327013	18°41'00"	98°55'00"	325.00	1,164.40
18	Chiang Mai	San Pa Tong	327014	18°37'00"	98°54'00"	315.00	826.30
19	Chiang Mai	San Khamphang	327015	18°45'00"	99°07'00"	300.00	848.40
20	Chiang Mai	Chiang Dao	327016	19°22'00"	98°59'00"	390.00	1,207.80
21	Chiang Mai	Mae Ai	327017	20°02'00"	99°17'00"	480.00	1,410.80
22	Chiang Mai	T.Ban An, A.Doï Tao	327018	17°56'00"	98°45'00"	270.00	633.10
23	Chiang Mai	Fang Horticultural Research Station	327019	19°56'00"	99°09'00"	460.00	1,391.40

Table D1 Average annual rainfall data are available from 1996 to 2005 (Continued).

No.	Province	Station	ID	Latitude (N)	Longitude (E)	Elevation (m)	Rainfall (mm)
24	Chiang Mai	Doi Suthep-Pui National Parks (A.Muang)	327020	18°47'00"	98°56'00"	1,040.00	1,600.70
25	Chiang Mai	Phuphing Ratchaniwet (A.Muang)	327021	18°47'00"	98°54'00"	1,400.00	1,694.80
26	Chiang Mai	Bhumibol Dam Self-Help Settlement (A.DoI Tao)	327022	17°56'00"	98°41'00"	270.00	908.80
27	Chiang Mai	Northern Thailand Petroleum Development Center (A.Fang)	327023	19°52'00"	99°13'00"	470.00	1,077.50
28	Chiang Mai	San Pa Tong Rice Research Station	327024	18°37'00"	98°54'00"	310.00	1,041.90
29	Chiang Mai	San Pa Tong Rice Research Station (A.Mae Taeng)	327025	19°04'00"	99°13'00"	560.00	1,237.60
30	Chiang Mai	Chiang Dao Watershed Preservation Research Station	327026	19°21'00"	98°46'00"	1,020.00	1,487.00
31	Chiang Mai	Bo Luang-Bo Kaew Plant Breeding Centre (A.Hot)	327027	18°09'00"	98°24'00"	1,020.00	1,129.70
32	Chiang Mai	Chom Thong Agricultural Program	327028	18°32'00"	98°47'00"	335.00	855.10
33	Chiang Mai	Wiang Hang	327029	19°33'00"	98°38'00"	-	1,123.20
34	Chiang Mai	Mae Chaem Forest Plantation (A.Mae Chaem)	327030	18°17'00"	98°23'00"	-	1,083.00
35	Chiang Mai	Moving Development Unit 32 (A.Chiang Dao)	327031	19°25'00"	98°58'00"	440.00	1,135.60
36	Chiang Mai	Mae wang	327032	18°31'14"	98°48'43"	360.00	1,290.30
37	Chiang Mai	Mae Cho	327301	18°55'00"	99°00'00"	316.53	1,120.00
38	Chiang Mai	Muang Chiang Mai	327501	18°47'24"	98°58'37"	304.51	1,188.90
39	Lamphun	Lamphun Administration Office	329001	18°32'00"	99°02'00"	-	883.10
40	Lamphun	Mae Tha	329002	18°27'00"	99°08'00"	400.00	1,133.80
41	Lamphun	Pa Sang	329003	18°31'00"	98°57'00"	280.00	1,085.70
42	Lamphun	Li	329004	17°45'00"	98°58'00"	-	1,027.00
43	Lamphun	Ban Hong	329005	18°19'00"	98°50'00"	310.00	1,030.60
44	Lamphun	Ban Goa Jadsan School (A.Li)	329006	17°38'00"	98°47'00"	-	978.90
45	Lamphun	Mae Li Forest Plantation (A.Li)	329007	17°56'00"	98°54'00"	460.00	1,030.30
46	Lamphun	Muang Lamphun	329201	18°34'00"	99°02'00"	296.42	1,031.00

Table D1 Average annual rainfall data are available from 1996 to 2005 (Continued).

No.	Province	Site Name	ID	Latitude (N)	Longitude (E)	Elevation (m)	Rainfall (mm)
47	Chiang Mai	Wat Chan	WA	19°04'00"	98°17'00"	990.00	980.20
48	Chiang Mai	Bo Kaeo	BO	18°52'00"	98°31'00"	1,400.00	1,594.90
49	Chiang Mai	Mae Sa	SA	18°49'00"	98°20'00"	650.00	1,097.25
50	Chiang Mai	Mae Yod	YO	18°50'00"	98°06'00"	1,180.00	1,778.80
51	Chiang Mai	Mae Ning	NI	18°37'00"	98°13'00"	1,630.00	2,085.75
52	Chiang Mai	Mae Jon Luang	JO	18°40'00"	98°28'00"	1,470.00	1,717.20
53	Chiang Mai	Doi Inthanon	DO	18°35'00"	98°29'00"	2,565.00	2,737.58
54	Chiang Mai	Mae Klang	KL	18°31'00"	98°29'00"	1,540.00	2,069.50
55	Chiang Mai	Research Station	RE	18°31'00"	98°18'00"	1,100.00	1,191.08
56	Chiang Mai	POU	PO	18°30'00"	98°22'00"	490.00	939.60
57	Chiang Mai	Mae Long	LO	18°27'00"	98°14'00"	1,450.00	1,512.80
58	Chiang Mai	Sirikit Plantation	SI	18°22'00"	98°28'00"	1,330.00	1,560.90
59	Chiang Mai	Ob Luang	OB	18°13'00"	98°29'00"	380.00	1,088.63
60	Chiang Mai	Huay Bong	HU	18°09'00"	98°26'00"	810.00	1,086.00
61	Chiang Mai	Mae Tho	TH	18°15'00"	98°13'00"	1,250.00	1,224.25

Source: Station number 1-46: Thai Meteorological Department (location of the 46 rain stations in northern Thailand)

Site number 47-61: The GAME-T project (location of the 15 rain gauges in the Mae Chaem watershed)

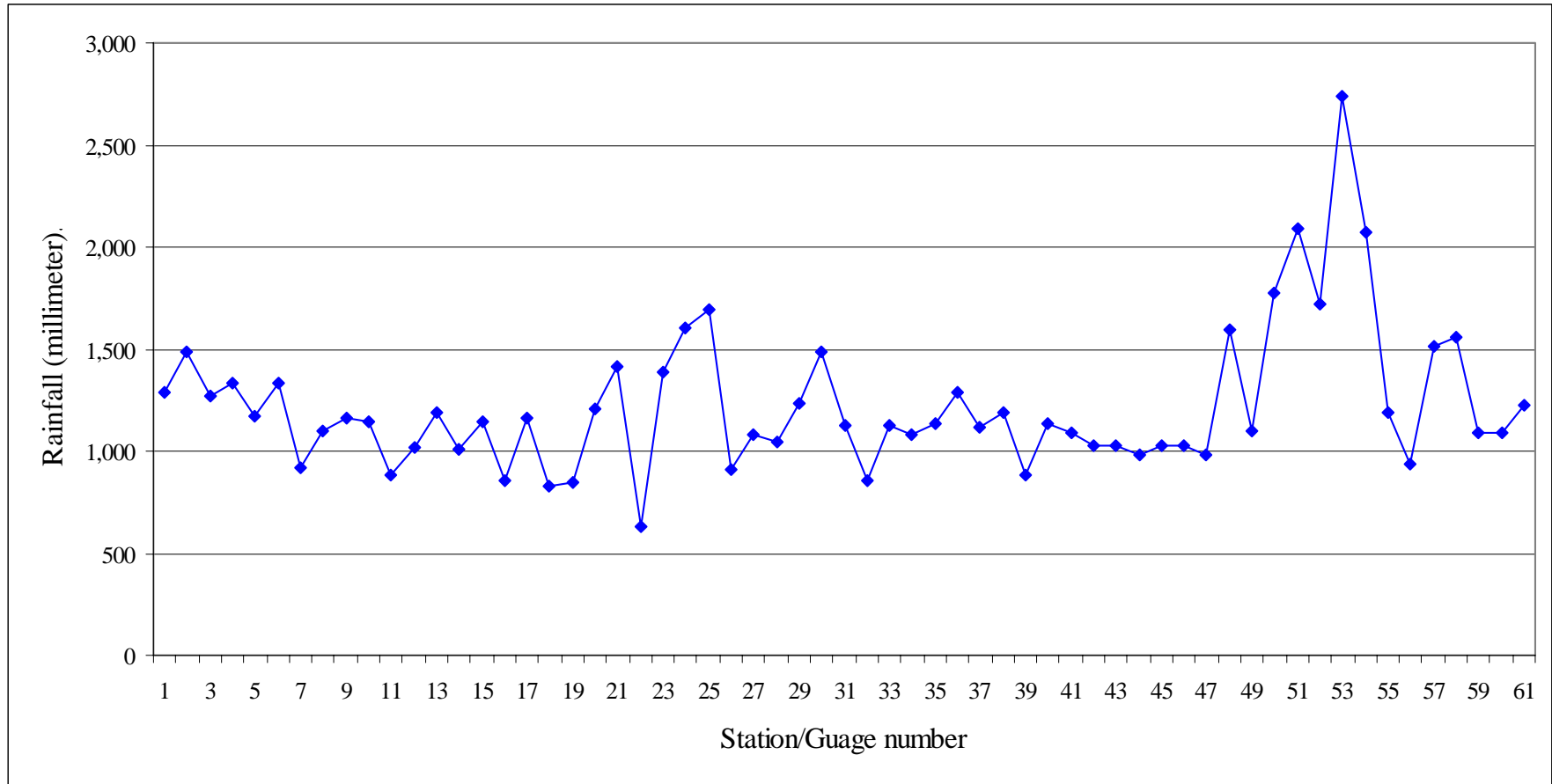


Figure D1 Graph showing the pattern distribution of average annual rainfall data are available from 1996 to 2005 on each station/gauge (Source: Thai Meteorological Department and the GAME-T project).

CURRICULUM VITAE

Miss Narumon Intarawichian was born in Chonburi Province, eastern Thailand on February 8, 1974. She received her B.Sc. degree in geography from Department of Geography, Faculty of Humanities and Social Sciences, Burapha University in 1995 and Master Degree in geography from Chulalongkorn University in 1998. During years 1996-1998, she worked as a part time employee (technician) at the Mapping and Survey Company Limited. After graduation (1998-1999), she had worked as a scientist (GIS technician) at the Centre for Industrial and Environmental Training (CIET), Burapha University and later (in 1999-2000) became a researcher for Education Quality Assurance at Faculty of Humanities and Social Sciences, Burapha University. During years 2000-2004, she was a lecturer at Department of Geography, Faculty of Humanities and Social Sciences, Burapha University. In 2004, she had a scholarship from the Commission on Higher Education, the Ministry of Education of Thailand to pursue her study for a Ph.D. at the School of Remote Sensing, Institute of Science, Suranaree University of Technology.

Her main research interest is on landslide susceptibility mapping using remote sensing and GIS modeling which is significantly inspired from the work achieved in her Ph.D. thesis.